Study on Kinematics and Movement Accuracy Improvement of Parallel Mechanisms

March 2015

PEI Zhanwu

Abstract

This thesis mainly comprises of two parts of contents, direct-kinematics and movement accuracy improvement of parallel mechanisms.

In Chapter 1, the background, purpose and necessity of this study will be introduced. As well-known mechanisms, parallel mechanisms have many outstanding advantages, such as high payload ability, high accuracy, high structural rigidity and high movement speed, however some drawbacks, smaller movement space and complicated kinematics, also limits their further applications and developments. A good idea to enlarge movement space by adding redundant joints has been seen, however it is hardly applied widely because of lack of a set of universal methods to do with direct-kinematics of parallel mechanisms with redundancy. Then again, due to the inherent defect of multi-joint mechanisms, the heterogeneity of movement accuracy in the movement space, accuracy deterioration will make some areas in the movement space unable to be used and the narrow workspace more narrow.

Based on the above, the purpose of this study will be set as follows,

1. To give a set of universal methods to establish direct-kinematic relations of parallel mechanisms. Especially they will be demanded to apply to parallel mechanisms with redundancy.

2. To provide a set of methods to improve movement accuracy of parallel mechanisms by using the movement information from passive joints. Workspaces of parallel mechanisms will be expanded in some accuracy deteriorating areas.

In Chapter 2, kinematics of parallel mechanisms will be discussed and a set of direct-kinematic relations applicable to parallel mechanisms with redundancy will be derived. Active joints which can determine and describe all movements of parallel mechanisms will be strictly defined. Mechanism DOF and end-effector DOF will be distinguished, a set of numerical approaches to calculate them will be provided and the definition of mechanism redundancy will be given. Joints in parallel mechanisms will be divided into two parts by selection matrices, active joints and passive joints, the movement relation between them will be derived. Finally the movement relation between active joints and end-effector will be presented. In the end of this chapter, manipulability of parallel mechanisms will be discussed, the conclusion will be used in the next chapter.

In Chapter 3, a set of approaches to improve movement accuracy of parallel mechanisms will be introduced. Kinematic sensors will be amounted to these joints, some active joints with better error performances will be picked out as sensing joints by evaluation measures, their accuracy movement information will be converted and delivered to driving joints to improve movement accuracy of parallel mechanisms.

In Chapter 4, Two numerical examples will be presented to verify some derivations and conclusions in chapter 2, high accuracy movement of parallel mechanisms will be simulated by using methods in chapter 3. Selection and use of sensing joints will be concretely introduced, and some significant improvements in some accuracy deteriorating areas will be seen from results of simulations.

In Chapter 5, A summary about works in the thesis will be given.

Contents

List of Figures

List of Tables

Chapter 1

Introduction

1.1 Parallel Mechanisms

In recent years, Parallel Mechanisms have attracted more and more interests on robotics research and application. A parallel mechanism (PM) shown in Fig.1.1 is a multi-DOF (degree of freedom) mechanism composed of one moving platform (or end-effector) and one base connected by at least two serial kinematic chains with multiple joints. All kinematic chains are parallel to each other, any of them can be looked as one single serial mechanism from the base to the end-effector, and they are also called legs or limbs.

The first application of PMs is in 1954, when a six-legged PM with six prismatic actuators was invented and used as a tire testing machine shown in Fig.1.2 by V. E. Gough. Its design later was publicized in a 1965 paper by D.Stewart, so it is called as Gough-Stewart platform. Compared to conventional serial mechanisms (SMs), PMs have many outstanding advantages such as higher payload ability, higher accuracy and higher structural rigidity, as well as high speed [1][2].

In term of these good properties of PMs, lots of applications have been developed, such as flight simulators shown in Fig.1.3, satellite dish positioning shown in Fig.1.4, machine tool shown in Fig.1.5, haptic devices shown in Fig.1.6, medical

robots shown in Fig.1.7, alignment devices shown in Fig.1.8, coordinate measuring machines as well as force sensors even weapon systems shown in Fig.1.9. Some of PMs have been popular mechanism, such as the Gough-Stewart platform and the Delta robot shown in Fig.1.10. Now they have covered a wide range of application fields, for instance, assembly, inspection, processing etc. [3]-[7].

1.2 Background Research on Parallel Mechanisms

Though many types of PMs have been proposed and lots of them have been also applied to many fields, due to some drawbacks such as smaller workspace, complicated kinematics, many further works are still needed to be done.

Now researches on PMs mainly focused on the following a few aspects:

1. New structure, new applications and optimization of architecture
2. Kinematics, movement planning, control and algorithm
3. Movement accuracy and error evaluation

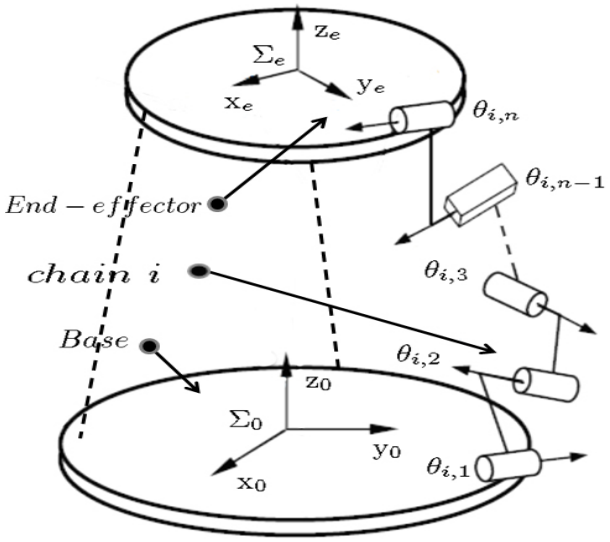

Fig. 1.1: Schematic representation of a parallel mechanism

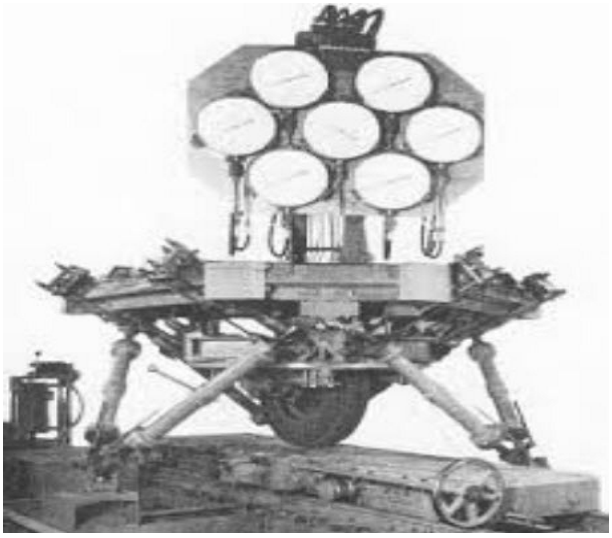

Fig. 1.2: Original Gough-Stewart platform

Fig. 1.3: Flight simulator

Fig. 1.4: Satellite antenna

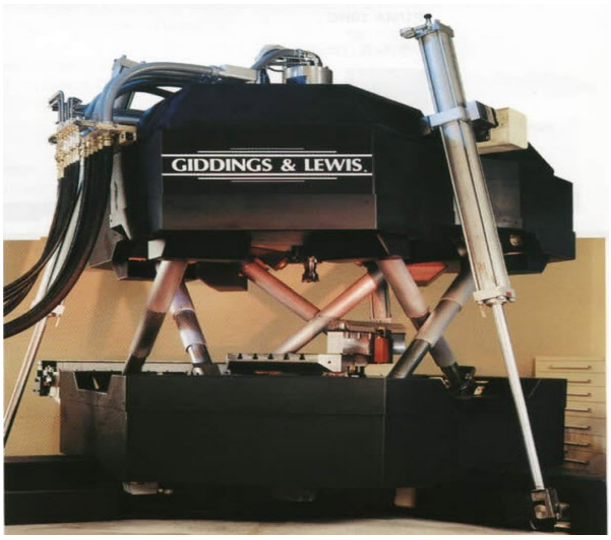

Fig. 1.5: Variax from Giddings & Lewis

4. Stiffness, vibration

Exploration of the new structure is in order to generate desired movements, achieve better movement requirements and architecture optimization is to obtain bigger movement space, best movement quality or higher movement accuracy. Some new structures are being continually developed, such as lower-mobility parallel mechanisms [8]-[13], serial-parallel mechanisms [14] and hybrid kinematic mechanisms. Lower-mobility PMs have been used to achieve some particular movements. Hybrid kine-

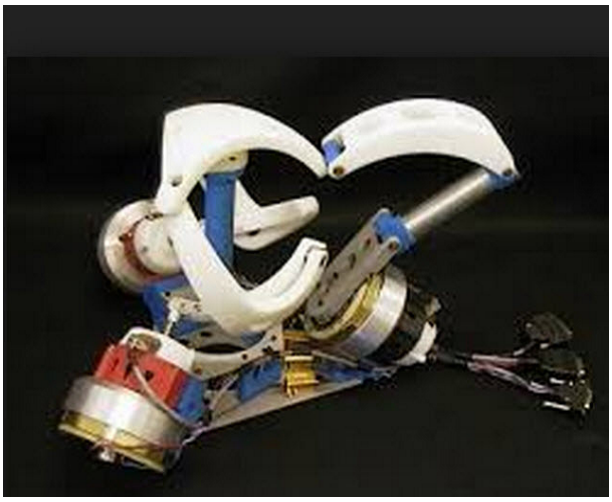

Fig. 1.6: A 3-DOF Spherical Haptic Device

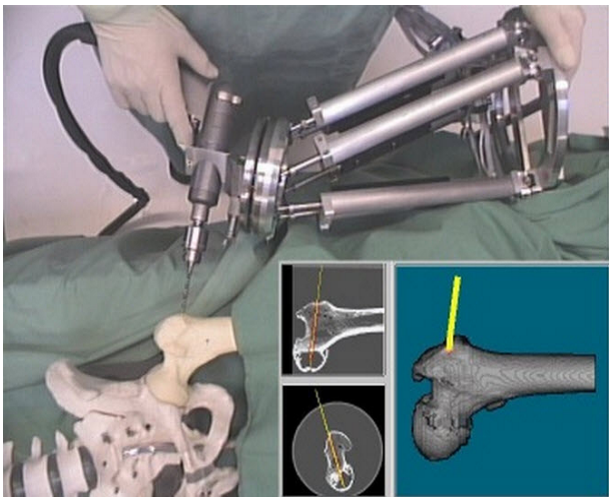

Fig. 1.7: Medical robot

Fig. 1.8: A active secondary mirror for Telescope from IPA

matic machine tools, where two PMs are used cooperatively, are to realize flexible motions. Moreover some attempts, which add redundant joints to kinematic chains of PMs to avoid singularity and enlarge workspace, have been also seen [15].

Kinematics are essential in all researches of PMs, no matter architecture optimization, movement planning, or others, kinematic relations must be firstly established.

In former researches, some works about kinematic relation of parallel structures

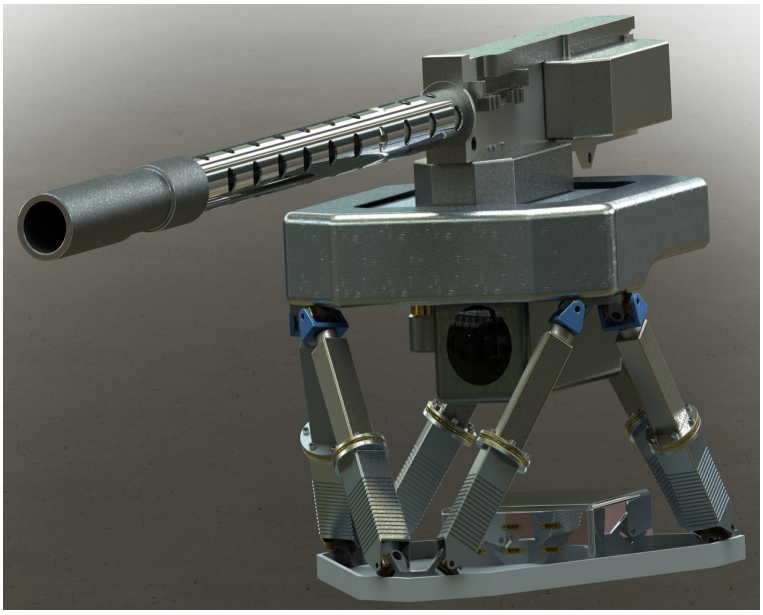

Fig. 1.9: a lightweight steerable gun mount based on a Stewart platform from Terra Engineering

Fig. 1.10: Delta robot from ABB

have been done. Stefan Dutr*é* provided one closed-form expression about the velocity closure, then derived a analytical Jacobian for 6-DOF parallel manipulator by using selection-matrices [16]. Doik kim suggested a approach to obtain the instantaneous kinematic relation by extending screw theory [17][18]. C.M.Gosselin and J.Angeles gave one Jacobian of parallel manipulator for singularity analysis [19].

However the PMs with redundancy has not still been touched in these researches, and a set of kinematic relations capable to be applied to PMs with redundancy has not been found. It will limit applications and developments of PMs and some good ideas,such as [15] will be hardly applied widely because of lack of a set of universal methods to do with direct-kinematics of parallel mechanisms with redundancy. So it is very necessary to find a set of universal and effective methods to build kinematic relations, especially capable to be used to PMs with redundancy.

As another important aspect of researches about PMs, the accuracy analysis, error model and error compensation also drew greatly attention, especially when PMs were applied to machine tools, medical robots, alignment devices, coordinate measuring machines as well as force sensors.

The accuracy of PMs relies on many factors, such as manufacturing tolerances and clearances, assembly errors, the actuator control errors, movement planning and algorithms, even imperfections from the architecture design, elastic deformations and thermal deformations also will degrade it. Some of these error sources can be calibrated, analyzed and evaluated by establishing effective error models.

Some papers have discussed the accuracy of PMs. In [20] the error analysis to a serial-parallel hybrid type PM was done and an error model caused by link dimensions was derived by using the differential vector. In [21] an error model was established, then the efficient particle swarm optimization approach was used to a translational 3-PUU on the base of this model. A set of algorithm to estimate the pose error of PMs was contributed, which was derived from some basic models of joint clearances and clearance constraints in [22]. The influence of manufacturing error on the accuracy of a Steward platform was discussed in [23]. Several papers also introduced the accurate movement control on PMs [24].

However studies on improving the movement accuracy of a given PM is very

rare. Better accuracy is always expected to a given PM, so it is very necessary to find new methods to improve the movement accuracy of PMs. Moreover accuracy deterioration also will cause some movement areas of PMs unable to be used and the cost of the whole mechanism will also rise significantly with using of precision machining technology and high precision control components for seeking a good accuracy. If ways to improve the movement accuracy of PMs can be found without any modifications of the hardware, the workspace of PMs will be expanded and the cost will be reduced too.

The paper [24] introduced an error compensation method by using a PSD sensor amounted to the end-effector. which can directly provide the movement information of the end effector to the controller without any kinematic or dynamic inaccuracy. Unfortunately this method can not be completely used in many cases like a work condition full of smoke, although this method achieved a quite high movement accuracy.

However the paper disclosed a fact that if more accurate movement information is obtained, movement accuracy of PMs can be improved. Fortunately structure of PMS provide possibility for obtaining more accurate information, because they are with lots of passive joints, accurate movement information can be probably gotten from these joints.

1.3 Purpose of This Research

In this thesis we will discuss the two things:

1. To find a set of universal method to establish direct kinematic relations of parallel mechanisms. Especially they will be demanded to apply to parallel mechanisms with redundant joints.

2. To provide a set of approaches to improve movement accuracies of parallel mechanisms by using more accurate movement information from joints.

1.4 Organization of This Thesis

This thesis will be organized as follows:

1. In chapter 2, kinematics of parallel mechanism will be discussed. A set of universal kinematic relations applicable to parallel mechanisms with redundant joints will be derived. Active joints that can determine all movements of parallel mechanisms will be strictly defined. Mechanism DOF and end-effector DOF will be distinguished. The definition of mechanism redundancy will be given. Then joints of parallel mechanisms will be divided into two parts, active joints and passive joints, the kinematic relation of them will be derived. Finally the kinematic relation between active joints and end-effector will be presented. In the end of this chapter, manipulability of parallel mechanisms will be discussed, its result will be used in the next chapter as a base of discussions.

2. In chapter 3, some approaches to improve movement accuracy of parallel mechanisms will be discussed by using more accurate movement information from joints. Kinematic sensors will be amounted to passive joints and some joints with better error performances will be picked out as sensing joints by evaluation measures, their accuracy movement information will be converted and delivered to driving joints to improve movement accuracy of parallel mechanisms. The chapter will firstly discuss error performances on the end-effector of different active joints, then selection and usage of sensing joints will be introduced.

3. In chapter 4, a 2-DOF planar PM and 3-DOF spatial PM with redundancy as

numerical examples will be provided to demonstrate how to use equations in chapter 2 and verify their validity. And high accuracy movement of parallel mechanisms will be simulated by using methods in chapter 3 and selections and usage of sensing joints will be concretely introduced. Some outstanding improvement in some areas of accuracy deterioration will be seen.

4. Finally, a summary about the thesis will be given.

Chapter 2

Kinematics of Parallel Mechanisms

2.1 Introduction

In robotic mechanism, movements of the end-effector are realized by joints, or they are decided by movements of joints. Different from SMs, because all kinematic chains were rigidly connected together on the end-effector, movements of kinematic chains are affected each other in PMs. All kinematic chains will own the same position and velocities on the end-effector, movements of the end-effector and joints can be decided by only a part of joints. Movement relations in PMs can be divided into the one from the part of joints to other joints (or all joints) and the one from the part of joints to the end-effector.

It can be also explained from the viewpoint of movement space. Movements of all joints can be seen as one space, called as the joint movement space, movements of end-effector can be seen as another space, called as the movement space of end-effector. If there are no constraints, movements of all chains and joint movements on each of kinematic chains are free and independent, and movement relations will be mappings from the subspace of the joint movement space from each of kinematic chains to the movement space of the end-effector. Because all kinematic chains were rigidly connected together on the end-effector and own a common end-effector,

movements of kinematic chains are affected each other, movements of joints are not independent, and movements from a part of joints can determine movements of other joints and end-effector, or all movements in PMs can and only need be decided or described by part joint movements. This part of joints will be called as *Active Joints*, the rest part of joints will be called as *Passive Joints*. Movement relations in PMs will be mappings from the subspace of the joint movement space from part joint movements to the movement space of the end-effector and from the subspace to the joint movement space. The dimensionality of the subspace of the joint movement space will be decided by the quantity of part joints, such subspaces are not unique.

In this chapter, DOFs, redundancies, movement relations and the manipulability of PMs will be discussed in sequence.

2.2 Movements and DOFs of Parallel Mechanisms

2.2.1 Symbols and Definitions in this chapter

Some basic definitions about PMs will be firstly given with reference to Fig.1.1. Kinematic chain refers to one assembly of rigid bodies connected by joints, all of them begin from the base and end at the end-effector in PMs, own the same position and velocities (or displacements) on the end-effector. The displacement vector on the end-effector can be written as:

$$\Delta\vec{x}_e = \begin{bmatrix} \Delta x_e & \Delta y_e & \Delta z_e & \Delta\alpha_e & \Delta\beta_e & \Delta\gamma_e \end{bmatrix}^T \tag{2.1}$$

If the PMs contains m kinematic chains, the joint displacement vector of the ith kinematic chain can be written as follows:

$$\Delta\vec{\theta}_i = \begin{bmatrix} \Delta\theta_{i1} & \Delta\theta_{i2} & \dots & \Delta\theta_{in_i} \end{bmatrix}^T \tag{2.2}$$

The symbol, $\Delta\theta_{ij}$, means one joint displacement locating to the jth joint of the ith

chain, θ_{ij}, and n_i is the quantity of joints on this chain. Joint displacements of all chains composed one joint displacement vector,

$$\Delta\vec{\theta} = \left[\begin{array}{cccc} \Delta\vec{\theta}_1{}^T & \Delta\vec{\theta}_2{}^T & \ldots & \Delta\vec{\theta}_m{}^T \end{array} \right]^T \quad . \tag{2.3}$$

The total quantity of joints in PMs is

$$N = \sum_{t=1}^{m} n_j \quad . \tag{2.4}$$

2.2.2 Position and Velocity Constraints

In PMs, all serial kinematic chains are rigidly connected together, all serial kinematic chains own the same position and movements on the end-effector. It is called as *Structural Constraint*, or respectively called as *Position Constraint* and *Velocity Constraint* [16].

Position constraint can be described as a set of nonlinear transition matrix relations, and written as:

$$\begin{array}{rcccc} T_e & = & T_{11} & T_{12} & \ldots & T_{1n_1} \\ & = & \ldots & \ldots & \ldots & \ldots \\ & = & T_{m1} & T_{m2} & \ldots & T_{mn_m} \end{array} \tag{2.5}$$

The symbol T_e is the transition matrix from the base to end-effector along any serial chain, and the symbol T_{ij} is the transition matrix over the jth joint of the ith chain. Position constraint is mainly used to do with the inverse kinematics of PMs, it will be used to calculate original positions of all kinematic chains.

Velocity constraint can be described by the following kinematic relation.

$$\begin{array}{rcccc} \Delta\vec{x}_e & = & J_1 & \Delta\vec{\theta}_1 \\ & = & J_2 & \Delta\vec{\theta}_2 \\ & = & \ldots & \ldots \\ & = & J_m & \Delta\vec{\theta}_m \end{array} \tag{2.6}$$

The symbol J_i is the Jacobian matrix of the ith chain, it can be obtained by many methods, D-H coordinate method will be used [25] in this study. From Eq.2.6, the closed-form expression of velocity constraint can be obtained as follows:

$$\begin{bmatrix} J_1 & -J_2 & 0 & \dots & 0 \\ J_1 & 0 & -J_3 & \dots & 0 \\ \vdots & \vdots & \vdots & \ddots & \vdots \\ J_1 & 0 & 0 & \dots & J_m \end{bmatrix} \begin{bmatrix} \Delta\,\vec{\theta}_1 \\ \Delta\,\vec{\theta}_2 \\ \vdots \\ \Delta\,\vec{\theta}_m \end{bmatrix} \triangleq A\,\Delta\vec{\theta} = \mathbf{0} \tag{2.7}$$

All discussions and derivations in this study will be based on velocity constraint to do.

2.2.3 Mechanism DOF and End-effector DOF

In practical robotic mechanism all the movements should be knowable and controllable. Different from SMs, PMs contains at least two kinematic chains and joint movements in every chains are dependent because of the structural constraint, and movements of the mechanism can be realized by controlling movements of active joints.

The quantity of active joints by which all movements of PMs can and only need be decided is named *Mechanism DOF*. It is equal to the dimensionality of the subspace from the joint movement space.

Mechanism DOF can be calculated by many methods, the most well-known one among them is:

$$N_a = \lambda(n_l - n_j - 1) + \Sigma n_j \tag{2.8}$$

the symbol N_a is the mechanism DOF of the PM, n_l is the quantity of links, n_j is the quantity of joints, and N_j is DOF of the jth joint, the symbol λ is 6 in spatial

mechanisms or 3 in planar mechanisms. This equation is so simply and widely used, but it can't apply to all PMs [26].

Mechanism DOF can also be calculated from the movement space of joints. From velocity constraint, the displacement vector $\Delta\vec{\theta}$ can be obtained as follows:

$$\Delta\,\vec{\theta} \;=\; \left(\; I_N - A^{+}A \;\right)\vec{k} \tag{2.9}$$

The symbol $\vec{k}$ is an arbitrary N dimensional coefficient vector, the right of Eq.2.9 is a set of total solutions of joint displacements. Because velocity Constraint is only one factor to restrict joint movements, the dimensionality of the solution space in Eq.2.9 must be the quantity of active joints, the mechanism DOF can be decided by the equation as follows,

$$N_a = Rank\left(I_N - A^{+}A\right) = N - Rank(A) \tag{2.10}$$

Here the matrix in the Eq.2.9 will be written as A_k for using conveniently it later.

$$A_k \;=\; \left(\; I_N - A^{+}A \;\right) \tag{2.11}$$

The quantity of movements of the end-effector able to be realized in the whole movement space of PMs is named *End-effector DOF*. It is impossible that the quantity of movements is greater than end-effector DOF on one position. If the quantity of movements is less than the end-effector DOF, the end-effector is locating at a singular position.

Movements on end-effector need to be realized by active joints. From Eq.2.6 the following equation can be obtained:

$$\begin{bmatrix} I_{6(3)} \\ I_{6(3)} \\ \cdots \\ I_{6(3)} \end{bmatrix} \Delta\vec{x}_e = \begin{bmatrix} J_1 & 0 & 0 & \cdots & 0 \\ 0 & J_2 & 0 & \cdots & 0 \\ \cdots & \cdots & \cdots & \cdots & \\ 0 & 0 & 0 & \cdots & J_m \end{bmatrix} \Delta\vec{\theta} \tag{2.12}$$

$[\, I_{6(3)} \;\; I_{6(3)} \;\; \cdots \;\; I_{6(3)} \,]^T$ is a $6m \times 6$ matrix (or $3m \times 3$ in a planar PM) and its rank is 6 (or 3), so the Eq.2.12 call be rewritten as follows,

$$\Delta\vec{x}_e = \begin{bmatrix} I_{6(3)} \\ I_{6(3)} \\ \vdots \\ I_{6(3)} \end{bmatrix}^{+} \begin{bmatrix} J_1 & 0 & 0 & \ldots & 0 \\ 0 & J_2 & 0 & \ldots & 0 \\ \vdots & \vdots & \vdots & \ddots & \vdots \\ 0 & 0 & 0 & \ldots & J_m \end{bmatrix} \Delta\vec{\theta} \tag{2.13}$$

Substituting Eq.2.9 into Eq.2.13, Eq.2.14 can be obtained. It can be considered as one total solutions of displacements on the end-effector.

$$\Delta\,\vec{x}_e = \begin{bmatrix} I_{6(3)} \\ I_{6(3)} \\ \vdots \\ I_{6(3)} \end{bmatrix}^{+} \begin{bmatrix} J_1 & 0 & 0 & \ldots & 0 \\ 0 & J_2 & 0 & \ldots & 0 \\ \vdots & \vdots & \vdots & \ddots & \vdots \\ 0 & 0 & 0 & \ldots & J_m \end{bmatrix} \left[\; I_N - A^{+}A \;\right] \vec{k} \tag{2.14}$$

The matrix of Eq. 2.14 will also be written as J_k for using conveniently.

$$J_k = \begin{bmatrix} I_{6(3)} \\ I_{6(3)} \\ \vdots \\ I_{6(3)} \end{bmatrix}^{+} \begin{bmatrix} J_1 & 0 & 0 & \ldots & 0 \\ 0 & J_2 & 0 & \ldots & 0 \\ \vdots & \vdots & \vdots & \ddots & \vdots \\ 0 & 0 & 0 & \ldots & J_m \end{bmatrix} \left[\; I_N - A^{+}A \;\right] \tag{2.15}$$

Eq. 2.14 is also derived from structural sonstraint which is the only one condition to restrict all movements in the PMs. Hence, end-effector DOF can be calculated as follows,

$$N_e = Rank\,(J_k) \qquad . \tag{2.16}$$

2.2.4 Redundancies in Parallel Mechanisms

Movements able to be realized on the end-effector can not exceed three-dimensional space, so end-effector DOF of the robotic mechanism must be equal to 6 or less than

6. And all movements on the end-effector are determined and realized by joint movements of PMs, so mechanism DOF or the quantity of active Joints must be equal to or greater than the dimensionality of the movement space on the end-effector.

When the quantity of active joints or mechanism DOF is greater than the dimensionality of movement space on the end-effector or end-effector DOF, the mechanism will be called with *Movement redundancy* or *Mechanism redundancy*.

All movements in PMs need be realized by a certain quantity of active Joints. But sometimes movements of the end-effector in PMs with redundancy can be realized by the insufficient quantity of joints. For example, in the PMs shown in Fig.2.1, five joints will be needed to make up active joints to control all movements of the mech-

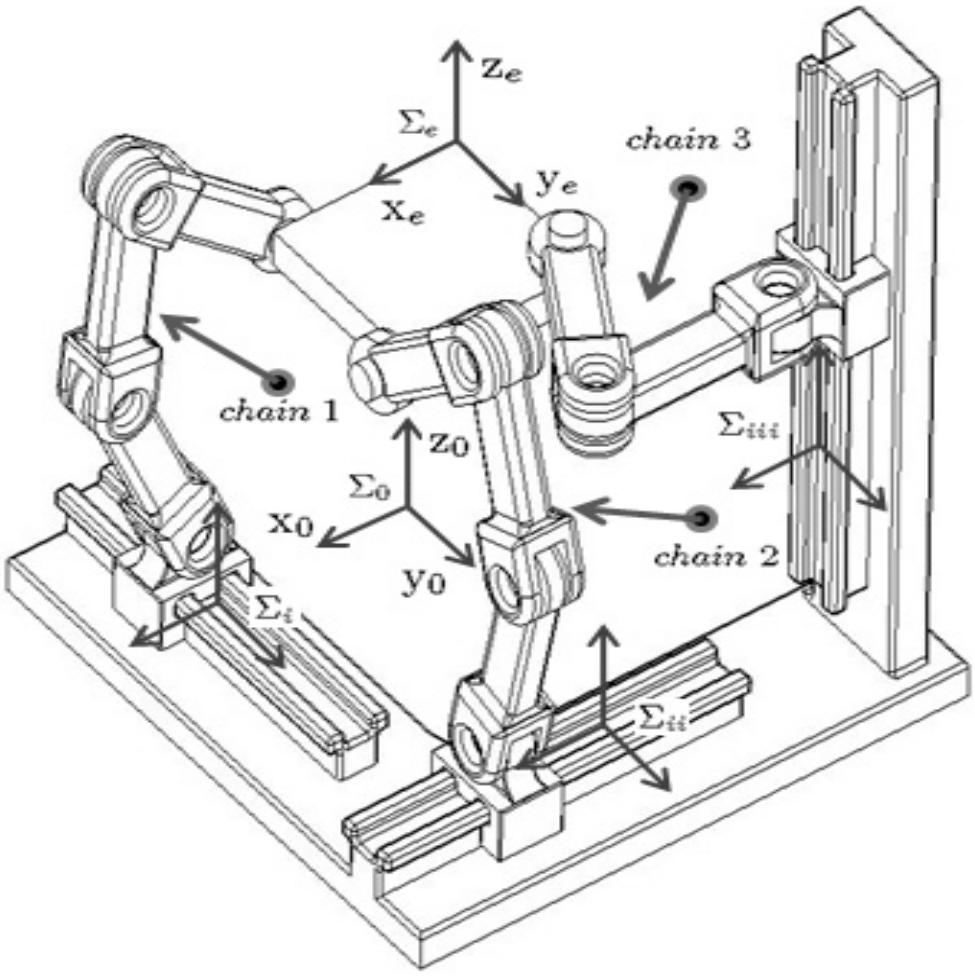

Fig. 2.1: A 3-DOF spatial PM with 2 redundant joints

anism, but movements of the end-effector can be realized by the first three joints in every chains. Of course, it will make movements of all chains to be uncontrollable. But in some type mechanisms, such as Steward platform which is made up by prismatic joints and ball-joints, the mechanism will be redundant if ball-joints were used on both ends of prismatic joint in every kinematic chain, but movements on the end-effector are still controllable and realizable by controlling all prismatic joints.

Movements of joints are executed by actuators, all accurate movements on the end-effector are also realized by controlling actuators of active joints. But it do not mean that only actuators equal to quantity of active Joints are permitted to use. More actuators can be applied to PMs, but the redundant part of them must be controlled cooperatively with active joints to move.

When the quantity of actuators applied to PMs is greater than the quantity needed to realize movements of the end-effector, the PMs will be called with *Driving redundancy*.

Obviously, driving redundancy does not mean the mechanism with mechanism redundancy. but if all movements of PMs with Mechanism redundancy can be controlled, it must mean the mechanism with Driving redundancy. It is the one of reasons that this thesis distinguishes joints of PMs as active joints and driving joints to avoid confusions.

2.3 Direct Jacobian of Parallel Mechanisms

As well known from section 2.2, movements of joints in PMs are dependent, all movements of the PMs can be realized by controlling movements of active joints. In this section, the displacement relation from active joints to end-effector will be established.

2.3.1 Selection Matrices

Marking displacements of active joints as one vector $\Delta\vec{\theta}_a$ and its quantity of joints as N_a, writting displacements of passive joints as one vector $\Delta\vec{\theta}_u$, its quantity of joints as N_u ($= N - N_a$), joint displacements in PMs can be written as follows [16],

$$\begin{aligned} \Delta\vec{\theta} &= I_N\ \Delta\vec{\theta} \\ &= \phi_a\ \Delta\vec{\theta}_a\ +\ \phi_u\ \Delta\vec{\theta}_u \\ &= \left[\ \phi_a\ \ \phi_u\ \right] \begin{bmatrix} \Delta\vec{\theta}_a \\ \Delta\vec{\theta}_u \end{bmatrix} \end{aligned} \tag{2.17}$$

The matrix I_N is a identity matrix with N dimension. $\phi_a \in R^{N\times N_a}$, Rank($\phi_a$) = N_a, is the matrix built by extracting the column vectors from I_N with correspondence with displacements of active joints. $\phi_u \in R^{N\times N_u}$, Rank($\phi_u$) = N_u, is the remaining part of the identity matrix I_N extracted. They are called as selection matrices.

Selection matrices, ϕ_a and ϕ_u, are a pair of orthogonal matrices and following relations can be obtained [16].

$$\begin{cases} \Delta\vec{\theta}_a &= \phi_a^T \Delta\vec{\theta} \\ \Delta\vec{\theta}_u &= \phi_u^T \Delta\vec{\theta} \end{cases} \tag{2.18}$$

2.3.2 Movement Relation between Joints in Parallel Mechanisms

Multiplying matrix A to both sides of Eq.2.17, the equation

$$A\,\Delta\vec{\theta}\ = A\phi_a\Delta\vec{\theta}_a + A\phi_u\Delta\vec{\theta}_u\ = 0 \tag{2.19}$$

can be gotten. It can be rewritten as follows,

$$A\phi_u\Delta\vec{\theta}_u\ = -A\phi_a\Delta\vec{\theta}_a \tag{2.20}$$

In this equation, $A\phi_u \in R^{6(m-1)\times N_u} (\in R^{3(m-1)\times N_u})$ and Rank $(A\phi_u)$ = N_u, so the following equation can be obtained.

$$\Delta\vec{\theta}_u\ = -(A\phi_u)^+ A\phi_a\Delta\vec{\theta}_a \tag{2.21}$$

Substituting Eq.2.21 to Eq.2.17, the displacement mapping from active joints to all joints can be obtained:

$$\begin{aligned} \Delta\,\vec{\theta} &= [\phi_a - \phi_u(A\phi_u)^{+}A\phi_a]\,\Delta\,\vec{\theta}_a \\ &= A_{\Phi}\Delta\,\vec{\theta}_a \end{aligned} \tag{2.22}$$

2.3.3 Direct Jacobian of Parallel Mechanisms

Substituting Eq.2.22 to Eq.2.13, the next equation can be gotten:

$$\Delta\,\vec{x_e} = \begin{bmatrix} I_{6(3)} \\ I_{6(3)} \\ \vdots \\ I_{6(3)} \end{bmatrix}^{+} \begin{bmatrix} J_1 & 0 & 0 & \ldots & 0 \\ 0 & J_2 & 0 & \ldots & 0 \\ \vdots & \vdots & \vdots & \ddots & \vdots \\ 0 & 0 & 0 & \ldots & J_m \end{bmatrix} A_{\phi}\Delta\vec{\theta}_a \tag{2.23}$$

It is an equation determined the instantaneous kinematic relation from active joints to the end-effector. Obviously, Jacobian matrix in the PMs can be written as:

$$J_a = \begin{bmatrix} I_{6(3)} \\ I_{6(3)} \\ \vdots \\ I_{6(3)} \end{bmatrix}^{+} \begin{bmatrix} J_1 & 0 & 0 & \ldots & 0 \\ 0 & J_2 & 0 & \ldots & 0 \\ \vdots & \vdots & \vdots & \ddots & \vdots \\ 0 & 0 & 0 & \ldots & J_m \end{bmatrix} A_{\phi} \tag{2.24}$$

The Jacobian matrix J_a ($\in R^{N_e \times N_a}$), $\mathrm{Rank}(J_a) = N_e$ is a mapping matrix from movement space of active joints to the movement space on the end-effector.

At the initial design stage, it is often needed to know which set of joints can be used as active joints. Here one method to identify will be provided. As is metioned above, because the mechanism DOF of PMs is always equal to the quantity of active joints, joints can be chosen arbitrarily, the sub-matrix can be extracted from the matrix in Eq.2.13 with correspondence to active joints. Examining its rank, if this

rank is equal to mechanism DOF, this set of joints will be able to be used as active joints.

2.4 Manipulability of Parallel Mechanism

Manipulability indicates the level of difficulty to realizes movements on the end-effector in all directions of the movement space by controlling joints. In SMs, Manipulability is unchanged at any a given position. But in PMs, it will be able to to be changed by choosing different active joints. Now the ellipsoid of manipulability in PMs will be given.

Similarly to SMs, the ellipsoid of manipulability in PMs can be written as follows:

$$(\Delta\vec{X}_e)^T(J_a^+)^T J_a^+ \Delta\vec{X}_e \leq 1 \tag{2.25}$$

Singular value decomposition can be done to J_a^+,

$$J_a^+ = V\Sigma^+ U^T, \tag{2.26}$$

matrices U$\in R^{N_e \times N_e}$ and V$\in R^{N_a \times N_a}$ are two orthogonal matrices.

The matrix Σ^+ is $N_a \times N_e$ matrix, it can be written as:

$$\Sigma^+ = \begin{bmatrix} \sigma_1^{-1} & 0 & \dots & 0 \\ 0 & \sigma_2^{-1} & \dots & 0 \\ \vdots & \vdots & \ddots & \vdots \\ 0 & 0 & \dots & \sigma_e^{-1} \\ 0 & 0 & \dots & 0 \\ \vdots & \vdots & \ddots & \vdots \\ 0 & 0 & \dots & 0 \end{bmatrix} \tag{2.27}$$

the σ_i is the ith axial length of ellipsoid. Axises of the manipulability ellipsoid can be written as follows:

$$\begin{bmatrix} \sigma_1\vec{u}_1 & \sigma_2\vec{u}_2 & \dots & \sigma_e\vec{u}_e \end{bmatrix} \tag{2.28}$$

It gave all directions of movement realizable on end-effector and the level of difficulty to realize these movements in these directions of movement space.

2.5 Conclusion

In PMs, all movements of mechanism can be realized by controlling movements of active joints. This chapter distinguished DOFs of PMs, derived two the instantaneous kinematic relations applicable to all PMs, the one is from active joints to all joints and the other is from active joints to the end-effector. In final the manipulability of the PMs was given.

A significant fact about PMs is disclosed that manipulability of PMs can be changed by choosing different active joints. It made it possible to realize better movement control on the end-effector by selecting different active joints [28].

Chapter 3

Movements Accuracy Improvement of Parallel Mechanisms

3.1 Introduction

The chapter will discuss the movement accuracy improvement of PMs. Lots of sensors will be amounted to passive joints, the movement information of joints will be obtained and recognized. Usable information will be converted into real-time positions and velocities of driving joints, then they will be transfered to driving joints to realize desired movements of PMs. It can be seen as another redundancy, *Information Redundancy*. Error performances will vary with variety of the position of the end-effector and active joints with better or more accurate movement information can be found at any a given position.

3.2 Error Performance on End-effector of Different Active Joints and Evaluation

As well known, actuators can be allocated to any joints possible in PMs, but taking into account the good dynamic response and high-speed movements of the end-

effctor, they were usually fixed to those joints relatively near the base. In this study allocation of driving joints will not be changed, but accuracy of movement information will be promoted by using sensors of different active joints. Error performances on end-effector of different active joints will firstly be discussed.

3.2.1 Establishment of Error Models

Joint errors are transfered by links and joints along each kinematic chains in PMs. Regardless of manufacturing and assembly errors from links and joints, the transition matrix of actuator control errors will be same as the Jacobian from active joints to the end-effector. It can be derived in a variety of ways, here the algebraic method in chapter 2 will be used, and its derivation will be introduced in brief as follows.

Firstly all coordinate frames in PMs will be set along kinematic chains from the base to end-effector with the D-H coordinate method, the Jacobian of each kinematic chain will derived by referring to [25], the error formula of ith kinematic chain can be written as

$$\delta \mathscr{X}_e \;=\; J_i \, \delta \Theta_i, \tag{3.1}$$

where the symbol, $\delta \mathscr{X}_e = (\, \delta x_e,\, \delta y_e,\, \delta z_e,\, \delta \alpha_e,\, \delta \beta_e,\, \delta \gamma_e \,)^T$ is one error vector on the end-effector, and $\delta \Theta_i = (\, \delta \theta_{i1},\, \delta \theta_{i2},\, \cdots, \delta \theta_{in_i} \,)^T$ is joint error vector of the ith kinematic chain.

Error formulas from all kinematic chains,

$$\begin{aligned} \delta \mathscr{X}_e &= J_1 \, \delta \Theta_1 \\ &= J_2 \, \delta \Theta_2 \\ &= \quad \cdots \\ &= J_m \, \delta \Theta_m \end{aligned} \tag{3.2}$$

can be obtained.

It can be rewritten as

$$\delta\mathscr{X}_e = \begin{bmatrix} I_{6(3)} \\ I_{6(3)} \\ \vdots \\ I_{6(3)} \end{bmatrix}^{+} \begin{bmatrix} J_1 & 0 & 0 & \cdots & 0 \\ 0 & J_2 & 0 & \cdots & 0 \\ \vdots & \vdots & \vdots & \ddots & \vdots \\ 0 & 0 & 0 & \cdots & J_m \end{bmatrix} \delta\Theta, \tag{3.3}$$

where $\delta\Theta = \begin{bmatrix} \delta\Theta_1{}^T & \delta\Theta_2{}^T & \cdots & \delta\Theta_m{}^T \end{bmatrix}^T$.

From Eq.3.2, the next formula can be derived

$$\begin{bmatrix} J_1 & -J_2 & 0 & \cdots & 0 \\ J_1 & 0 & -J_3 & \cdots & 0 \\ \vdots & \vdots & \vdots & \ddots & \vdots \\ J_1 & 0 & 0 & \cdots & J_m \end{bmatrix} \begin{bmatrix} \delta\Theta_1 \\ \delta\Theta_2 \\ \vdots \\ \delta\Theta_m \end{bmatrix} = A\,\delta\Theta = \mathbf{0}. \tag{3.4}$$

Using a pair of selection matrices, ϕ_a and ϕ_p, to PMs, the joint error vector will be divided into two parts, $\delta\Theta_a$ from active joints and $\delta\Theta_p$ from passive joints,

$$\begin{aligned} \delta\Theta &= I_N\ \delta\Theta \\ &= \phi_a\ \delta\Theta_a\ +\ \phi_p\ \delta\Theta_p \\ &= \begin{bmatrix} \phi_a & \phi_p \end{bmatrix} \begin{bmatrix} \delta\Theta_a \\ \delta\Theta_p \end{bmatrix}. \end{aligned} \tag{3.5}$$

From Eq.3.4 and 3.5, error projections on passive joints of active joints can be gotten,

$$\delta\Theta_p = -(A\phi_p)^{+} A\phi_a\,\delta\Theta_a. \tag{3.6}$$

From Eq.3.5 and 3.6, the error formula from active joints to all joints can be obtained,

$$\delta\Theta = \left[\phi_a - \phi_p(A\phi_p)^{+}A\phi_a\right]\ \delta\Theta_a = A_\Phi\,\delta\Theta_a. \tag{3.7}$$

A_Φ is error transition matrix from active joints to all joints, error performances on the driving joints of active joints can be discussed by this matrix.

Finally substituting Eq.3.7 to Eq.3.3, the error model from active joints to the end-effector will be obtained,

$$\begin{aligned}\delta \mathscr{X}_e &= \begin{bmatrix} I_{6(3)} \\ I_{6(3)} \\ \vdots \\ I_{6(3)} \end{bmatrix}^{+} \begin{bmatrix} J_1 & 0 & 0 & \cdots & 0 \\ 0 & J_2 & 0 & \cdots & 0 \\ \vdots & \vdots & \vdots & \ddots & \vdots \\ 0 & 0 & 0 & \cdots & J_m \end{bmatrix} A_\Phi \, \delta\Theta_a \\ &= J_a \, \delta\Theta_a. \end{aligned} \tag{3.8}$$

Error model from active joints to the end-effector has been built, it will be used to analyze error performances of different active joints.

3.2.2 Error Performances on the End-effector from Different Active Joints

The discussion will be begun from a 1-DOF PM, it is shown in Fig.3.1 and can produce one movement along the rod. Before this discussion, **Hypothesis** *I* in this thesis will be firstly given, that is all senors used in the discussion are assumed at the same level of accuracy.

Because any one of joints can be used as active joints, the joint 1, 2 and 3 will be respectively selected to study. Setting coordinate frames as shown in Fig.3.1, Jacobians from the 1st and 2nd kinematic chain can be respectively given as follows,

$$J_1 = \begin{bmatrix} -\sin(\theta_1) l_1 - \sin(\theta_1+\theta_2) l_2 & -\sin(\theta_1+\theta_2) l_2 & 0 \\ \cos(\theta_1) l_1 + \cos(\theta_1+\theta_2) l_2 & \cos(\theta_1+\theta_2) l_2 & 0 \\ 1 & 1 & 1 \end{bmatrix} \tag{3.9}$$

$$J_2 = \begin{bmatrix} 1 & 0 & 0 \end{bmatrix}^T. \tag{3.10}$$

If joint 1 is selected as active joints, error transition matrix from the joint 1 to all the joints can be gotten from Eq.3.7,

$$A_{\Phi} = \begin{bmatrix} 1 \\ -1 - l_1 \cos(\theta_1) \sec(\theta_1 + \theta_2) / l_2 \\ l_1 \cos(\theta_1) \sec(\theta_1 + \theta_2) / l_2 \\ l_1 \sec(\theta_1 + \theta_2) \sin(\theta_2) \end{bmatrix}. \tag{3.11}$$

Using Eq.3.8, the error formula from the joint 1 to the end-effector,

$$\delta \mathscr{X}_e = \begin{bmatrix} l_1 \sec(\theta_1 + \theta_2) \sin(\theta_2) & 0 & 0 \end{bmatrix}^T \delta\theta_1, \tag{3.12}$$

can be obtained

In the same way, error transition matrices and error formulas of all other active

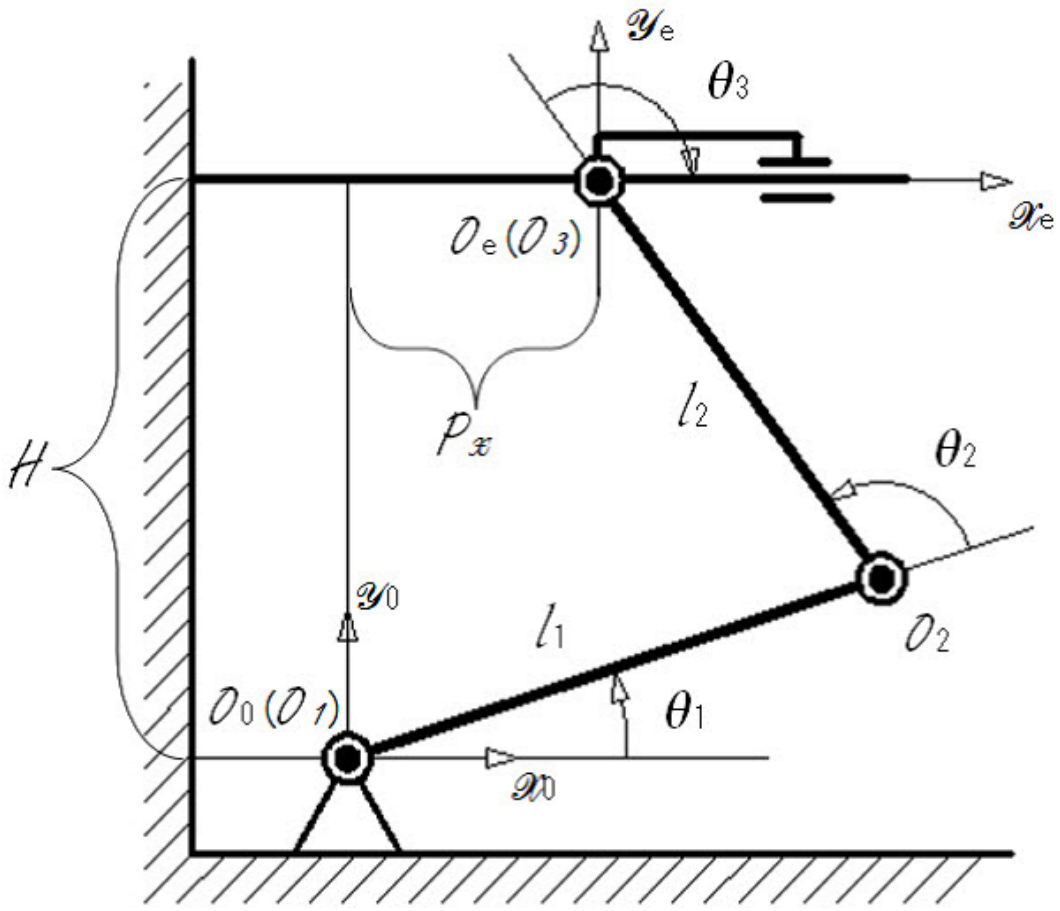

Fig. 3.1: A 1-DOF PM of type 3RRR-P

joints can be also obtained. Here error formulas of joint 2 and 3 are given respectively as follows,

$$\delta\mathscr{X}_e = \begin{bmatrix} \dfrac{-l_1 l_2 \sin(\theta_2)}{l_1\cos(\theta_1)+l_2\cos(\theta_1+\theta_2)} & 0 & 0 \end{bmatrix}^T \delta\theta_2 \tag{3.13}$$

$$\delta\mathscr{X}_e = \begin{bmatrix} l_2\sec(\theta_1)\sin(\theta_2) & 0 & 0 \end{bmatrix}^T \delta\theta_3. \tag{3.14}$$

Setting the margin of the joint error as $|\delta\theta_i| <= 0.001$, denoting $l_1 = 140$ [mm]、$l_2 = 120$ [mm] and $H = 140$ [mm], when the end-effector locates at $P_x = 50\sqrt{3}/2$ [mm], errors on the end-effector of different active joints can be calculated by Eq.3.12 $\sim$ 3.14 and listed at table 3.1.

Table 3.1: Errors from different active joints for the PM in Fig.3.1

Active Joint	θ_1	θ_2	θ_3
Error $\left(_{\lvert\delta\mathscr{X}_e\rvert}\right)$	$\leqslant 0.1936$	$\leqslant 0.5391$	$\leqslant 0.1424$

Obviously errors are different when different active joints are selected at a certain position.

Referring to Fig.3.2, Errors from different active joints also vary with the variety of end-effector's position in the workspace, error difference is very enormous at some regions. At any position, joints with the more accurate movement information can be found by evaluating their error performances on the end-effector.

3.2.3 Error Ellipsoid and Evaluation Functions

It is easy to find joints with the more accurate movement information for 1-DOF PM and only need to compare magnitudes of errors on the end-effector of different joints. For a multi-DOF PM, it will be difficult because error owns both magnitudes

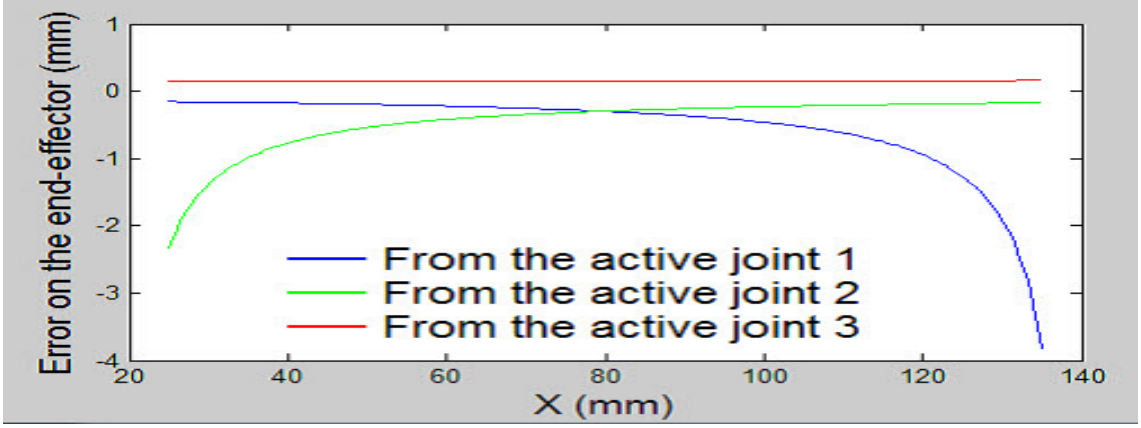

Fig. 3.2: Varieties of errors in workspace for the PM in Fig.3.1

and directions on the end-effector. A often used way is to evaluate error performances on the end-effector of different active joints by their error ellipsoids.

If the error margin of each joint is limited, errors on the end-effector can only emerge in a certain region in the movement space of the end-effector. The region can be called as the *error region of the end-effector*, and the region formed by joint errors in the joint movement space can be named as the *error region of joints*. When joint errors from active joints is defined in one spheroid, errors on the end-effector will be limited in one error ellipsoid in the movement space of end-effector.

Error ellipsoid can be built by Eq.3.8. Before beginning to build, the normalization to $\delta\Theta_a$ and $\delta\mathscr{X}_e$ is needed. Assuming normalized errors are respectively $\delta\hat{\mathscr{X}}_e$ and $\delta\hat{\Theta}_a$, from Eq.3.8, the normalized error transformation equation can be rewritten as

$$\delta\hat{\mathscr{X}}_e = \hat{J}_a\,\delta\hat{\Theta}_a. \tag{3.15}$$

Similarly to manipulability ellipsoid, if errors of active joints are set as

$$\delta\hat{\Theta}_a^T\,\delta\hat{\Theta}_a \leq 1,$$

the error ellipsoid can be written as

$$(\delta\hat{\mathscr{X}}_e)^T(\hat{J}_a^+)^T\hat{J}_a^+\,\delta\hat{\mathscr{X}}_e \leq 1. \tag{3.16}$$

Making a singular value decomposition to $\hat{J}_a^+$, two orthogonal matrices U, V and all singular values can be obtained.

$$\hat{J}_a^+ = V\Sigma^+ U^T, \tag{3.17}$$

From Eq.3.16 and 3.17, the error ellipsoid can be rewritten as

$$(U^T\delta\hat{\mathscr{X}}_e)^T\mathscr{D}iag(\sigma_1^{-2},\sigma_2^{-2}\cdots\sigma_{n_a}^{-2})U^T\delta\hat{\mathscr{X}}_e \leq 1. \tag{3.18}$$

The singular value σ_i denotes magnitudes of errors along different directions defined by the matrix U.

From the error transition matrix, $\hat{J}_a$, three evaluation functions, also called as Error Amplification Factors (EAF), can be obtained [27]

$$EAF_1 = \prod_{i=1}^{n_a}\sigma_i \tag{3.19}$$

$$EAF_2 = \mathscr{M}ax(\sigma_1,\sigma_2\cdots\sigma_{n_a}) \tag{3.20}$$

$$EAF_3 = \mathscr{M}ax(\sigma_1,\sigma_2\cdots\sigma_{n_a})/\mathscr{M}in(\sigma_1,\sigma_2\cdots\sigma_{n_a}) \tag{3.21}$$

Three EAFs defined receptively the volume of the error ellipsoid, the maximum singular value and the condition number. The smaller EAF means the smaller error on the end-effector. Therefore, Any one of them can be used as a criterion to measure the accuracy. One example will be used to explain how to evaluate error performances of different active joints by EAFs.

A 2-DOF planar PM with 5 revolute joints is shown in Fig.3.3. It has two kinematic chains from the base to the end-effector and two joints will be needed to realize movements of the end-effector. Because any two of all joints can be assigned as active joints, 10 pairs of active joints can be applied.

Error models from different active joints will be built by Eq.3.1$\sim$3.8. Jacobians from two kinematic chains

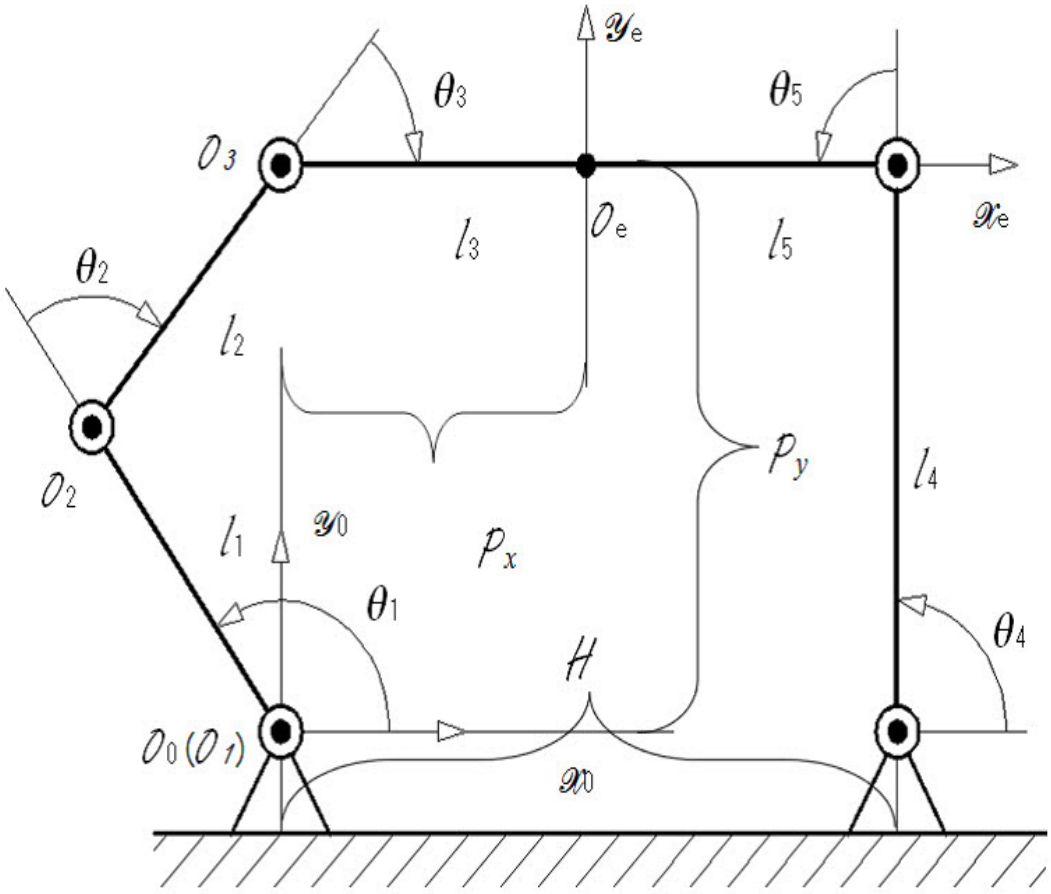

Fig. 3.3: A 2-DOF planar PM of type RRR-RR

$$J_1 = \begin{bmatrix} -l_1\mathrm{S}_1 - l_2\mathrm{S}_{12} - l_3\mathrm{S}_{123} & -l_2\mathrm{S}_{12} - l_3\mathrm{S}_{123} & -l_3\mathrm{S}_{123} \\ l_1\mathrm{C}_1 + l_2\mathrm{C}_{12} + l_3\mathrm{C}_{123} & l_2\mathrm{C}_{12} + l_3\mathrm{C}_{123} & l_3\mathrm{C}_{123} \\ 1 & 1 & 1 \end{bmatrix} \tag{3.22}$$

$$J_2 = \begin{bmatrix} -l_4\mathrm{S}_4 - l_5\mathrm{S}_{45} & -l_5\mathrm{S}_{45} \\ l_4\mathrm{C}_4 + l_5\mathrm{C}_{45} & l_5\mathrm{C}_{45} \\ 1 & 1 \end{bmatrix} \tag{3.23}$$

can be derived. Here the symbol “S” and “C” respectively represent the “sin” and “cos” function, for example, the “S_{12-3}” means as “$\sin(\theta_1 + \theta_2 - \theta_3)$”.

If joint 1, 4 are selected as active joints, the error transition matrix from active joints to all joints

$$A_\Phi = \begin{bmatrix} 1 & 0 \\ A_\Phi(2,1) & A_\Phi(2,2) \\ A_\Phi(3,1) & A_\Phi(3,2) \\ 0 & 1 \\ A_\Phi(5,1) & A_\Phi(5,2) \end{bmatrix} \tag{3.24}$$

$$A_\Phi(2,1) = -\frac{l_1 l_3 S_{23} + l_1 l_5 S_{1-4-5} + l_2 l_3 S_3 + l_2 l_5 S_{12-4-5}}{l_2 l_3 S_3 + l_5 l_2 S_{12-4-5}}$$

$$A_\Phi(2,2) = \frac{l_3 l_4 S_{123-4} - l_4 l_5 S_5}{l_2 l_3 S_3 + l_2 l_5 S_{12-4-5}}$$

$$A_\Phi(3,1) = \frac{l_1 l_2 S_2 + l_1 l_3 S_{23} + l_1 l_5 S_{1-4-5}}{l_2 l_3 S_3 + l_2 l_5 S_{12-4-5}}$$

$$A_\Phi(3,2) = -\frac{l_2 l_4 S_{12-4} + l_3 l_4 S_{123-4} - l_4 l_5 S_5}{l_2 S_3 l_3 + l_2 l_5 S_{12-4-5}}$$

$$A_\Phi(5,1) = \frac{l_1 S_2}{l_3 S_3 + l_5 S_{12-4-5}}$$

$$A_\Phi(5,2) = -\frac{l_3 S_3 + l_4 S_{12-4} + l_5 S_{12-4-5}}{l_3 S_3 + l_5 S_{12-4-5}}$$

and the error transition matrix from active joints to the end-effector can be obtained.

$$J_a = \begin{bmatrix} -\dfrac{l_1 l_5 S_2 S_{45}}{l_3 S_3 + l_5 S_{12-4-5}} & \dfrac{-l_3 l_4 S_3 S_4 + l_4 l_5 S_{12} S_5}{l_3 S_3 + l_5 S_{12-4-5}} \\ \dfrac{l_1 l_5 C_{45} S_2}{l_3 S_3 + l_5 S_{12-4-5}} & \dfrac{l_3 l_4 C_4 S_3 - l_4 l_5 C_{12} S_5}{l_3 S_3 + l_5 S_{12-4-5}} \\ \dfrac{l_1 S_2}{l_3 S_3 + l_5 S_{12-4-5}} & -\dfrac{l_4 S_{12-4}}{l_3 S_3 + l_5 S_{12-4-5}} \end{bmatrix} \tag{3.25}$$

Error transition matrices of other active joints can be also derived in the same way.

Setting the margin of joint error as $|\delta\theta_i| <= 0.001$ and denoting $l_1 = l_2 = l_3 = l_5 = 75$ [mm], $l_4 = 75\sqrt{3}$ [mm] and $H = 150$ [mm], when the end-effector locates at

the position, $P_x = 75$ [mm] and $P_y = 75\sqrt{3}$ [mm], all EAFs and maximum errors on the end-effector from different active joints can be calculated and active joints with best error performances can be selected. They are listed at table 3.2.

Table 3.2: EAFs and selections of active joints for the PM in Fig.3.3

Active Joint	EAF_1	EAF_2	EAF_3
1 & 2	3247.60	107.657	3.5688
1 & 3	1948.56	58.0948	1.7321
1 & 4	9742.79	206.836	4.3911
1 & 5	3247.60	67.5591	1.4054
2 & 3	2435.70	91.8559	3.4641
2 & 4	4871.39	135.638	3.7767
2 & 5	3247.60	97.5539	2.9304
3 & 4	4871.39	135.638	3.7767
3 & 5	9742.79	307.607	9.7120
4 & 5	9742.79	155.573	2.4842
Selected Joint	1 & 3	1 & 3	1 & 5

Adjusting the order of items in table 3.2 in accordance with evaluation function values, a new table can be gotten.

Table 3.3: Adjusting the order of items in table 3.2 in accordance with EAFs

EAF_1	1948.56	2435.70	3247.60	3247.60	3247.60	4871.39	4871.39	9742.79	9742.79	9742.79
Active Joint	1&3	2&3	1&5	2&5	1&2	2&4	3&4	4&5	1&4	3&5
EAF_2	58.0948	67.5591	91.8559	97.5539	107.657	135.638	135.638	155.573	206.836	307.607
Active Joint	1&3	1&5	2&3	2&5	1&2	2&4	3&4	4&5	1&4	3&5
EAF_1	1.4054	1.7321	2.4842	2.9304	3.4641	3.5688	3.7767	3.7767	4.3911	9.7120
Active Joint	1&5	1&3	4&5	2&5	2&3	1&2	2&4	3&4	1&4	3&5

As is seen from Table 3.2 and 3.3, active joints with the smallest EAF can be

found, however active joints found by different EAFs are not same and several different active joints own the same value of evaluation function in some EAFs.

3.2.4 Comparison Method of Error Ellipsoids (CMEE)

Evaluation of error performances from different active joints can be also done by directly comparing their error ellipsoids on the end-effector. If the error ellipsoid of a set of active joints is embodied wholly by the one of other sets, this set of active joints will own better error performance on the end-effector.

Selecting active joints 1,3 and 4,5 in the PM of Fig.3.3, their error ellipsoids and the comparison of error ellipsoids can be given in Fig.3.4. The condition above is one very strict, and can not be met in many cases.

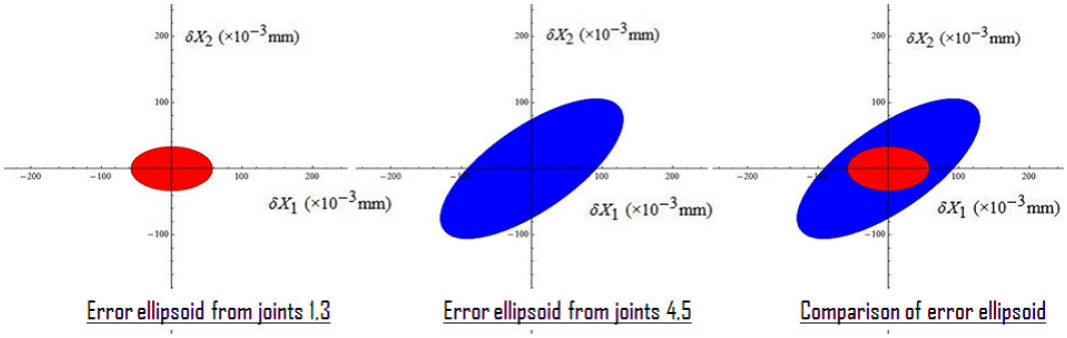

Fig. 3.4: Error ellipsoid and new ellipsoid after transformation

Some inclusions between error ellipsoids are extremely subtle and hardly to be distinguished. To be easily observed or compared by computer, coordinate conversion can be used to error ellipsoids, which is firstly to transform a error ellipsoid into one spheroid by coordinate transformation, then to apply the matrix transformation to other error ellipsoids and obtain new ellipsoids for comparisons.

With reference to Eq.3.16 and 3.17, the error ellipsoid of any active joints can be written as

$$(\delta\hat{\mathscr{X}}_e)^T(\hat{J}_i^+)^T\hat{J}_i^+\delta\hat{\mathscr{X}}_e = (\Sigma_i^+U_i^T\delta\hat{\mathscr{X}}_e)^T\Sigma_i^+U_i^T\delta\hat{\mathscr{X}}_e \leq 1 \tag{3.26}$$

Setting a new coordinate frame $\Sigma_{\mathscr{W}}$, and the mapping relation of displacements

between two coordinates

$$\delta \mathscr{W} = \Sigma_i^{+} U_i^T \delta \hat{\mathscr{X}}_e, \tag{3.27}$$

the error ellipsoid in Eq.3.26 will be transformed into one spheroid,

$$\delta \mathscr{W}^T \delta \mathscr{W} \leq 1. \tag{3.28}$$

Applying the transformation to the other error ellipsoid, a new error ellipsoid

$$\delta \mathscr{W}^T (\hat{J}_a^{+} U_i \Sigma_i)^T \hat{J}_a^{+} U_i \Sigma_i \delta \mathscr{W} \leq 1. \tag{3.29}$$

can be gotten in the coordinate frame $\Sigma_{\mathscr{W}}$.

Comparisons of error ellipsoids between active joints to driving joints in the PM of Fig.3.3 have been made and are listed at Fig.3.5∼Fig3.13 .

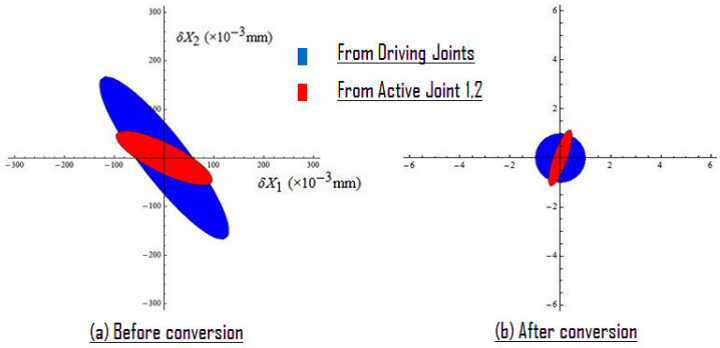

Fig. 3.5: Comparison error ellipsoids for active joints 1,2

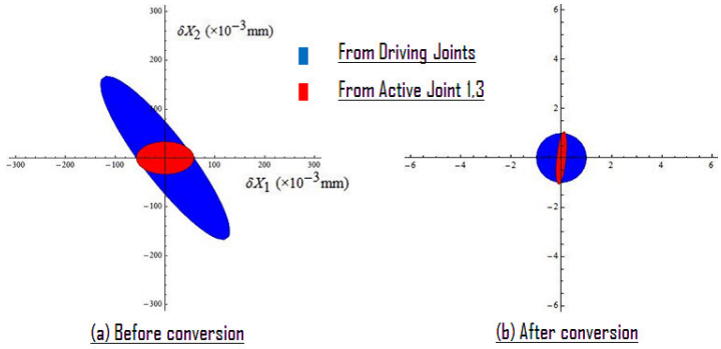

Fig. 3.6: Comparison error ellipsoids for active joints 1,3

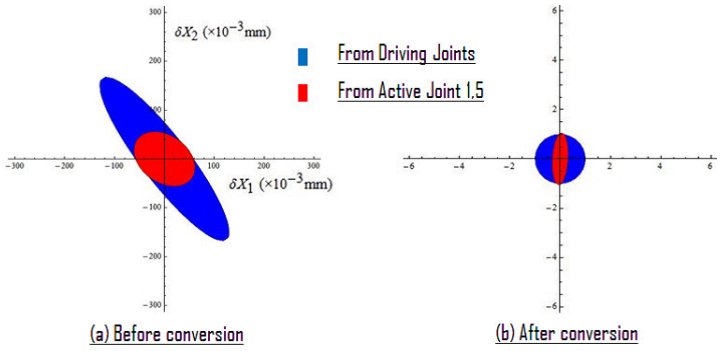

Fig. 3.7: Comparison error ellipsoids for active joints 1,5

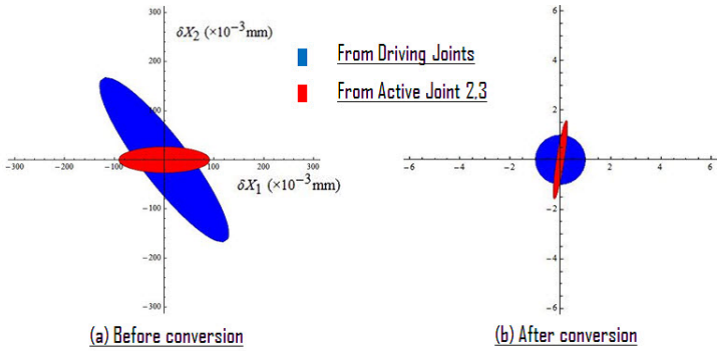

Fig. 3.8: Comparison error ellipsoids for active joints 2,3

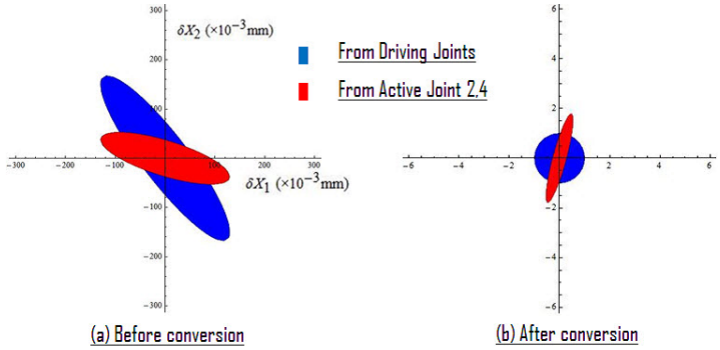

Fig. 3.9: Comparison error ellipsoids for active joints 2,4

None of error ellipsoids is included by the one of driving joints. It means error regions of all other active joints have transcended the boundary of the error ellipsoid of driving joints.

In fact a allowable error is often given, it can be described as a spheroid (or a ellipsoid if accuracy requirements in directions are different) and called as *allowable error spheroid* (or *allowable error ellipsoid*) in the movement space of the end-

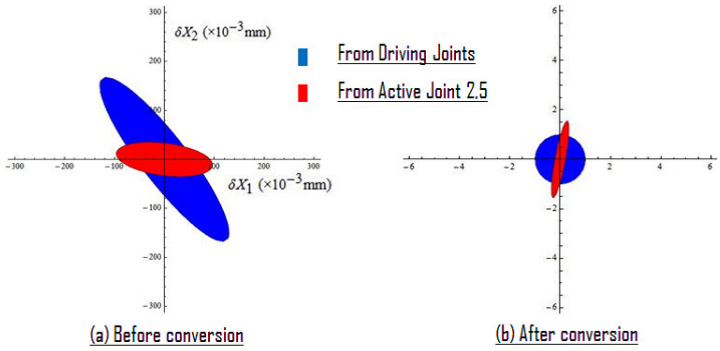

Fig. 3.10: Comparison error ellipsoids for active joints 2,5

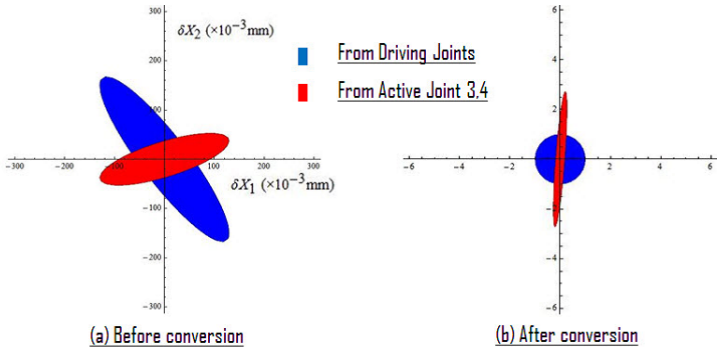

Fig. 3.11: Comparison error ellipsoids for active joints 3,4

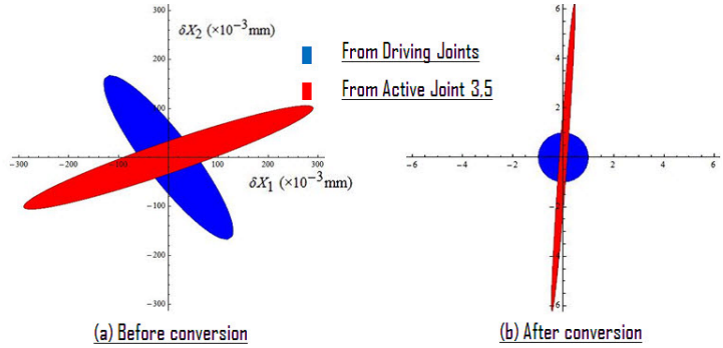

Fig. 3.12: Comparison error ellipsoids for active joints 3,5

effector.

Inclusions of two error ellipsoids can be divided into two cases, which is to be holden wholly or not. As mentioned above, the evaluation of error performances from different active joints is intend to find active joints with better accuracy than driving joints, so comparison of error ellipsoids should be done between driving joints and active joints.

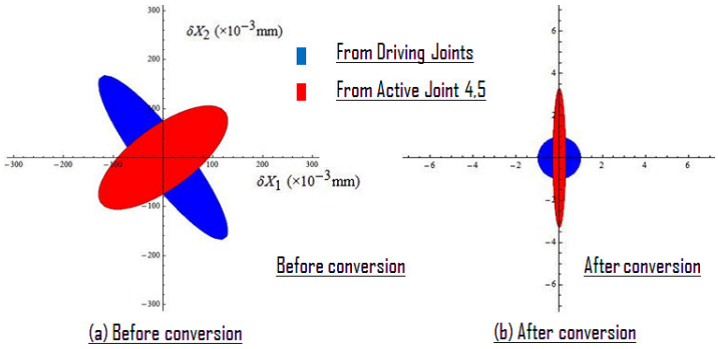

Fig. 3.13: Comparison error ellipsoids for active joints 4,5

Taking into account allowable error spheroid, inclusions will be distinguished into three cases if other two cases, which error ellipsoids are included entirely by allowable error spheroid or allowable error spheroid are holden fully by all error ellipsoids, are disregarded,

1. the error ellipsoid is embodied wholly by the one of driving joints and allowable error spheroid.

2. the error ellipsoid is include partly by the one of driving joints and holden wholly by the allowable error spheroid.

3. the error ellipsoid transcended boundaries of the one of driving joints and allowable error spheroid

Setting the allowable error, $|error_{allow}| <= 0.1$, comparisons of error ellipsoids from different active joints with driving joints have been made and results will be shown in Fig.3.14. Case 1 does not emerge, Case 2 appears in Fig.(b), (c), (d) and (f), Case 3 is shown in Fig.(a), (e), (g), (h) and (i).

Error ellipsoids of active joints 1,3, 1,5, 2,3 and 2,5 are wholly embodied by allowable error spheroid, hence errors from them are less than the allowable error, they are considered with better error performances than driving joints in most regions and meet the accuracy requirement.

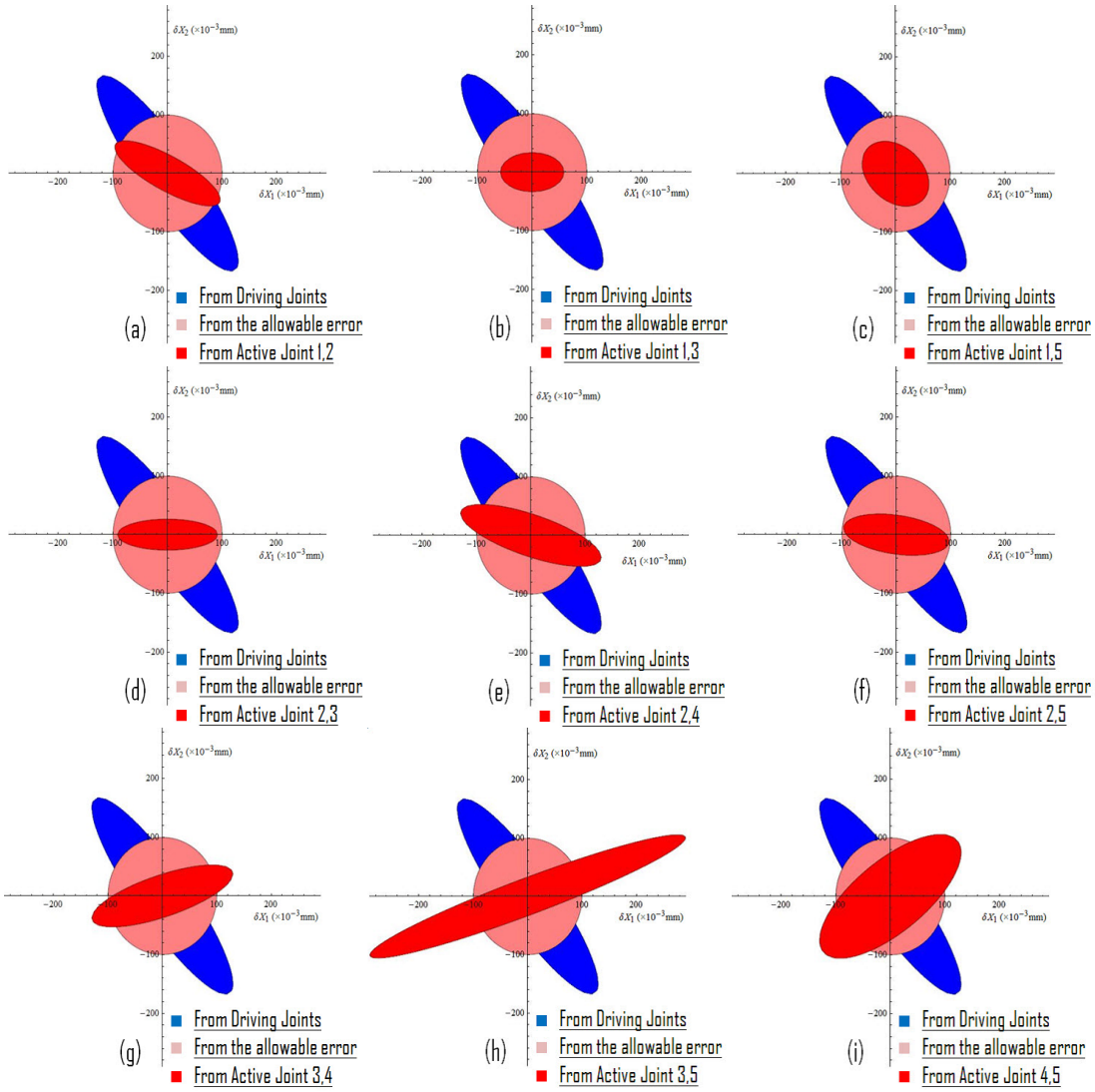

Fig. 3.14: Comparison of ellipsoids

3.2.5 Comparison Method of Error Polyhedrons (CMEP)

When all joints are set at the same accuracy level, the error region of active joints can be described as a hypercube in joint movement space. If the hypercube is projected into the movement space of end-effector, the error region of the will be formed on the end-effector and it will be a polyhedron with consideration of the PM with redundancy.

Error mapping relations from the diving joints 1,4 to the end-effector is shown in Fig.3.15, some correspondences can be seen.

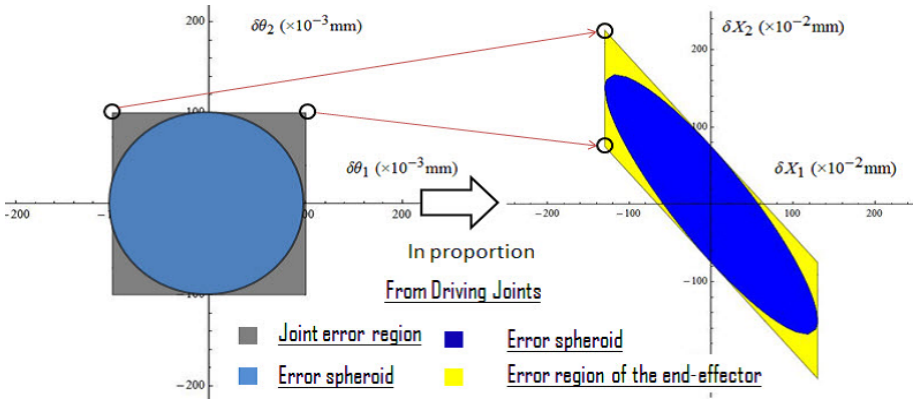

Fig. 3.15: Joint error region and error region of the end-effector

Error evaluations can be done by error polyhedrons of different active joints. Error ellipsoids and error polyhedrons from all other active joints of the PM shown in Fig.3.3 have been drawn and shown in Fig.3.16.

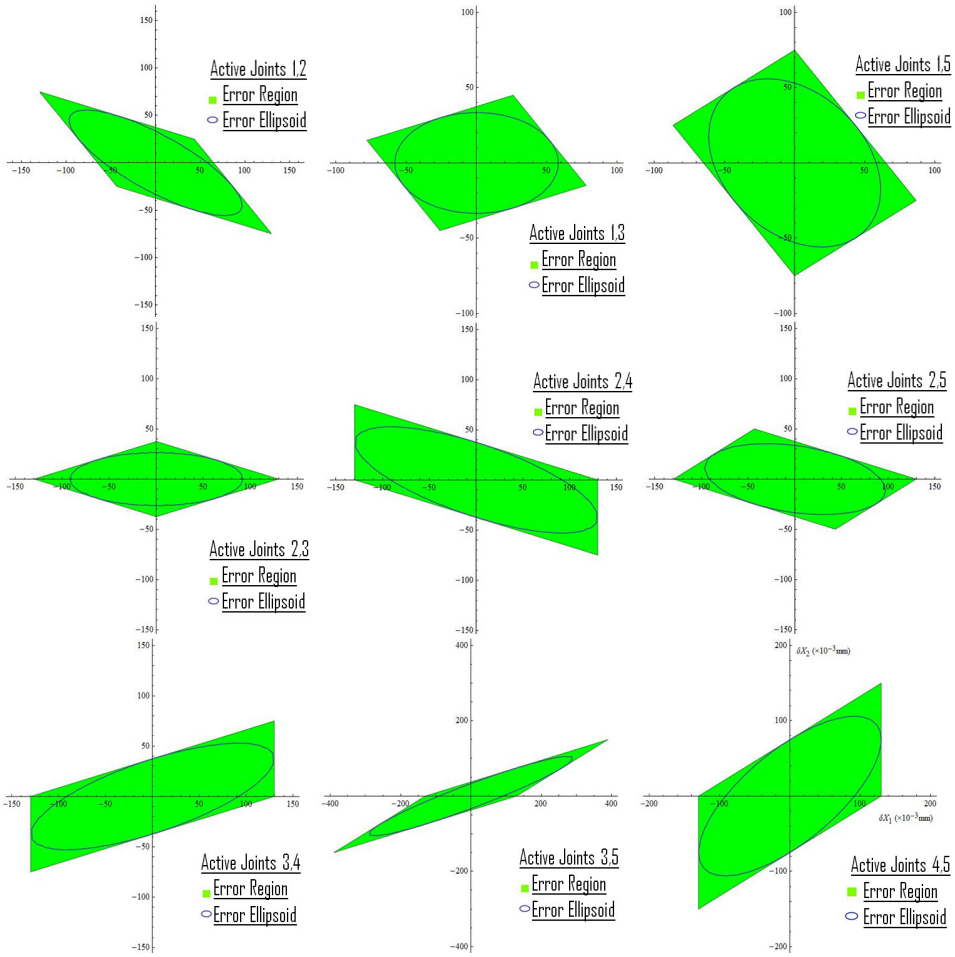

Fig. 3.16: Error ellipsoids and error polyhedrons

From Fig.3.16, it can be well known that error ellipsoids are wholly included by error polyhedrons, and they can be determined from given error polyhedrons, conversely error polyhedrons can not be decided by error ellipsoids.

Vertexes of the polyhedron are from projections of vertexes from the hypercube, and the maximum error on the end-effector can be directly calculated by Eq.3.8. So a evaluation of error performance can be done by comparing maximum errors at vertexes of polyhedrons instead of EAF2.

Evaluations of error performances can also be done from comparisons of error polyhedrons. When the error polyhedron on the end-effector of a set of active joints is embodied wholly by the one of driving joints, its error performances on the end-effector will be better than driving joints. all comparisons of error polyhedrons have been done and shown in Fig.3.17.

From Fig.3.17, it can be known that error polyhedrons of active joints 1,2, 1,3 and 1,5 are holden totally and they can be considered with better error performances on the end-effector.

3.3 Accuracy Improvement of Parallel Mechanisms Using the Information of Passive Joints

In Section 3.2, error performances on the end-effector of different active joints were discussed, some evaluation methods have been presented. Some active joints with better error performances or more accurate movement information can be found by these methods. In this section it will be discussed how to used these joints to improve the movement accuracy of PMs.

A direct way is to allocate actuators and sensors to all joints, then move joints with better error performances by switching control in different work area to realize

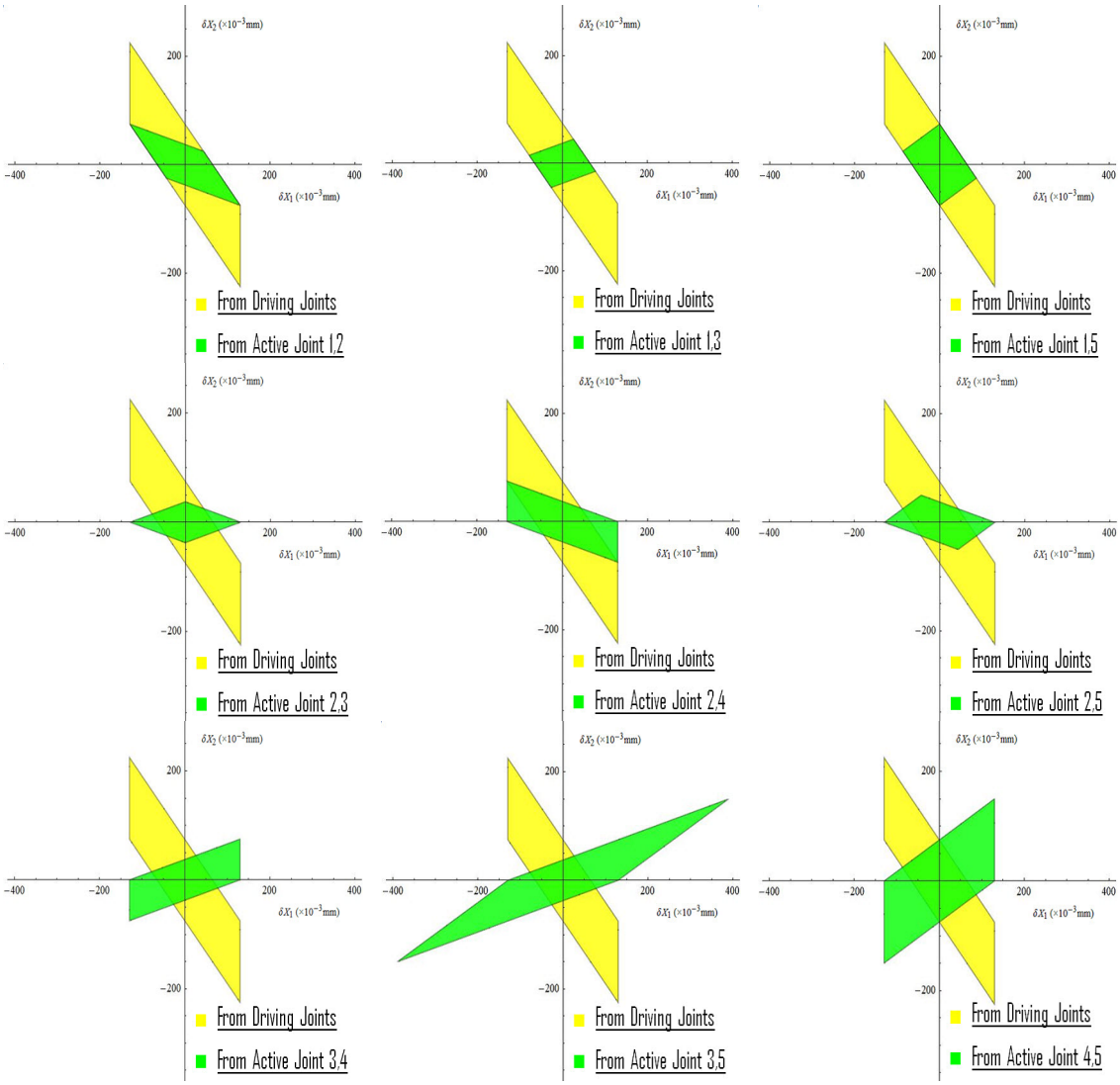

Fig. 3.17: Comparisons of error polyhedrons

movements of end-effector. But the redundant weight will affect the rapid movement of PMs, and the cost will also rise with usage of more actuators and components.

A more realistic idea is to only equip sensors to passive joints without any other modifications, then obtain and discriminate their movement information, convert and transfer good movement information to driving joints to realize movements.

Firstly error causes and transmission will be discussed. The other *hypothesis II* in this thesis will be given, that is movement accuracies of actuators are higher than sensors. It means that the impact on accuracy of the actuator will be ignored.

3.3.1 Error Causes and Transmissions

The joint error is caused by the precision of the sensor. If the accuracy of the sensor is set at Δ, the error of any joint i, δ_i, can be defined as

$$\delta\theta_i = \Delta\theta_i - [\frac{\Delta\theta_i}{\Delta}]\Delta \tag{3.30}$$

the symbol, [ ], represents the round function. If the precision of the sensor approaches infinity, $\Delta \to 0$, its measured result will is close to the true value,

$$[\frac{\Delta\theta_i}{\Delta}]\Delta \to \Delta\theta_i$$

and the joint error will be near to zero, $\delta\theta_i \to 0$.

Movement errors of the end-effector are resulted from errors of driving joints, can be written as

$$\delta\mathscr{X}_e = J_d\delta\Theta_d \tag{3.31}$$

where J_d is the Jacobian of driving joints and $\delta\Theta_d$ is a vector comprises of joint errors from driving joints.

If the projection on active joints j of joint errors from driving joints is set as $\Delta\Theta_j$, the equation

$$\delta\mathscr{X}_e = J_d A_j \Delta\Theta_j \tag{3.32}$$

can be obtained from Eq.3.7, where the symbol, A_j, is the corresponding sub-matrix extracted from the matrix $A_{\Phi j}$.

From Eq.3.30, one joint error vector caused by accuracies of sensors,

$$\delta\Theta_j = \Delta\Theta_j - [[\frac{\Delta\theta_j}{\Delta}]\Delta] \tag{3.33}$$

can be obtained, where $[[\frac{\Delta\theta_j}{\Delta}]\Delta]$ is one vector from measured values of sensors.

Measured values of sensors will be transfered to driving joints as error compensations,

$$\delta_{cj} = -A_j[[\frac{\Delta\theta_j}{\Delta}]\Delta] \tag{3.34}$$

Displacements of the end-effector which result from error compensations of driving joints can be written as

$$\Delta_{cj} = -J_d A_j[[\frac{\Delta\theta_j}{\Delta}]\Delta] \tag{3.35}$$

Rest errors on the end-effector after the compensation,

$$\begin{aligned} \Delta_{rj} &= \delta X_e - J_d A_j[[\tfrac{\Delta\theta_j}{\Delta}]\Delta] \\ &= \delta X_e - J_d A_j \Delta\Theta_j + J_d A_j \delta\Theta_j \\ &= J_d A_j \delta\Theta_j \\ &= J_j \delta\Theta_j \end{aligned} \tag{3.36}$$

can be obtained, it is equal to errors on the end-effector of active joints j and can also be seen as projections on the end-effector of joint error from active joints j.

Due to accuracies of joints, rest errors will persist after error compensations are made. From Eq.3.36, the error vector, δ_d,

$$\delta_d = A_j \delta\Theta_j \tag{3.37}$$

can be obtained. It is comprised of projections on driving joints of joint errors from active joints and different from $\delta\Theta_d$ above.

Derivations above have given error causes and shown their transmission, and the relation between joint errors and accuracies has been built. In fact, Error performances, ellipsoids, error regions and error polyhedrons can be also discussed or explained from the accuracy point of view. As well known, the equation

$$\delta\hat{\Theta}_j^T \delta\hat{\Theta}_j \leq 1 \tag{3.38}$$

represents one spheroid (or ellipsoid) in joint movement space. It can be called as the error region of active joints, the projection of it on the movement space of the end-effector is the error ellipsoid.

If the sphere,

$$\delta\hat{\Theta}_j^T \delta\hat{\Theta}_j = 1 \tag{3.39}$$

is looked as the boundary that the precision of sensors on active joints can reach and named as *accuracy sphere* of active joints, it will divide the movement space of active joints into two parts, the interior and exterior of the sphere. Its interior is the region where errors can not be measured, so they will not be detected by sensors when errors on the end-effector are projected into the region.

The error ellipsoid and sphere above can be also defined from Eq.3.33 respectively as

$$\| \Delta\Theta_j - [[\frac{\Delta\theta_j}{\Delta}]\Delta] \| \leq 1 \tag{3.40}$$

and

$$\| \Delta\Theta_j - [[\frac{\Delta\theta_j}{\Delta}]\Delta] \| = 1 \tag{3.41}$$

From Eq.3.36, 3.40, the rest error ellipsoid

$$(\Delta_{rj})^T (J_i^+)^T J_i^+ \Delta_{rj} \leq 1 \tag{3.42}$$

can be obtained. From Eq.3.41, the projection on the end-effector of *accuracy sphere* from active joints can be written as,

$$(\Delta_{rj})^T (J_i^+)^T J_i^+ \Delta_{rj} = 1. \tag{3.43}$$

The projection of the accuracy sphere on the end-effector will be the surface of the error ellipsoid. It also divides the movement space of the end-effector into two parts,

errors within the surface will be projected onto the interior of the accuracy sphere and errors without the surface will be projected onto the exterior. Only errors outside error ellipsoid can be measured by sensors of active joints. So the relation between accuracies of sensors and error ellipsoids have been built.

When two error ellipsoids are compared, the movement space of the end-effector can be distinguished into several regions shown in Fig.3.15.

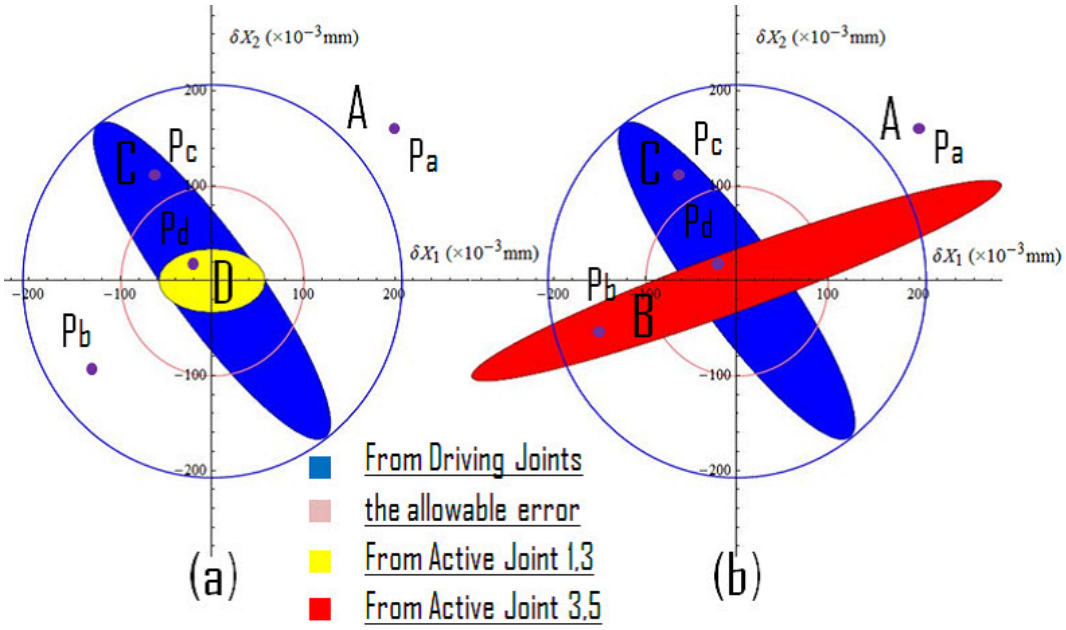

Fig. 3.18: Different region in the error region of the end-effector

Setting a few positions in region A, B, C and D, projections on several different active joints can be gotten and listed at table 3.4.

From Fig.3.15 and table 3.4, position P_a in region A is without all error ellipsoids, so its errors can be captured by sensors of all active joints, P_b in region B is inside the error ellipsoid of active joints 3,5 and outside the one of driving joints, so its errors can be detected by sensors of driving joints but can not be done by sensors of active joints 3,5. Contrarily P_c in region C is included by the error ellipsoid of driving joints and outside active joints 3,5, so its errors can be detected by sensors of active joints 3,5 but can not be done by sensors of driving joints. P_d in region D is within all error ellipsoids, so its errors can not be measured by sensor of any active joints.

Table 3.4: Projections on different active joints from errors of the end-effector

Position	δx,δy	Active Joints		Active Joints		Active Joints	
	($\times 10^{-3}$mm)	1	4	1	3	3	5
P_a	200,170	-0.005 (-0.005346)	-0.001 (-0.001540)	-0.005 (-0.005346)	-0.002 (-0.002994)	-0.002 (-0.002994)	0 (-0.000727)
P_b	-150,-60	0.003 (0.003110)	0.001 (0.001155)	0.003 (0.003110)	0 (0.000445)	0 (0.000445)	0 (-0.000355)
P_c	-80,110	0 (-0.000235)	0 (0.000616)	0 (-0.000235)	-0.003 (-0.003550)	-0.003 (-0.003550)	-0.002 (-0.002083)
P_d	-60,40	0 (0.000041)	0 (0.000154)	0 (0.000041)	0 (-0.000687)	0 (-0.000687)	0 (-0.000421)

It needs to be noted that round-down function has been used in calculations in table 3.4, if round function is used, some reactions of errors on sensors will need to be ignored because they are on the accuracy sphere, and errors maybe come from the interior of the ellipsoids.

3.3.2 Two Ways to Improve Movement Accuracy of Parallel Mechanisms

Active joints that present accurate movement information to driving joints are called as *Sensing Joints*. Errors measured by sensors of sensing joints will be converted, then transfered to driving joints as error compensations to modify movements of driving joints. Movement information can be provided by one set or several sets of sensing joints. It can be also seen as two ways to improve movement accuracy of PMs.

$\mathscr{W}_1$ is to use active joints with the best error performance on the end-effector as sensing joints, obtain their joint errors measured by sensors, convert and transfer joint errors to driving joints to modify movements of the end-effector. It is shown in Fig.3.19.

From Eq.3.34, the compensation equation from sensing joints to driving joints

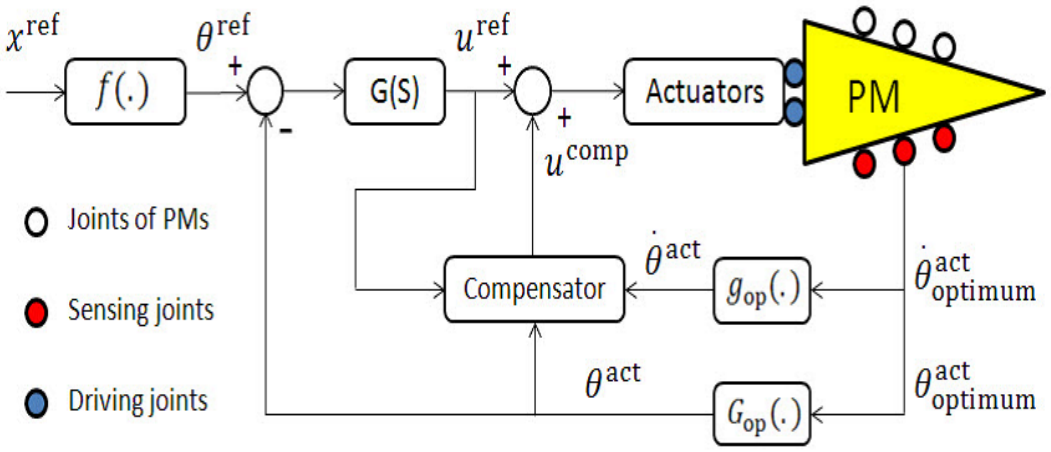

Fig. 3.19: $\mathscr{W}_1$: Using a optimum set of sensing joints

can be rewritten as,

$$\delta_c = -A_s[[\frac{\Delta\theta_s}{\Delta}]\Delta] \tag{3.44}$$

the matrix, A_s, is the corresponding sub-matrix extracted from the mapping matrix $A_{\Phi s}$ from sensing joints, the vector, $[[\frac{\Delta\theta_s}{\Delta}]\Delta]$, is a vector comprised of measured values of projections on sensing joints of errors on the end-effector.

Setting joint errors from driving joints, $\delta\theta_1 = 0.00015$ and $\delta\theta_4 = -0.00042$ in the PM shown in Fig.3.3, errors on the end-effector and their projections on other active joints can be calculated from Eq.3.7 and 3.8.

Table 3.5: Errors on the end-effector and their projections on joints

Original Error ($\|\delta\mathscr{X}_e\|$)	δx_e (mm)	δy_e (mm)	$\delta\theta_1$	$\delta\theta_2$	$\delta\theta_3$	$\delta\theta_4$	$\delta\theta_5$
0.09214	0.05456	-0.07425	0.00015	-0.00156	0.0024	-0.00042	0.00141

Setting the precision of joints $\Delta = 0.001$, measured values of sensors from all joints can be listed at table 3.6

Referring to Table 3.2, Fig.3.14 and 3.17, some optimum joints can be selected as sensing joints by using different evaluation methods. Joint error compensations to driving joints, error compensations on the end-effector and rest errors can be cal-

Table 3.6: Measured values of sensors

$[\frac{\Delta\theta_1}{\Delta}]\Delta$	$[\frac{\Delta\theta_2}{\Delta}]\Delta$	$[\frac{\Delta\theta_3}{\Delta}]\Delta$	$[\frac{\Delta\theta_4}{\Delta}]\Delta$	$[\frac{\Delta\theta_5}{\Delta}]\Delta$
0.000	-0.002	0.002	0.000	0.001

culated from Eq.3.34 $\sim$ 3.36,

Table 3.7: Joint error compensations, error compensations and rest errors using $\mathscr{W}_1$

Sensing joints	1,2	1,3	1,5	2,3	2,5
δ_c	{0., 0.0006667}	{0., 0.0004}	{0., 0.0003333}	{-0.001, 0.}	{-0.001, 0.}
Δ_c	{-0.0866025, 0.1}	{-0.0519615, 0.06}	{-0.0433013, 0.05}	{0., 0.075}	{0., 0.075}
Δ_r	{-0.03204, 0.02575}	{0.00260, -0.01425}	{0.01126, -0.02425}	{0.05456, 0.00075}	{0.05456, 0.00075}
$\lvert\Delta_r\rvert$	0.04111	0.01448	0.02674	0.05456	0.05456

As well known from table 3.7, rest errors from all sensing joints are less than original errors and movement accuracies of the end-effector have been improved by error compensations.

$\mathscr{W}_2$ is to use all active joints or a part of active joints with better error performance on the end-effector, obtain their joint errors measured by sensors, convert joint errors, average and transfer them to driving joints to modify movements of the end-effector. It is shown in Fig.3.20.

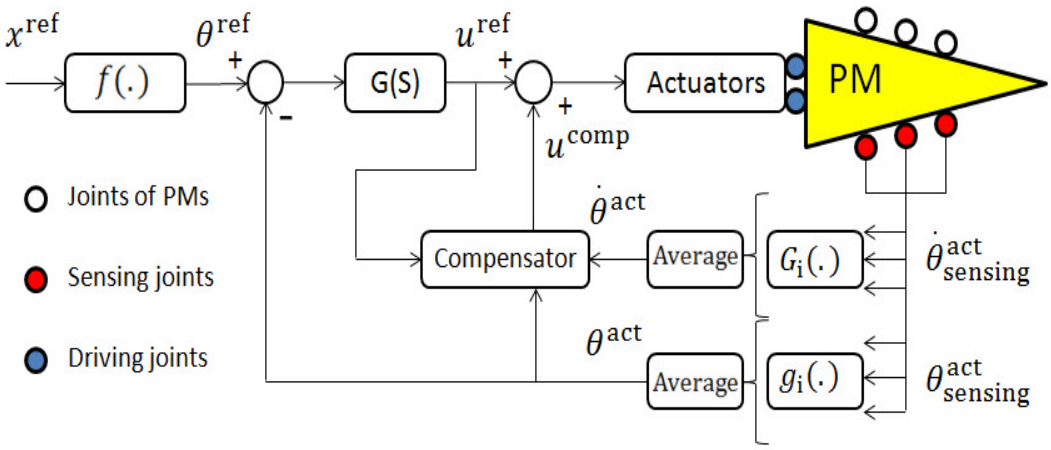

Fig. 3.20: $\mathscr{W}_2$: Using several sets of sensing joints

Joint error compensations to driving joints,

$$\delta c = -\frac{1}{m}\Sigma_{j=1}^{m}\{A_j[[\frac{\Delta\theta_j}{\Delta}]\Delta]\} \tag{3.45}$$

can be obtained from Eq.3.34.

Error compensations on the end-effector,

$$\Delta c = -J_d\frac{1}{m}\Sigma_{j=1}^{m}\{A_j[[\frac{\Delta\theta_j}{\Delta}]\Delta]\} \tag{3.46}$$

can be gotten from Eq.3.35.

Rest errors can be written as

$$\Delta_r = \delta X_e - J_d\frac{1}{m}\Sigma_{j=1}^{m}\{A_j[[\frac{\Delta\theta_j}{\Delta}]\Delta]\}. \tag{3.47}$$

Selecting all active joints and a part of active joints as sensing joints respectively, joint error compensations, error compensations on the end-effector and rest errors, can be gotten.

Table 3.8: Joint error compensations, error compensations and rest errors using $\mathscr{W}_2$

	All of joints	Part of joints 1,2‖1,3‖1,5‖2,3‖2,5
δ_c	{-0.006, 0.0014}	{-0.002, 0.0014}
Δ_c	{-0.0181865, 0.066}	{-0.0363731, 0.072}
Δ_r	{-0.03637, 0.00825}	{-0.01819, 0.00225}
$\mid \Delta_r \mid$	0.03730	0.01833

As well known from table 3.8, movement accuracies of the end-effector have been improved by error compensations. As is noted, when sensors of all joints are used in $\mathscr{W}_2$, error performances of different active joints will not need to be evaluated.

The main process can be summarized as follows,

1. To find all sets of active joints from joints with sensors, then building error models for them.

2. To disperse the workspace into points (x_i, y_i, z_i), build information maps. When $\mathscr{W}_1$ is used, active joints with the best error performance will be picked out by evaluation methods and identifiers of joint selected will be recorded to the file. When $\mathscr{W}_2$ is used, active joints with better error performances will be picked out and saved to the file. These files can be called as the *Information Map*s, they will be different with different evaluation methods.

3. To decide sensing joints by scanning information maps when a target position is given.

4. To convert movement information of sensing joints, transfer them to driving joints to produce movement compensations.

3.4 Conclusion

Improvement of movement accuracy has been discussed, and better movement accuracy on the end-effector can be achieved by using more accurate movement information to driving joints to compensate their movements. Several evaluation methods have been provided to find sensing joints. Error causes and transmissions, the relation between accuracy sphere and error regions have been also discussed. Finally two ways to improve the accuracy of the end-effector have been provided for obtaining better movement accuracy on the end-effector.

Chapter 4

Two Numerical Examples for Kinematics and Movement Accuracy Improvement of Parallel Mechanisms

4.1 Introduction

In the chapter kinematics of two PMs will be calculated by equations in chapter 2 to verify the validity of related conclusions. Then two movement simulations will be done by using methods in chapter 3.

Detailed contents are listed as following,

1. For kinematics of PMs

   (a) Calculating mechanism DOF and end-effector DOF, judging the redundancy of PMs.

   (b) Calculating Jacobians of PMs

   (c) Discussing the manipulability with using different active joints.

2. For movement accuracy improvement of PMs

   (a) Finding sensing joints and making Sensing map

One procedure flow will be presented in Fig. 4.1, it demonstrates the way to find sensing joints.

(b) Simulating one accurate movement of PMs along the given trajectory by using $\mathscr{W}_1$

Referring Fig.4.2, a movement simulation will be made by using $\mathscr{W}_1$.

(c) Simulating one accurate movement of PMs along the given trajectory by using $\mathscr{W}_2$ with reference of Fig.4.3

4.2 Numerical Example for a 2-DOF Planar Parallel Mechanism

In this section, one planar example will be done. It is a 2-DOF PM without redundant joints.

1. For kinematics of the PM

(a) Mechanism DOF, end-effector DOF and mechanism redundancy.

Firstly Jacobians of two kinematic chains will be derived.

The PM in Fig. 3.3 is a planar structure, Jacobians of two kinematic chains can be easily gotten by differentiating their position equations. Their position equations and Jacobians can be respectively written as following,

i. Kinematic chain 1:

$$\begin{cases} x = l_1\cos(\theta_1) + l_2\cos(\theta_1+\theta_2) + l_3\cos(\theta_1+\theta_2+\theta_3) \\ y = l_1\sin(\theta_1) + l_2\sin(\theta_1+\theta_2) + l_3\sin(\theta_1+\theta_2+\theta_3) \end{cases} \tag{4.1}$$

$$J_1 = \begin{bmatrix} -\mathrm{S}_1 l_1 - \mathrm{S}_{1+2} l_2 - \mathrm{S}_{1+2+3} l_3 & -\mathrm{S}_{1+2} l_2 - \mathrm{S}_{1+2+3} l_3 & -\mathrm{S}_{1+2+_3} l_3 \\ \mathrm{C}_1 l_1 + \mathrm{C}_{1+2} l_2 + \mathrm{C}_{1+2+3} l_3 & \mathrm{C}_{1+2} l_2 + \mathrm{C}_{1+2+3} l_3 & \mathrm{C}_{1+2+3} l_3 \\ 1 & 1 & 1 \end{bmatrix} \tag{4.2}$$

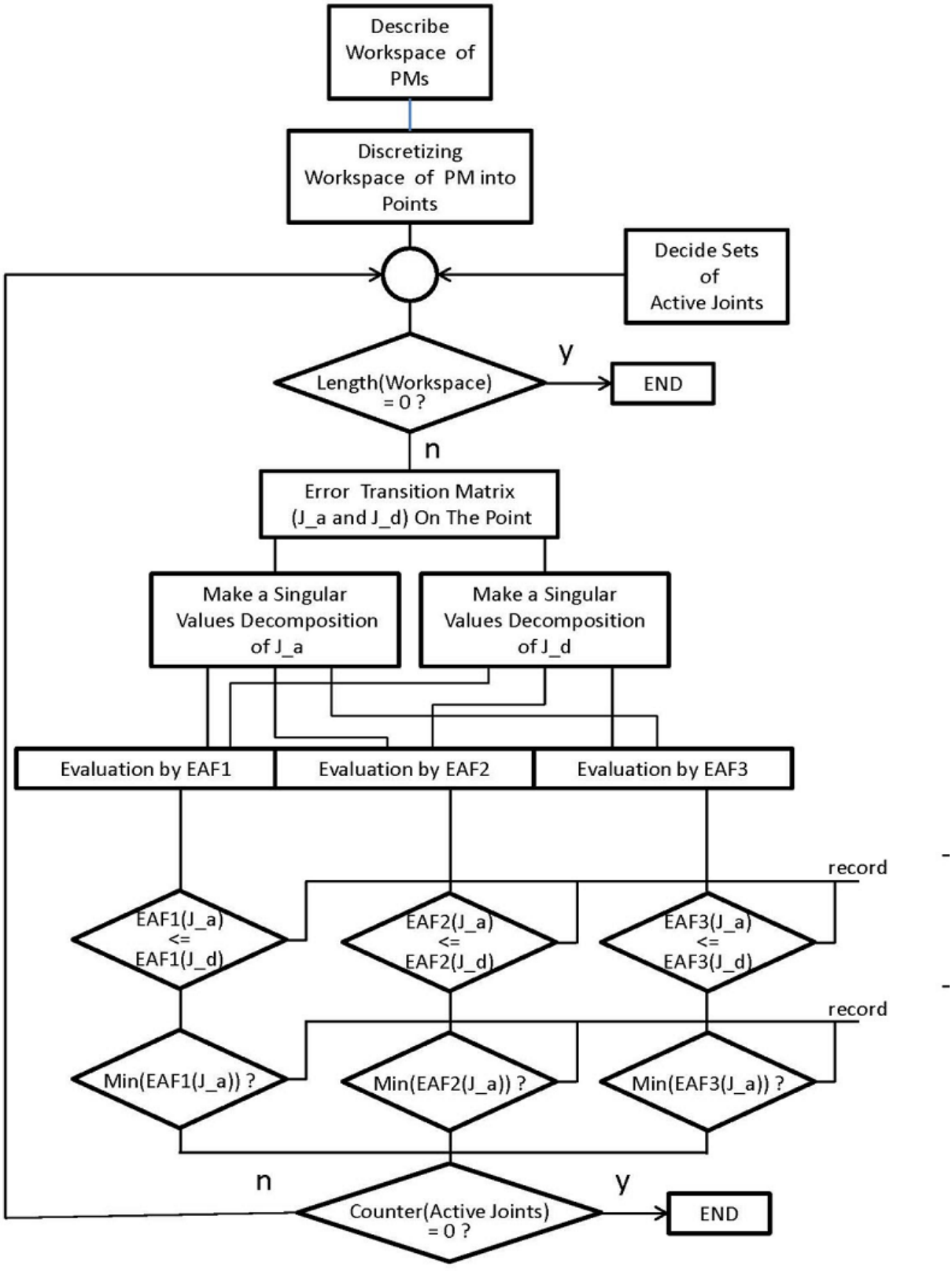

Fig. 4.1: One procedure flow for finding sensing joints

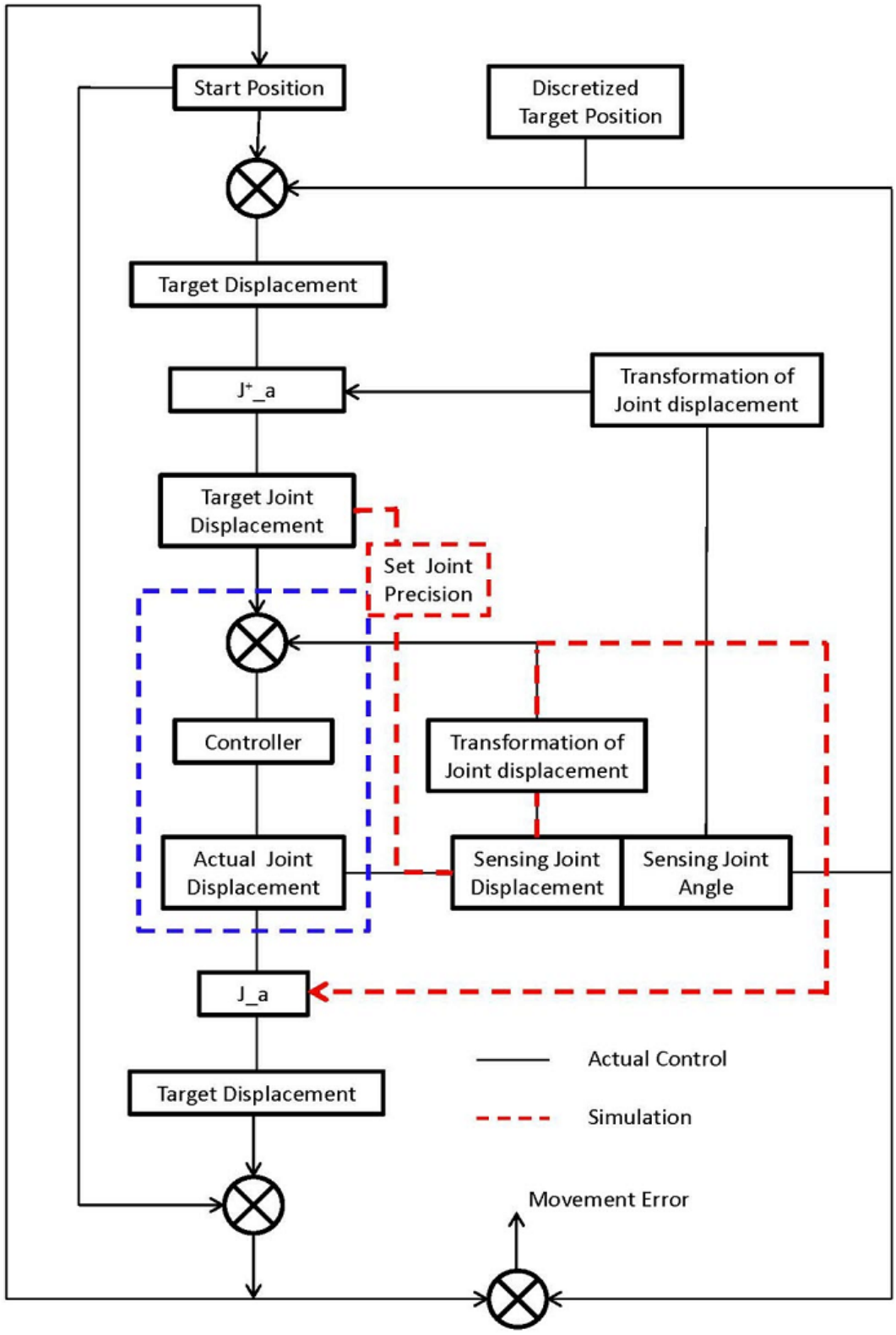

Fig. 4.2: One control and simulation flow to improve movement accuracy by $\mathscr{W}_1$

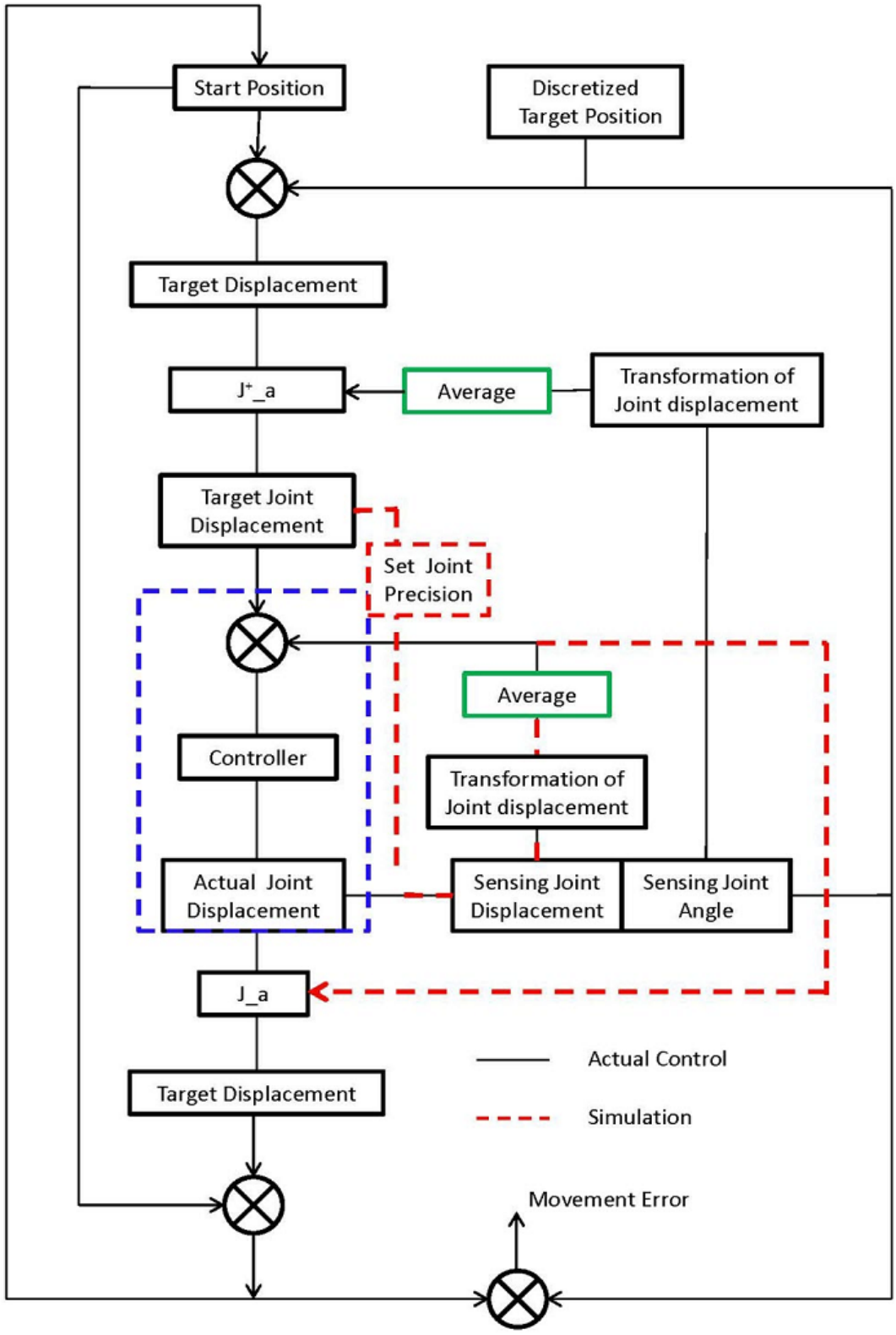

Fig. 4.3: One control and simulation flow to improve movement accuracy by $\mathscr{W}_2$

ii. Kinematic chain 2:

$$\begin{cases} x = l_4\cos(\theta_4) + l_5\cos(\theta_4+\theta_5) \\ y = l_4\sin(\theta_4) + l_5\sin(\theta_4+\theta_5) \end{cases} \tag{4.3}$$

$$J_2 = \begin{bmatrix} -\mathrm{S}_4 l_4 - \mathrm{S}_{4+5} l_5 & -\mathrm{S}_{4+5} l_5 \\ \mathrm{C}_4 l_4 + \mathrm{C}_{4+5} l_5 & \mathrm{C}_{4+5} l_5 \\ 1 & 1 \end{bmatrix} \tag{4.4}$$

Setting lengths of linkages

$$l_1 = 75\ [\mathrm{mm}], \quad l_2 = 75\ [\mathrm{mm}], \quad l_3 = 75\ [\mathrm{mm}],$$
$$l_4 = 75\sqrt{3}\ [\mathrm{mm}], \quad l_5 = 75\ [\mathrm{mm}], \quad H = 150\ [\mathrm{mm}],$$

if the end-effector locates at the position

$$P_x = 75\ [\mathrm{mm}],\ P_y = 75\sqrt{3}\ [\mathrm{mm}],$$

all angles of joints can be calculated by using the inverse kinematics,

$$\theta_1 = 120^\circ,\ \theta_2 = -60^\circ,\ \theta_3 = -60^\circ,\ \theta_4 = 90^\circ,\ \theta_5 = 90^\circ.$$

Substituting angles of joints, lengths of links to Eq.4.2 and 4.4, the matrix A_K can be gotten from Eq.2.7 and 2.11

$$A_k = \begin{bmatrix} \frac{38}{71} & -\frac{27}{71} & -\frac{2}{71} & \frac{20}{71} & -\frac{11}{71} \\ -\frac{27}{71} & \frac{36}{71} & -\frac{21}{71} & -\frac{3}{71} & -\frac{9}{71} \\ -\frac{2}{71} & -\frac{21}{71} & \frac{30}{71} & -\frac{16}{71} & \frac{23}{71} \\ \frac{20}{71} & -\frac{3}{71} & -\frac{16}{71} & \frac{18}{71} & -\frac{17}{71} \\ -\frac{11}{71} & -\frac{9}{71} & \frac{23}{71} & -\frac{17}{71} & \frac{20}{71} \end{bmatrix},$$

and its rank can be calculated,

$$Rank(A_k) = 2.$$

Scanning the whole movement space of the PM, the same result can be gotten, so mechanism DOF of the PM is 2.

The matrix J_K can be obtained from Eq.2.15,

$$J_k = \begin{bmatrix} -\frac{1500\sqrt{3}}{71} & \frac{225\sqrt{3}}{71} & \frac{1200\sqrt{3}}{71} & -\frac{1350\sqrt{3}}{71} & \frac{1275\sqrt{3}}{71} \\ -\frac{675}{71} & \frac{900}{71} & -\frac{525}{71} & -\frac{75}{71} & -\frac{225}{71} \\ \frac{9}{71} & -\frac{12}{71} & \frac{7}{71} & \frac{1}{71} & \frac{3}{71} \end{bmatrix},$$

and its rank can be calculated,

$$Rank(J_k) = 2.$$

Scanning the whole movement space, the same result can be gotten, so end-effector DOF of the PM is 2.

Because mechanism DOF of the PM is equal to its end-effector DOF, the PM is not with mechanism redundancy.

(b) Calculating Jacobian of the PM

Select a pair of joints as active joints. Because the joint 1 and 4 have been used in chapter 2, so a different pair, the joint 2 and 4, will be selected in the chapter.

Selection matrices with correspondence to selected joints can be written as

$$\phi_a = \begin{bmatrix} 0 & 0 \\ 1 & 0 \\ 0 & 0 \\ 0 & 1 \\ 0 & 0 \end{bmatrix}$$

$$\phi_u = \begin{bmatrix} 1 & 0 & 0 \\ 0 & 0 & 0 \\ 0 & 1 & 0 \\ 0 & 0 & 0 \\ 0 & 0 & 1 \end{bmatrix}.$$

From Eq.2.22, the displacement mapping matrix from active joints to all joints,

$$A_{\phi 14} = \begin{bmatrix} A_{\phi 14}[1,1] & A_{\phi 14}[1,2] \\ 1 & 0 \\ A_{\phi 14}[3,1] & A_{\phi 14}[3,2] \\ 0 & 1 \\ A_{\phi 14}[5,1] & A_{\phi 14}[5,2] \end{bmatrix}$$

$$A_{\phi 14}[1,1] = -\frac{l_2\left(\mathrm{S}_3 l_3 + \mathrm{S}_{1+2-4-5} l_5\right)}{l_1\left(\mathrm{S}_{2+3} l_3 + \mathrm{S}_{1-4-5} l_5\right) + l_2\left(\mathrm{S}_3 l_3 + \mathrm{S}_{1+2-4-5} l_5\right)}$$

$$A_{\phi 14}[1,2] = \frac{l_4\left(\mathrm{S}_{1+2+3-4} l_3 - \mathrm{S}_5 l_5\right)}{l_1\left(\mathrm{S}_{2+3} l_3 + \mathrm{S}_{1-4-5} l_5\right) + l_2\left(\mathrm{S}_3 l_3 + \mathrm{S}_{1+2-4-5} l_5\right)}$$

$$A_{\phi 14}[3,1] = -\frac{l_1\left(\mathrm{S}_2 l_2 + \mathrm{S}_{2+3} l_3 + \mathrm{S}_{1-4-5} l_5\right)}{l_1\left(\mathrm{S}_{2+3} l_3 + \mathrm{S}_{1-4-5} l_5\right) + l_2\left(\mathrm{S}_3 l_3 + \mathrm{S}_{1+2-4-5} l_5\right)}$$

$$A_{\phi 14}[3,2] = -\frac{l_4\left(\mathrm{S}_{1-4} l_1 + \mathrm{S}_{1+2-4} l_2 + \mathrm{S}_{1+2+3-4} l_3 - \mathrm{S}_5 l_5\right)}{l_1\left(\mathrm{S}_{2+3} l_3 + \mathrm{S}_{1-4-5} l_5\right) + l_2\left(\mathrm{S}_3 l_3 + \mathrm{S}_{1+2-4-5} l_5\right)}$$

$$A_{\phi 14}[5,1] = -\frac{\mathrm{S}_2 l_1 l_2}{l_1\left(\mathrm{S}_{2+3} l_3 + \mathrm{S}_{1-4-5} l_5\right) + l_2\left(\mathrm{S}_3 l_3 + \mathrm{S}_{1+2-4-5} l_5\right)}$$

$$A_{\phi 14}[5,2] = -\frac{l_1\left(\mathrm{S}_{2+3} l_3 + \mathrm{S}_{1-4} l_4 + \mathrm{S}_{1-4-5} l_5\right) + l_2\left(\mathrm{S}_3 l_3 + \mathrm{S}_{1+2-4} l_4 + \mathrm{S}_{1+2-4-5} l_5\right)}{l_1\left(\mathrm{S}_{2+3} l_3 + \mathrm{S}_{1-4-5} l_5\right) + l_2\left(\mathrm{S}_3 l_3 + \mathrm{S}_{1+2-4-5} l_5\right)}$$

can be derived.

Finally from Eq.2.24, the displacement mapping matrix from active joints to the end-effector,

$$J_{a14} = \begin{bmatrix} J_{a14}[1,1] & J_{a14}[1,2] \\ J_{a14}[1,1] & J_{a14}[1,2] \\ J_{a14}[1,1] & J_{a14}[1,2] \end{bmatrix}$$

$$J_{a14}[1,1] = \frac{S_2 S_{4+5} l_1 l_2 l_5}{l_1 (S_{2+3} l_3 + S_{1-4-5} l_5) + l_2 (S_3 l_3 + S_{1+2-4-5} l_5)}$$

$$J_{a14}[1,2] = \frac{l_4 (l_1 (-S_{2+3} S_4 l_3 + S_1 S_5 l_5) + l_2 (-S_3 S_4 l_3 + S_{1+2} S_5 l_5))}{l_1 (S_{2+3} l_3 + S_{1-4-5} l_5) + l_2 (S_3 l_3 + S_{1+2-4-5} l_5)}$$

$$J_{a14}[2,1] = -\frac{C_{4+5} S_2 l_1 l_2 l_5}{l_1 (S_{2+3} l_3 + S_{1-4-5} l_5) + l_2 (S_3 l_3 + S_{1+2-4-5} l_5)}$$

$$J_{a14}[2,2] = \frac{l_4 (l_1 (C_4 S_{2+3} l_3 - C_1 S_5 l_5) + l_2 (C_4 S_3 l_3 - C_{1+2} S_5 l_5))}{l_1 (S_{2+3} l_3 + S_{1-4-5} l_5) + l_2 (S_3 l_3 + S_{1+2-4-5} l_5)}$$

$$J_{a14}[3,1] = -\frac{S_2 l_1 l_2}{l_1 (S_{2+3} l_3 + S_{1-4-5} l_5) + l_2 (S_3 l_3 + S_{1+2-4-5} l_5)}$$

$$J_{a14}[3,2] = -\frac{(S_{1-4} l_1 + S_{1+2-4} l_2) l_4}{l_1 (S_{2+3} l_3 + S_{1-4-5} l_5) + l_2 (S_3 l_3 + S_{1+2-4-5} l_5)},$$

can be gotten.

(c) Manipulability of the PM

The manipulability ellipsoid can be gotten from Eq.2.25∼2.27. Making a singular-value decomposition to the Jacobian, axes of the manipulability ellipsoid, Σ^+, and their direction matrix, U, can be gotten.

Firstly if the joint 1 and 4 are selected as active joints,

$$U_{a14} = \begin{bmatrix} -0.601065 & -0.7992 & 0. \\ 0.799129 & -0.601012 & 0.0133321 \\ -0.0106551 & 0.00801349 & 0.999911 \end{bmatrix}$$

$$\Sigma^+_{a14} = \begin{bmatrix} 0.00483447 & 0. & 0. \\ 0. & 0.021229 & 0. \end{bmatrix}$$

Then if the joint 2 and 4 are selected,

$$U_{a24} = \begin{bmatrix} -0.954453 & -0.298361 & 0. \\ 0.298334 & -0.954368 & 0.0133321 \\ -0.00397779 & 0.0127249 & 0.999911 \end{bmatrix}$$

$$\Sigma^{+}_{a24} = \begin{bmatrix} 0.00737251 & 0. & 0. \\ 0. & 0.0278415 & 0. \end{bmatrix}$$

Finally if the joint 3 and 4 are selected as active joints,

$$U_{a34} = \begin{bmatrix} -0.954453 & -0.298361 & 0. \\ -0.298334 & 0.954368 & 0.0133321 \\ 0.00397779 & -0.0127249 & 0.999911 \end{bmatrix}$$

$$\Sigma^{+}_{a34} = \begin{bmatrix} 0.00737251 & 0. & 0. \\ 0. & 0.0278415 & 0. \end{bmatrix}$$

Obviously axes of manipulability ellipsoid and its direction matrix are completely different. It verified the conclusion in chapter 2 that the manipulability of PMs will be different when different active joints are used.

2. For movement accuracy improvement of the PM

   (a) i. Setting the trajectory in workspace

   The movement space of the PM is shown in Fig.4.4, it was computed by algebraic methods. The workspace will be set inside it. Here the whole movement space will be seen as workspace. A trajectory has been set in the workspace.

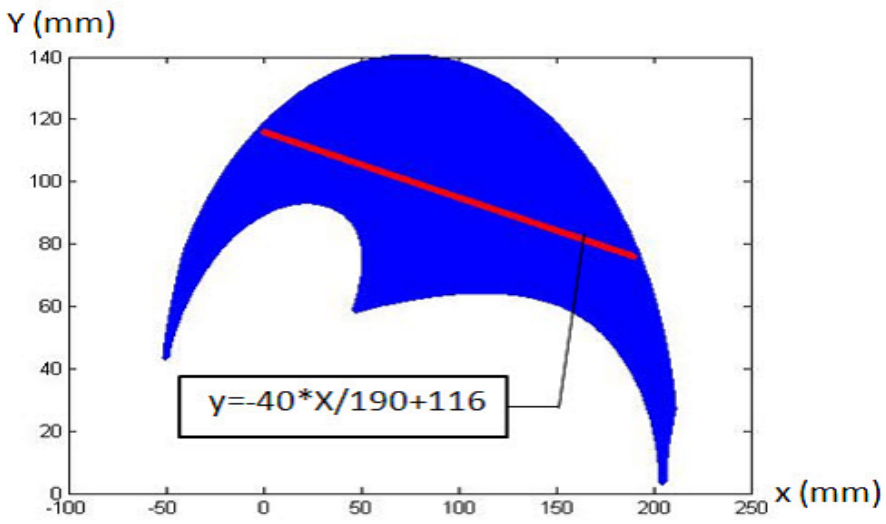

Fig. 4.4: A target trace in the workspace of a 2-DOF PM shown in Fig.3.3

ii. Decided sensing joints by using $\mathscr{W}_1$

By using the evaluation fuction, EAF1, EAF2, or EAF3, sensing joints on each discretized point in movement space can be found, they will be recorded to the file and form the information map of the whole movement space with reference of the procedure flow in Fig.4.1.

A map can be gotten by one evaluation function and one using way, so six maps will be made. All sensing joints can be found along the trajectory from information maps.

Using $\mathscr{W}_1$, all sensing joints along the trajectory have been determined and shown in Fig.4.5. They are three sets of optimum sensing joints by using different EAFs, only one set of active joints is selected on any a position as sensing joints.

iii. Decided sensing joints by using $\mathscr{W}_2$

Using $\mathscr{W}_2$, all sensing joints along the trajectory can be gotten and shown in Fig.4.6. Several sets of active joints with better error performances are selected on a position as sensing joints.

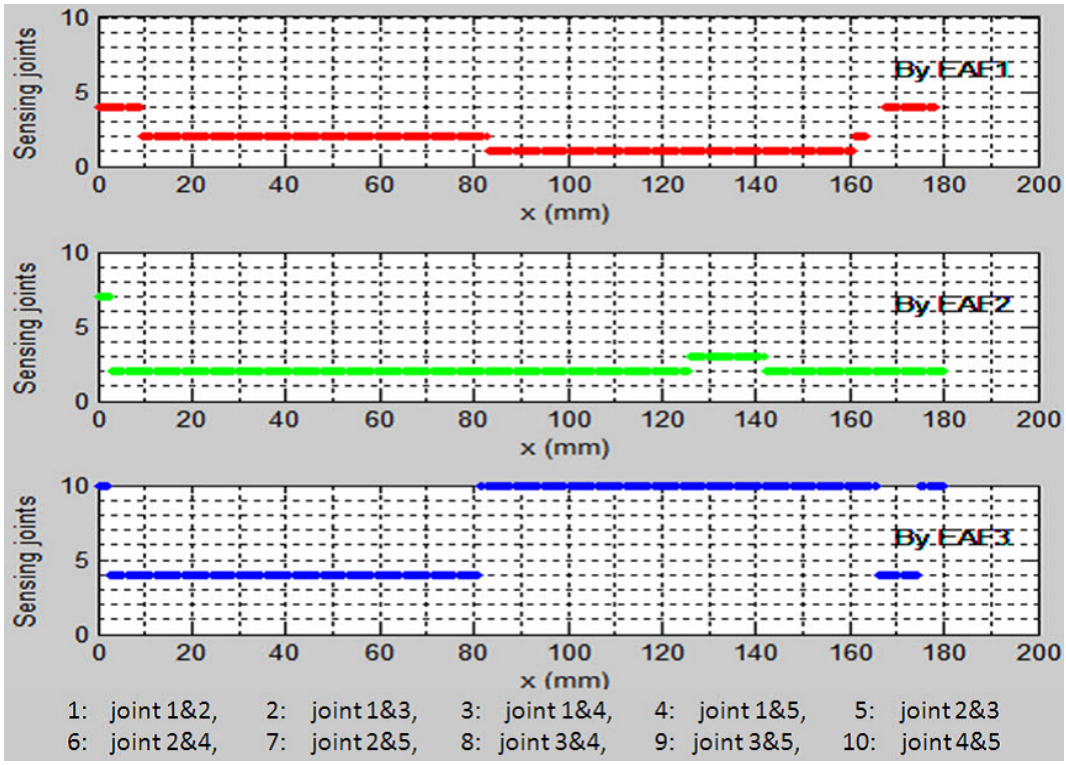

Fig. 4.5: Sensing joints selected along the target trace by using $\mathscr{W}_1$

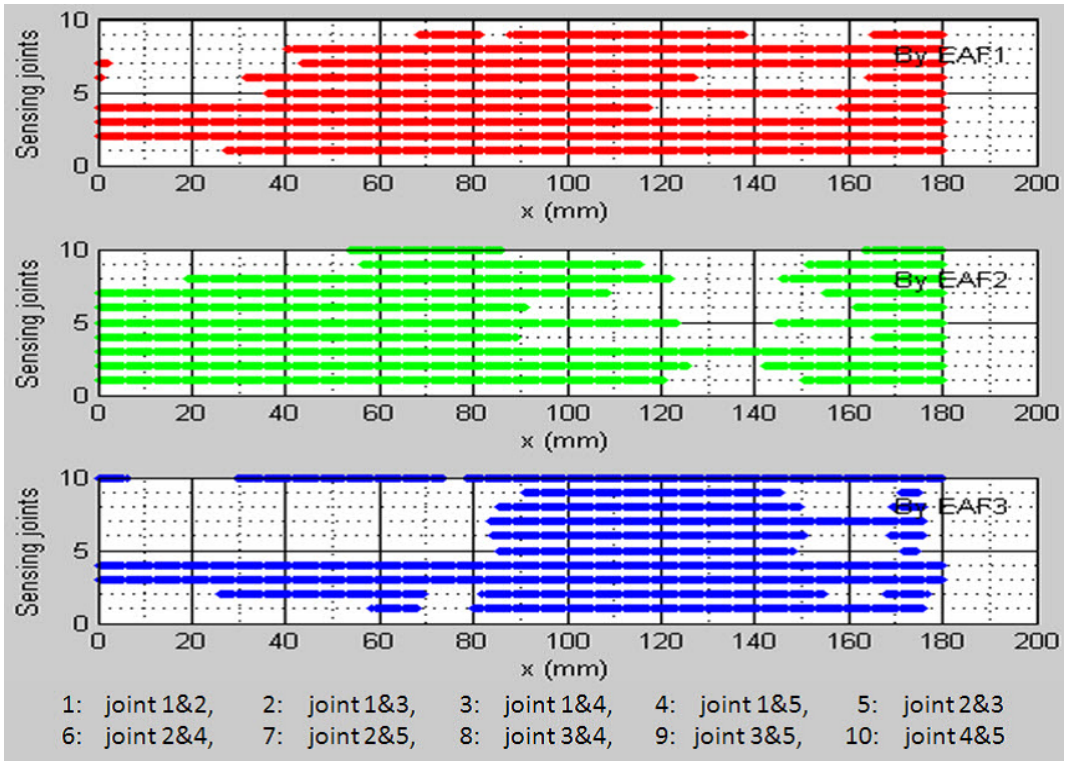

Fig. 4.6: Sensing joints selected along the target trace by using $\mathscr{W}_2$

(b) Improving movement accuracy of the PM by $\mathscr{W}_1$

Movement Errors are offsets from the actual position to the target. Its amplitude can be calculate from the following equation.

$$Error = \| \vec{X}_{tar} - \vec{X}_{act} \| \tag{4.5}$$

It will be used to measure movement accuracy as a criterion.

A movement simulation will be made along the trajectory shown in Fig.4.4. By $\mathscr{W}_1$, optimum sensing joints will be used. Referring to Fig.4.2, angles of sensing joints will be used to calculate angles of other joints by inverse kinematics. Displacements of sensing joints will be converted into displacements of driving joints, then delivered to driving joints to realize

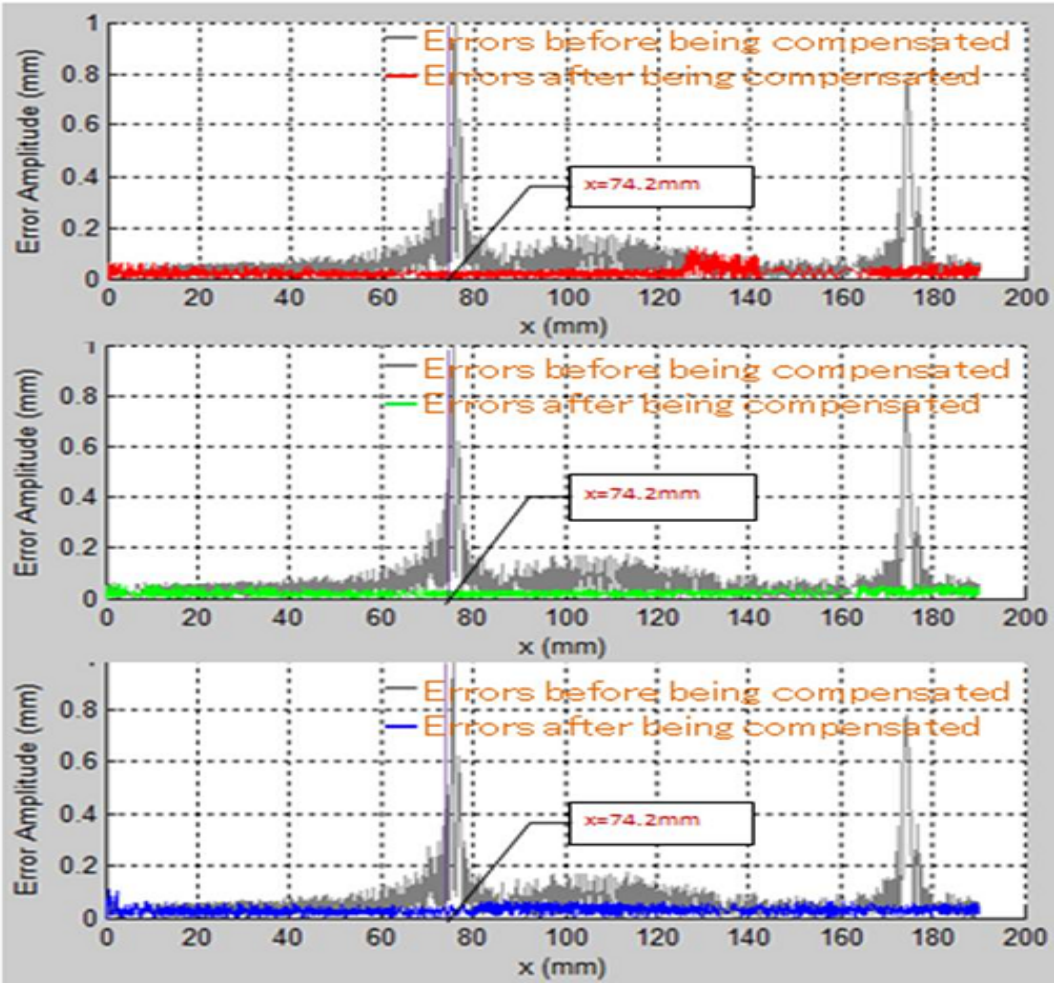

Fig. 4.7: Error on the end-effector by using the $\mathscr{W}_1$

movements of the end-effector.

Movement errors are shown in Fig.4.7, the gray line is errors from driving joints and amplitudes of errors after compensation are marked by the red line, green line and blue line. Obviously movement accuracies have been improved significantly.

Referring to Fig.4.8, if the end-effector at the position is located at (x=74.2mm, y=100.37895mm) of the trajectory, angles of joints can be listed as follows,

$$\theta_1 = 150.464^\circ, \quad \theta_2 = -121.507^\circ, \quad \theta_3 = -6.95571^\circ,$$
$$\theta_4 = 94.6584^\circ, \quad \theta_5 = 107.344^\circ$$

Setting the precision of joints, $\Delta = 0.001$, when joint errors of driving joints, $\delta\theta_1 \to 0.0005$ and $\delta\theta_4 \to -0.0005$, they will be detected by sensors of driving joints. Errors on the end-effector and measured values of joint errors from sensors can be listed at table 4.1,

Selecting each set of active joints as sensing joints, joint error compensa-

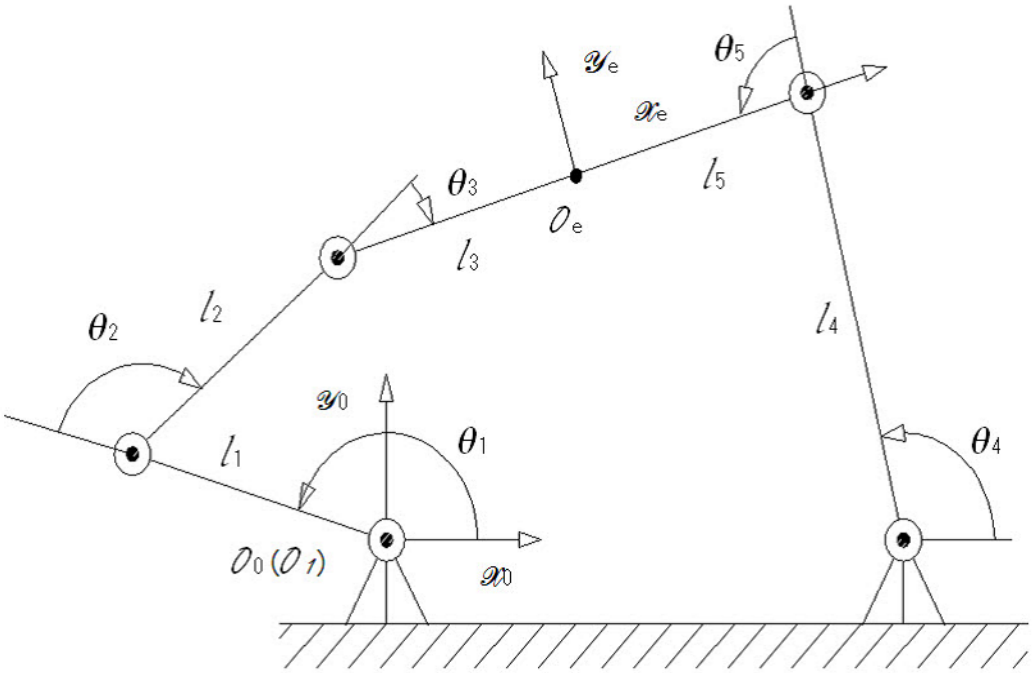

Fig. 4.8: A new position for the 2DOF PM

Table 4.1: Errors on the end-effector and measured values from sensors

Error ($\|\delta\mathscr{X}_e\|$)	δx_e (mm)	δy_e (mm)	$[\frac{\Delta\theta_1}{\Delta}]\Delta$	$[\frac{\Delta\theta_2}{\Delta}]\Delta$	$[\frac{\Delta\theta_3}{\Delta}]\Delta$	$[\frac{\Delta\theta_4}{\Delta}]\Delta$	$[\frac{\Delta\theta_5}{\Delta}]\Delta$
0.40062	0.20576	-0.34374	0	-0.011	0.015	0	-0.006

tions, δ_c, error compensations on the end-effector, Δ_c, and rest errors, Δ_r, can be gotten respectively from Eq.3.34 $\sim$ 3.36,

Table 4.2: Joint error compensations, error compensations and rest errors by $\mathscr{W}_1$

	1,2	1,3	1,4	1,5	2,3
δ_c	{0., 0.000805709}	{0., 0.000743662}	{0, 0}	{0., 0.000798097 }	{-0.001197, 0.000150 }
Δ_c	{0.25188, -0.35668 }	{0.23248, -0.32921 }	{0., 0. }	{0.24950, -0.35331 }	{0.16552, -0.35992 }
Δ_r	{-0.04611, 0.01294 }	{-0.02672, -0.01453 }	{0.20576, -0.34374 }	{-0.04373, 0.00957 }	{0.04024, 0.01618 }
$\|\Delta_r\|$	0.04790	0.03041	0.40062	0.04477	0.04337
	2,4	2,5	3,4	3,5	4,5
δ_c	{-0.00147336, 0. }	{-0.00009684, 0.000752 }	{-0.00150209, 0.}	{0.002028, 0.001748 }	{-0.00170446, 0.}
Δ_c	{0.14573, -0.36066 }	{0.24490, -0.35694 }	{0.14857, -0.36769 }	{0.34575, -0.27727 }	{0.16859, -0.41723 }
Δ_r	{0.06003, 0.01692 }	{-0.03914, 0.01320 }	{0.05720, 0.02400 }	{-0.13999, -0.06647 }	{0.03717, 0.07349 }
$\|\Delta_r\|$	0.06237	0.04130	0.06200	0.15496	0.08236

Referring to Fig.4.5, active joints 1,3 and 1,5 will be respectively selected as sensing joints in this movement simulation by $\mathscr{W}_1$. As well known from table 4.2 or Fig.4.7, movement accuracies on of the end-effector have been greatly improved by compensating joint errors of driving joints.

(c) Improving movement accuracy of the PM by $\mathscr{W}_2$

By $\mathscr{W}_2$, several sets of sensing joints will be used. Referring to Fig. 4.3, angles of sensing joints will be summed, then averaged to calculate angles of other joints. Displacements of sensing joints will be converted into displacements of driving joints, they will be averaged, then delivered to driving joints to realize movements of the end-effector.

Movement errors are shown in Fig.4.9, obviously movement accuracies have also been improved greatly.

Referring to Fig.4.6, if the evaluation function, EAF1, is used, nine sets of active joints will be selected as sensing joints, if the evaluation function,

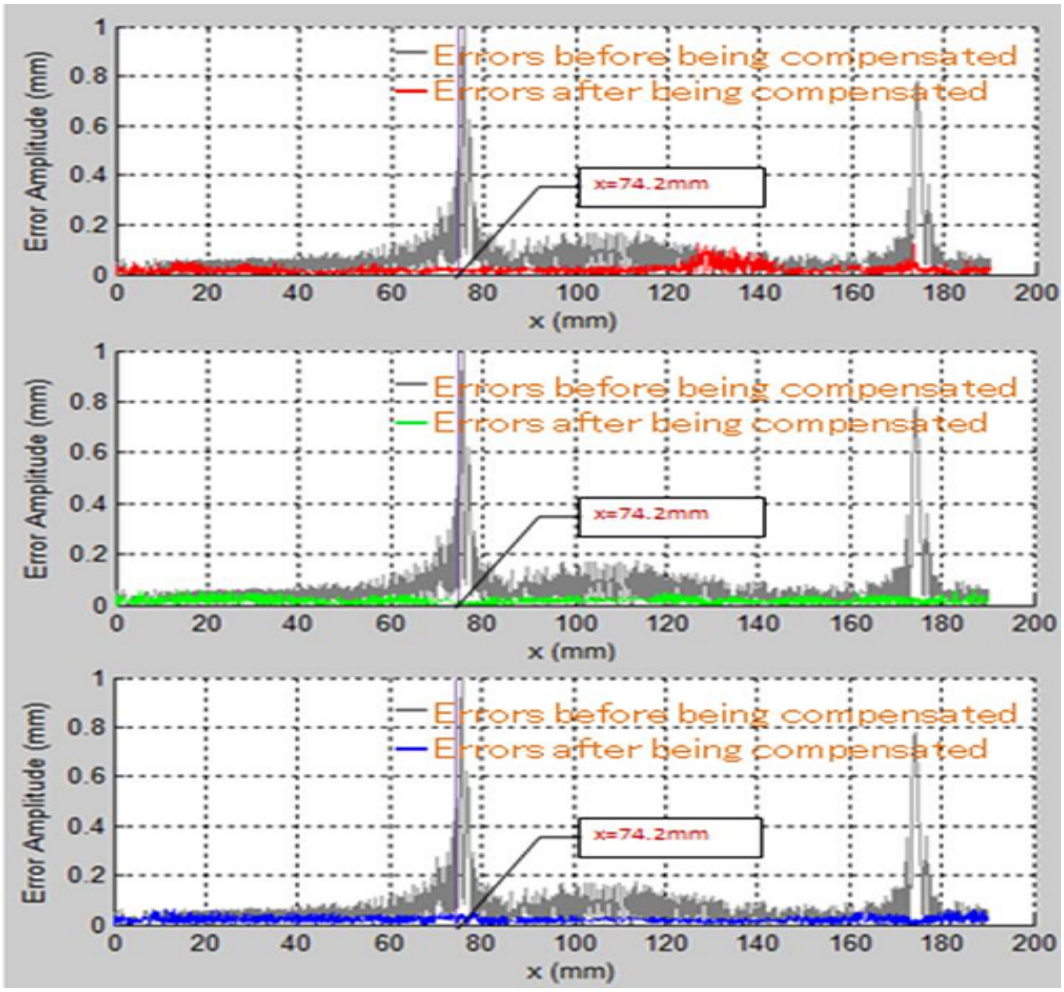

Fig. 4.9: Error on the end-effector by using the $\mathscr{W}_2$

EAF2, is used, all active joints will be selected,if the evaluation function, EAF3, is used, four sets of active joints will be selected. Joint error compensations, error compensations of the end-effector and rest errors can be calculated from Eq.3.43 $\sim$ 3.45.

Table 4.3: Joint error compensations, error compensations and rest errors by $\mathscr{W}_2$

	δ_c	Δ_c	Δ_r	$\mid \Delta_r \mid$
EAF1	{-0.00224321, 0.00499801}	{-0.19826, 0.30685}	{0.00750, -0.03686}	0.037641
EAF2	{-0.00394767, 0.00499801}	{-0.19530, 0.31789}	{0.01047, -0.02585}	0.02789
EAF3	{-0.00170446, 0.00154176}	{-0.1626, 0.2749}	{0.04312, -0.06880}	0.08120

As well known from table 4.3 or Fig.4.9, movement accuracies on of the

end-effector have been greatly improved by error compensations to driving joints by $\mathscr{W}_2$.

From Fig.4.8 and 4.9, movement errors before compensations are very enormous in some regions, it will make these regions unusable for the accuracy degradation and the workspace narrower. After compensations, movement accuracy have gotten great improvement in these areas, the workspace will be expanded with accuracy improvement.

4.3 Numerical Example for 3-DOF Spatial Parallel Mechanisms

In this section, one spatial example will be given. It is a 3-DOF PM with 2 redundant joints.

1. For kinematics of the PM

   (a) *Mechanism DOF, end-effector DOF and mechanism redundancy*

   Referring to Fig.2.1, lengths of all linkages in the PM are set at 120 [mm], and origins of initial coordinate frames of every kinematic chain are shown as follows,

$$\begin{aligned}
\Sigma_i &= \Sigma_O + [\,240 \quad 0 \quad 0\,]^T.\\
\Sigma_{ii} &= \Sigma_O + [\,0 \quad 240 \quad 0\,]^T.\\
\Sigma_{iii} &= \Sigma_O + [\,0 \quad 240 \quad 320\,]^T.
\end{aligned}$$

   A set of angles of joints can be set as:

$$\begin{aligned}
\vec{\theta} &= [\,\theta_{11}\ \theta_{12}\ \theta_{13}\ \theta_{14}\ t_1\ \theta_{21}\ \theta_{22}\ \theta_{23}\ \theta_{24}\ t_2\ \theta_{31}\ \theta_{32}\ \theta_{33}\ t_3\ \,]\\
&= [\,25.8253^\circ\ -32.1680^\circ\ -120.0573^\circ\ 36.4001^\circ\ -34.2373\\
&\quad 13.5270^\circ\ -32.0570^\circ\ -109.774^\circ\ -38.3040^\circ\ -32.4311\\
&\quad -0.0318^\circ\ -119.731^\circ\ 29.7628^\circ\ 28.0700\,]
\end{aligned}$$

From Eq.2.11, the matrix A_k can be gotten as follows.

$$A_k = \begin{bmatrix}
0.1970 & -0.3031 & 0.2272 & -0.1212 & 0 & 0 & 0 \\
-0.3031 & 0.4663 & -0.3496 & 0.1864 & 0 & 0 & 0 \\
0.2272 & -0.3496 & 0.2622 & -0.1398 & 0 & 0 & 0 \\
-0.1212 & 0.1864 & -0.1398 & 0.0746 & 0 & 0 & 0 \\
0 & 0 & 0 & 0 & 0.9998 & 0.0045 & -0.0005 \\
0 & 0 & 0 & 0 & 0.0045 & 0.1801 & -0.2983 \\
0 & 0 & 0 & 0 & -0.0005 & -0.2983 & 0.4943 \\
0 & 0 & 0 & 0 & -0.0043 & 0.2198 & -0.3642 \\
0 & -0.0001 & 0 & 0.0001 & 0.0003 & -0.1016 & 0.1682 \\
-0.0045 & -0.0009 & 0.0036 & 0.0017 & 0 & 0 & 0 \\
0 & 0 & 0 & 0 & 0.0083 & 0 & 0 \\
0 & 0 & 0 & 0 & -0.0083 & 0 & 0 \\
0 & 0 & 0 & 0 & 0 & 0 & 0 \\
-0.0003 & 0.0062 & 0.0035 & -0.0094 & 0 & 0.0001 & 0.0052
\end{bmatrix}$$

$$\begin{bmatrix}
0 & 0 & -0.0045 & 0 & 0 & 0 & -0.0003 \\
0 & -0.0001 & -0.0009 & 0 & 0 & 0 & 0.0062 \\
0 & 0 & 0.0036 & 0 & 0 & 0 & 0.0035 \\
0 & 0.0001 & 0.0017 & 0 & 0 & 0 & -0.0094 \\
-0.0043 & 0.0003 & 0 & 0.0083 & -0.0083 & 0 & 0 \\
0.2198 & -0.1016 & 0 & 0 & 0 & 0 & 0.0001 \\
-0.3642 & 0.1682 & 0 & 0 & 0 & 0 & 0.0052 \\
0.2684 & -0.1240 & 0 & 0 & 0 & 0 & 0.0031 \\
-0.1240 & 0.0574 & 0 & 0 & 0 & 0 & -0.0085 \\
0 & 0 & 0.9998 & -0.0048 & -0.0048 & 0.0096 & 0 \\
0 & 0 & -0.0048 & 0.0001 & 0 & 0 & 0 \\
0 & 0 & -0.0048 & 0 & 0.0001 & 0 & 0 \\
0 & 0 & 0.0096 & 0 & 0 & 0.0001 & 0 \\
0.0031 & -0.0085 & 0 & 0 & 0 & 0 & 0.9998
\end{bmatrix}$$

It needs to be ranked for calculating mechanism DOF of the PM. A singular value decomposition to the matrix is recommended to use for avoiding errors with numerical calculations. The results is written below,

$$[\ 1\ 1\ 1\ 1\ 1\ 0\ 0\ 0\ 0\ 0\ 0\ 0\ 0\ 0\ ]^{T}.$$

so the rank of the matrix is 5.

Scanning the whole movement space, the same result can be gotten, so the mechanism DOF of the PM is 5.

From Eq.2.15, the matrix J_k can be obtained as follows,

$$J_k = \begin{bmatrix} -0.0003 & 0.0062 & 0.0035 & -0.0094 & 0 & 0.0001 & 0.0052 \\ 0.0045 & 0.0009 & -0.0036 & -0.0017 & 0 & 0 & 0 \\ 0 & 0 & 0 & 0 & 0.9998 & 0.0045 & -0.0005 \\ 0 & 0 & 0 & 0 & 0 & 0 & 0 \\ 0 & 0 & 0 & 0 & 0 & 0 & 0 \\ 0 & 0 & 0 & 0 & 0 & 0 & 0 \end{bmatrix}$$

$$\begin{bmatrix} 0.0031 & -0.0085 & 0 & 0 & 0 & 0 & 0.9998 \\ 0 & 0 & -0.9998 & 0.0048 & 0.0048 & -0.0096 & 0 \\ -0.0043 & 0.0003 & 0 & 0.0083 & -0.0083 & 0 & 0 \\ 0 & 0 & 0 & 0 & 0 & 0 & 0 \\ 0 & 0 & 0 & 0 & 0 & 0 & 0 \\ 0 & 0 & 0 & 0 & 0 & 0 & 0 \end{bmatrix}$$

Making a singular value decomposition to this matrix, the result below can be obtained,

$$[\ 0.9999\ 0.9999\ 0.9999\ 0\ 0\ 0\ ]^{T}$$

so the rank of this matrix is 3. The same result can be obtained by scanning the total movement space, so the end-effector DOF of the PM is 3.

Comparing the end-effector DOF and mechanism DOF, the PM is with mechanism redundancy.

(b) Calculating Jacobian of the PM

Referring to Fig. 2.1, a set of joints

$$\{\theta_{12}, \theta_{13}, \theta_{22}, \theta_{23}, \theta_{31}\}$$

can be selected.

Extracting row vectors from the matrix, A_k, according to displacements of selected joints, a sub-matrix can be gotten as following,

$$A_s = \begin{bmatrix} -0.3031 & 0.4663 & -0.3496 & 0.1864 & 0 & 0 & 0 \\ 0.2272 & -0.3496 & 0.2622 & -0.1398 & 0 & 0 & 0 \\ 0 & 0 & 0 & 0 & -0.0005 & -0.2983 & 0.4943 \\ 0 & 0 & 0 & 0 & -0.0043 & 0.2198 & -0.3642 \\ 0 & 0 & 0 & 0 & 0.0083 & 0 & 0 \end{bmatrix}$$

$$\begin{bmatrix} 0 & -0.0001 & -0.0009 & 0 & 0 & 0 & 0.0062 \\ 0 & 0 & 0.0036 & 0 & 0 & 0 & 0.0035 \\ -0.3642 & 0.1682 & 0 & 0 & 0 & 0 & 0.0052 \\ 0.2684 & -0.1240 & 0 & 0 & 0 & 0 & 0.0031 \\ 0 & 0 & 0.0048 & 0.0001 & 0 & 0 & 0 \end{bmatrix}$$

Its rank is 5, so this set of joints can be used as active joints.

From Eq.2.17, selection matrices of selected joints can be given as follows,

$$\phi_s = \begin{bmatrix} 0\ 1\ 0\ 0\ 0\ 0\ 0\ 0\ 0\ 0\ 0\ 0\ 0\ 0 \\ 0\ 0\ 1\ 0\ 0\ 0\ 0\ 0\ 0\ 0\ 0\ 0\ 0\ 0 \\ 0\ 0\ 0\ 0\ 0\ 0\ 1\ 0\ 0\ 0\ 0\ 0\ 0\ 0 \\ 0\ 0\ 0\ 0\ 0\ 0\ 0\ 1\ 0\ 0\ 0\ 0\ 0\ 0 \\ 0\ 0\ 0\ 0\ 0\ 0\ 0\ 0\ 0\ 0\ 1\ 0\ 0\ 0 \end{bmatrix}^T$$

$$\phi_u = \begin{bmatrix} 1&0&0&0&0&0&0&0&0&0&0&0&0&0&0 \\ 0&0&0&1&0&0&0&0&0&0&0&0&0&0&0 \\ 0&0&0&0&1&0&0&0&0&0&0&0&0&0&0 \\ 0&0&0&0&0&1&0&0&0&0&0&0&0&0&0 \\ 0&0&0&0&0&0&0&0&1&0&0&0&0&0&0 \\ 0&0&0&0&0&0&0&0&0&1&0&0&0&0&0 \\ 0&0&0&0&0&0&0&0&0&0&0&1&0&0&0 \\ 0&0&0&0&0&0&0&0&0&0&0&0&1&0&0 \\ 0&0&0&0&0&0&0&0&0&0&0&0&0&1&0 \\ 0&0&0&0&0&0&0&0&0&0&0&0&0&0&1 \end{bmatrix}^T$$

From Eq.2.24, the Jacobian can be obtained,

$$J_d = \begin{bmatrix} 46.8602 & -122.6959 & 70.1629 & 0 & 0 & 0 \\ 62.4954 & -163.6341 & 93.5731 & 0 & 0 & 0 \\ 52.0736 & 141.1727 & -80.7287 & 0 & 0 & 0 \\ 70.6716 & 191.5922 & -109.5608 & 0 & 0 & 0 \\ 39.3882 & 106.7824 & 58.9752 & 0 & 0 & 0 \end{bmatrix}^T .$$

Designating a set of joint displacements

$$[\ 0.02^\circ\ \ 0.04^\circ\ \ 0.06^\circ\ \ 0.03^\circ\ \ 2.86^\circ\ ]^T$$

to active joints

$$[\ \Delta\theta_{12}\ \ \Delta\theta_{13}\ \ \Delta\theta_{22}\ \ \Delta\theta_{23}\ \ \Delta\theta_{31}\ ]^T$$

all joint displacements,

$$\begin{aligned} \Delta\vec{\theta} = [\,&\Delta\theta_{11}\ \Delta\theta_{12}\ \Delta\theta_{13}\ \Delta\theta_{14}\ \Delta t_1\ \Delta\theta_{21}\ \Delta\theta_{22} \\ &\Delta\theta_{23}\ \Delta\theta_{24}\ \Delta t_2\ \Delta\theta_{31}\ \Delta\theta_{32}\ \Delta\theta_{33}\ \Delta t_3] \\ =[\,&2.01^\circ\ \ 0.02^\circ\ \ 0.04^\circ - 2.07^\circ\ \ 2.90 \\ &1.06^\circ\ \ 0.06^\circ\ \ 0.03^\circ - 1.15^\circ - 5.43 \\ &2.86^\circ\ \ 0.12^\circ - 2.99^\circ\ \ 2.12\,] \end{aligned}$$

can be gotten from Eq.2.22.

Displacements of the end-effector,

$$\Delta\vec{X}_e = [\ 2.1209\ \ 5.4302\ \ 2.8967\ \ 0\ \ 0\ \ 0\ ]^T$$

can be obtained from Eq.2.23.

At the same position, selecting

$$\{\theta_{11}, \theta_{13}, \theta_{22}, \theta_{24}, \theta_{32}\}$$

as active joints, their joint displacements have been calculated and can be rewritten as,

$$\begin{aligned}&[\ \Delta\theta_{11}\ \Delta\theta_{13}\ \Delta\theta_{22}\ \Delta\theta_{24}\ \ \Delta\theta_{32}]\\ &= [\ 2.01^\circ\ \ 0.04^\circ\ \ 0.06^\circ\ -1.15^\circ\ \ 0.12^\circ\ ],\end{aligned}$$

the Jacobian of this set of active joints can be gotten as follows,

$$J_d = \begin{bmatrix} 3.3521 & 132.3514 & 76.7297 & 0 & 0 & 0 \\ -2.9060 & -114.7371 & -66.5180 & 0 & 0 & 0 \\ 33.5371 & 14.6720 & 8.5060 & 0 & 0 & 0 \\ -98.5089 & -43.0962 & -24.9847 & 0 & 0 & 0 \\ -5.2995 & -2.3184 & -121.3055 & 0 & 0 & 0 \end{bmatrix}^T$$

Displacements of the end-effector

$$[\ 2.1209\ \ 5.4302\ \ 2.8967\ \ 0\ \ 0\ \ 0\ ]^T$$

can be calculated from Eq.2.23.

Obviously displacements of the end-effector from two sets of active joints are same, it proved that direct kinematic relations derived in chapter 2 are correct.

(c) Manipulability of the PM

Manipulability ellipsoid can be gotten from Eq.2.25∼2.27.

Selecting the set of joints,

$$\{\theta_{12}, \theta_{13}, \theta_{22}, \theta_{23}, \theta_{31}\}$$

as active joints, axes of the manipulability ellipsoid,

$$\{\ 368.2712\ \ 129.9061\ \ 91.6928\ \ 0\ \ 0\ \}$$

and their direction matrix,

$$\begin{bmatrix} 0.0695 & 0.8920 & -0.4467 & 0 & 0 \\ -0.8651 & -0.1691 & -0.4722 & 0 & 0 \\ 0.4967 & -0.4192 & -0.7599 & 0 & 0 \\ 0 & 0 & 0 & -0.7581 & -0.2296 \\ 0 & 0 & 0 & -0.0994 & -0.8844 \\ 0 & 0 & 0 & 0.6445 & -0.4064 \end{bmatrix}$$

can be gotten.

Selecting the set of joints

$$\{\theta_{11}, \theta_{13}, \theta_{22}, \theta_{24}, \theta_{32}\}$$

as active joints, axes of the manipulability ellipsoid and their direction matrix will be,

$$\{\ 223.5614\ \ 101.3582\ \ 95.4276\ \ 0\ \ 0\ \}$$

and their direction matrix is:

$$\begin{bmatrix} -0.1690 & -0.7585 & -0.6294 & 0 & 0 \\ 0.7186 & 0.3422 & -0.6054 & 0 & 0 \\ -0.6746 & 0.5546 & -0.4872 & 0 & 0 \\ 0 & 0 & 0 & -0.5201 & 0.8498 \\ 0 & 0 & 0 & -0.3508 & -0.3035 \\ 0 & 0 & 0 & 0.7787 & 0.4309 \end{bmatrix}$$

can be gotten.

Obviously manipulability ellipsoids from different active joints are completely different. It verified the conclusion in chapter 2 once again.

2. For movement accuracy improvement of the PM

(a) i. Setting the trajectory in workspace

For a PM with redundancy, extra movement conditions must be provided in order to control movements of redundant joints. It is in favor of movement planing and keeping away from singular positions, but it will make calculation more complicated and does not need to be discussed in the chapter.

To avoid complicated calculation, the PM in Fig.2.1 will be simplified, a 3-DOF PM without redundancy can be obtained and shown in Fig.4.10.

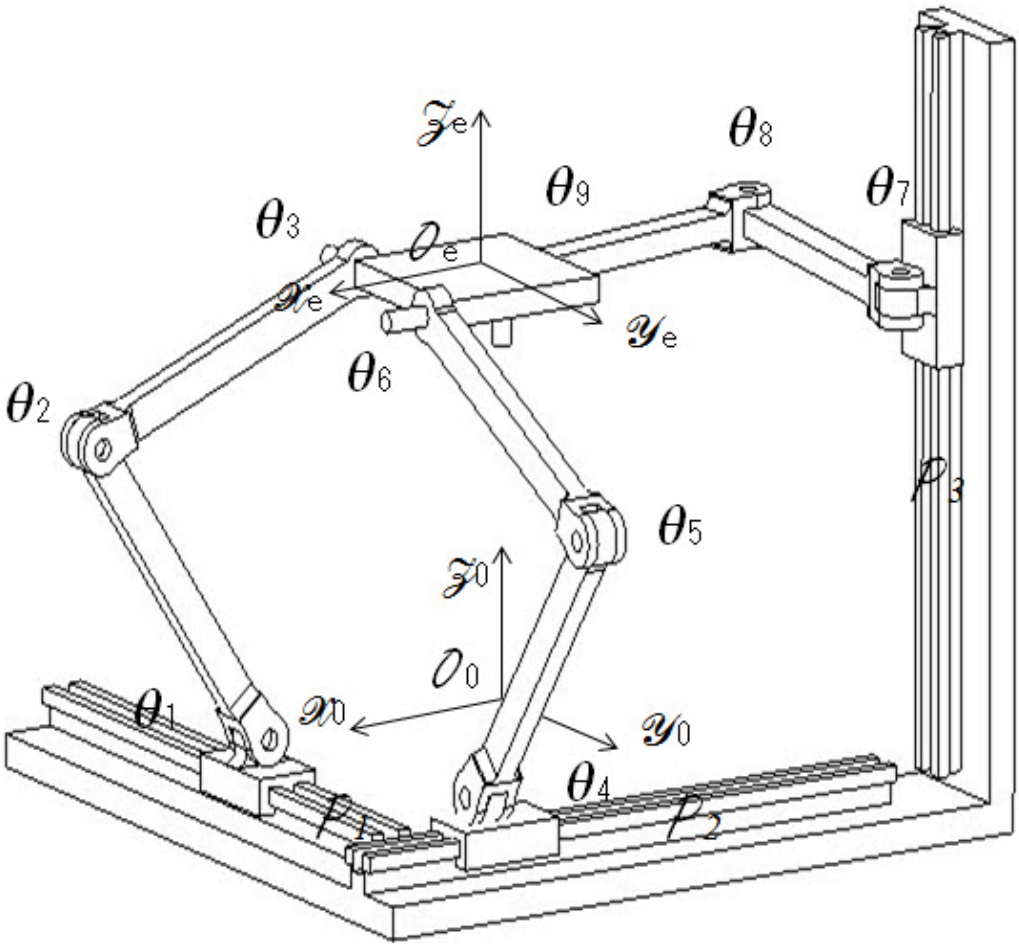

Fig. 4.10: A 3-DOF spatial PM without redundant joints

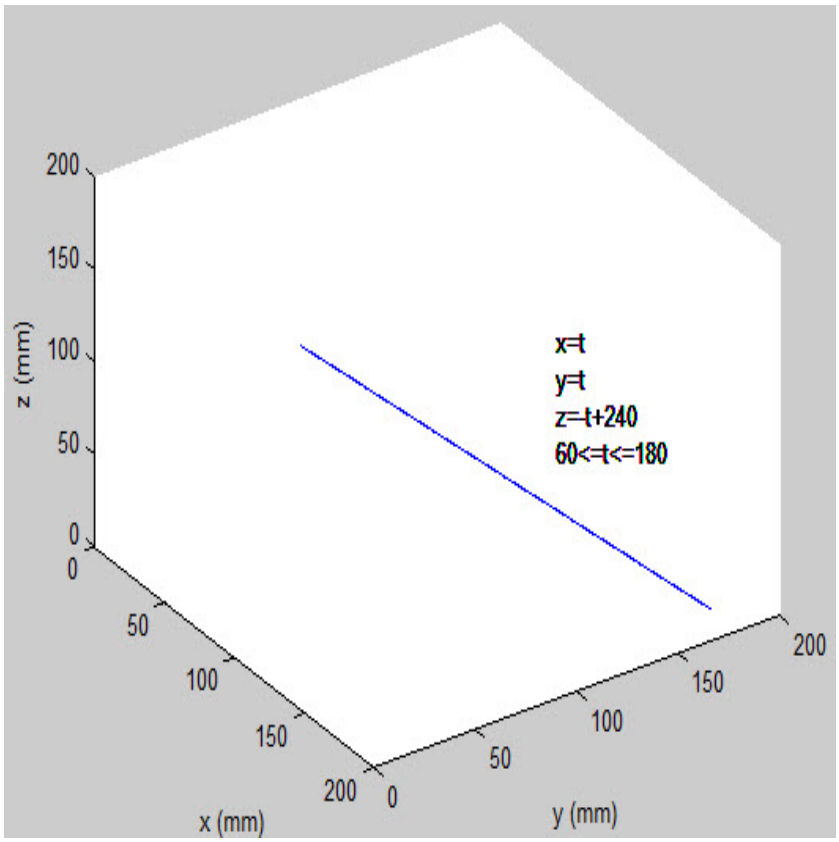

Fig. 4.11: A Target Trace in the Workspace of a 3-DOF PM

A trajectory is set as shown in Fig.4.11, movement simulations will be made along this trajectory. Referring to Fig.4.2 and 4.3, error compensations can be done on every position by using $\mathscr{W}_1$ and $\mathscr{W}_2$.

Sensing joints will be decided by evaluation functions, EAF1, EAF2 and EAF3. Referring Fig.4.1, information maps, which hold identification numbers of sensing joints selected, have been made in advance. All identification numbers and corresponding sets of active joints have been listed at table 4.4.

When a movement simulation is made, sensing joints on every position along the trajectory can be decided from information maps. Identification numbers of sensing joints on every position can be shown by graphes along the trajectory.

Table 4.4. Sets of active joints and their identification numbers

ID NO.	Active Joints	ID NO.	Active Joints	ID NO.	Active Joints	ID NO.	Active Joints	ID NO.	Active Joints
1	1,2,3	2	1,2,4	3	1,2,5	4	1,2,6	5	1,2,7
6	1,2,8	7	1,2,9	8	1,2,10	9	1,2,11	10	1,2,12
11	1,3,4	12	1,3,5	13	1,3,6	14	1,3,7	15	1,3,8
16	1,3,9	17	1,3,10	18	1,3,11	19	1,3,12	20	1,4,5
21	1,4,6	22	1,4,7	23	1,4,8	24	1,4,9	25	1,4,10
26	1,4,11	27	1,4,12	28	1,5,6	29	1,5,7	30	1,5,8
31	1,5,9	32	1,5,10	33	1,5,11	34	1,5,12	35	1,6,7
36	1,6,8	37	1,6,9	38	1,6,10	39	1,6,11	40	1,6,12
41	1,7,8	42	1,7,9	43	1,7,10	44	1,7,11	45	1,7,12
46	1,8,9	47	1,8,10	48	1,8,11	49	1,8,12	50	1,9,10
51	1,9,11	52	1,9,12	53	1,10,11	54	1,10,12	55	1,11,12
56	2,3,4	57	2,3,5	58	2,3,6	59	2,3,7	60	2,3,8
61	2,3,9	62	2,3,10	63	2,3,11	64	2,3,12	65	2,4,5
66	2,4,6	67	2,4,7	68	2,4,8	69	2,4,9	70	2,4,10
71	2,4,11	72	2,4,12	73	2,5,6	74	2,5,7	75	2,5,8
76	2,5,9	77	2,5,10	78	2,5,11	79	2,5,12	80	2,6,7
81	2,6,8	82	2,6,9	83	2,6,10	84	2,6,11	85	2,6,12
86	2,7,8	87	2,7,9	88	2,7,10	89	2,7,11	90	2,7,12
91	2,8,9	92	2,8,10	93	2,8,11	94	2,8,12	95	2,9,10
96	2,9,11	97	2,9,12	98	2,10,11	99	2,10,12	100	2,11,12
101	3,4,5	102	3,4,6	103	3,4,7	104	3,4,8	105	3,4,9
106	3,4,10	107	3,4,11	108	3,4,12	109	3,5,6	110	3,5,7
111	3,5,8	112	3,5,9	113	3,5,10	114	3,5,11	115	3,5,12
116	3,6,7	117	3,6,8	118	3,6,9	119	3,6,10	120	3,6,11
121	3,6,12	122	3,7,8	123	3,7,9	124	3,7,10	125	3,7,11
126	3,7,12	127	3,8,9	128	3,8,10	129	3,8,11	130	3,8,12
131	3,9,10	132	3,9,11	133	3,9,12	134	3,10,11	135	3,10,12
136	3,11,12	137	4,5,6	138	4,5,7	139	4,5,8	140	4,5,9
141	4,5,10	142	4,5,11	143	4,5,12	144	4,6,7	145	4,6,8
146	4,6,9	147	4,6,10	148	4,6,11	149	4,6,12	150	4,7,8
151	4,7,9	152	4,7,10	153	4,7,11	154	4,7,12	155	4,8,9
156	4,8,10	157	4,8,11	158	4,8,12	159	4,9,10	160	4,9,11
161	4,9,12	162	4,10,11	163	4,10,12	164	4,11,12	165	5,6,7
166	5,6,8	167	5,6,9	168	5,6,10	169	5,6,11	170	5,6,12
171	5,7,8	172	5,7,9	173	5,7,10	174	5,7,11	175	5,7,12
176	5,8,9	177	5,8,10	178	5,8,11	179	5,8,12	180	5,9,10
181	5,9,11	182	5,9,12	183	5,10,11	184	5,10,12	185	5,11,12
186	6,7,8	187	6,7,9	188	6,7,10	189	6,7,11	190	6,7,12
191	6,8,9	192	6,8,10	193	6,8,11	194	6,8,12	195	6,9,10
196	6,9,11	197	6,9,12	198	6,10,11	199	6,10,12	200	6,11,112
201	7,8,9	202	7,8,10	203	7,8,11	204	7,8,12	205	7,9,10
206	7,9,11	207	7,9,12	208	7,10,11	209	7,10,12	210	7,11,12
211	8,9,10	212	8,9,11	213	8,9,12	214	8,10,11	215	8,10,12
216	8,11,12	217	9,10,11	218	9,10,12	219	9,11,12	220	10,11,12

ii. Decided sensing joints by using $\mathscr{W}_1$

Identification numbers of sensing joints on every dispersed position along the trajectory in Fig. 4.11 will be shown in Fig. 4.12 when $\mathscr{W}_1$ is used.

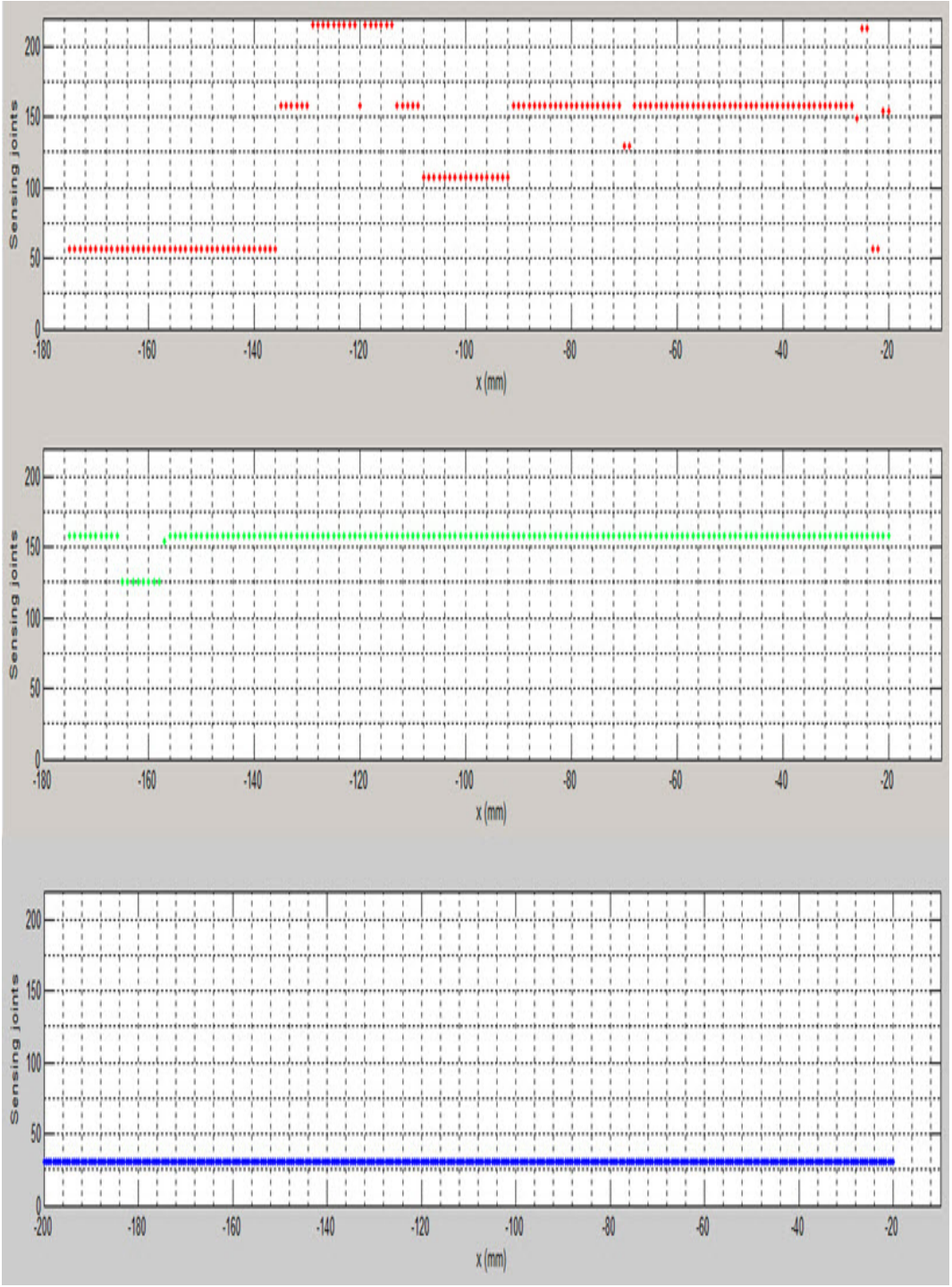

Fig. 4.12: Sensing joints selected along the trajectory by using $\mathscr{W}_1$

iii. Decided sensing joints by using $\mathscr{W}_2$

Identification numbers of sensing joints on every dispersed position along the trajectory in Fig. 4.11 will be shown in Fig. 4.13 when $\mathscr{W}_2$ is used.

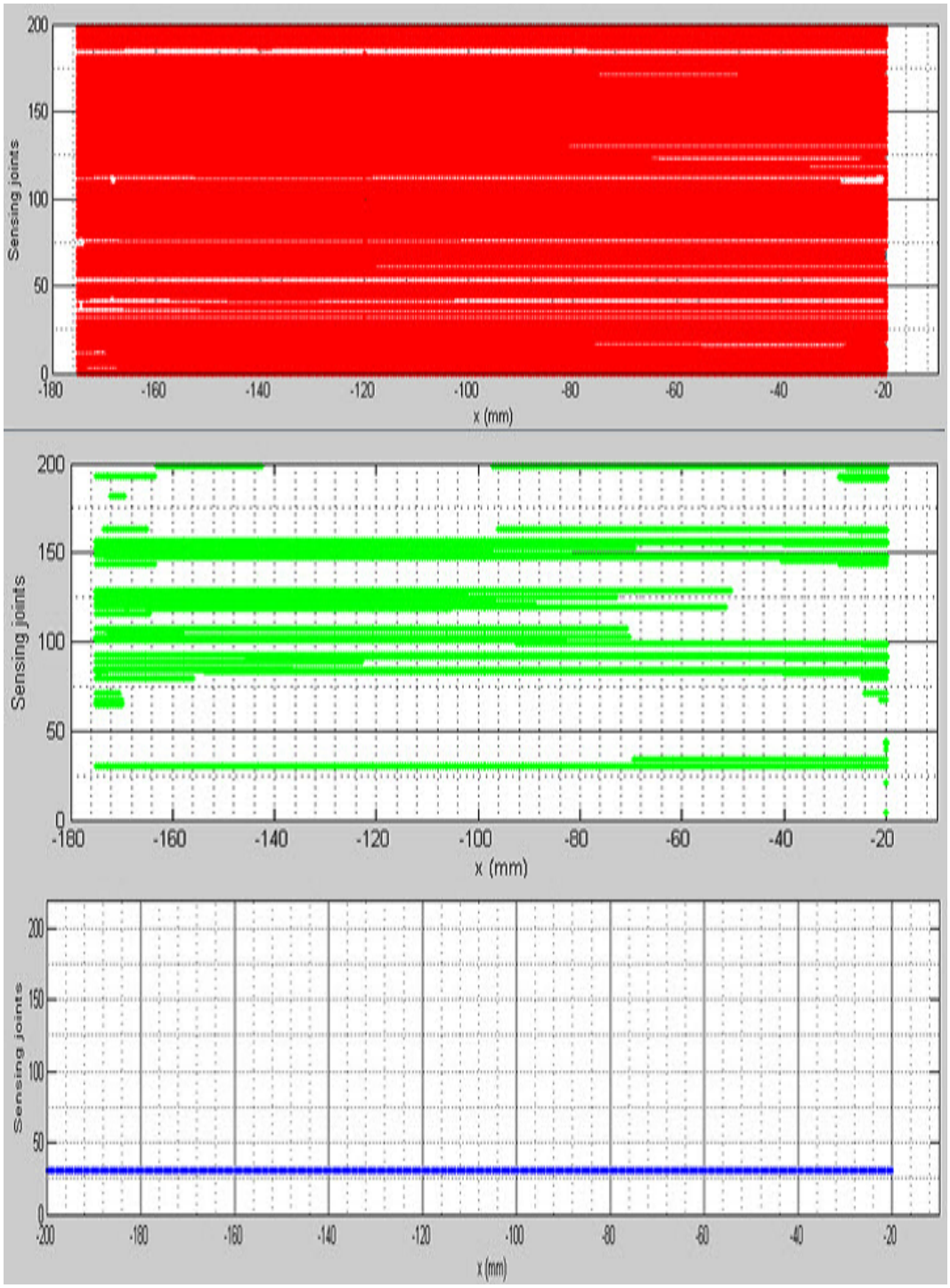

Fig. 4.13: Sensing joints selected along the trajectory by using $\mathscr{W}_2$

Six information maps can be gotten, but EAF3 can not be used as evaluation measure in this PM, because displacements of the end-effector, δX_e, δY_e *and* δZ_e, are always equal to ones of prismatic joints, δP_2, δP_1 *and* δP_3, in this PM and EAF3 will be invalid.

When

$$\delta P_1 = \delta P_2 = \delta P_3$$

is set, their error ellipsoids on the end-effector will be a ball and

$$EAF3 = \mathscr{M}ax(\sigma_1, \sigma_2 \cdots \sigma_{n_a}) / \mathscr{M}in(\sigma_1, \sigma_2 \cdots \sigma_{n_a})$$

will be 1 forever and only one set of active joints can be selected.

A line can be seen in Fig.4.12 or 4.13, it means only one set of active joints will be selected along the trajectory.

(b) Improving movement accuracy of the PM by $\mathscr{W}_1$

In $\mathscr{W}_1$, sensing joints will be active joints with the best error performance. Referring to Fig.4.2, angles of sensing joints will be used to calculate angles of other joints by inverse kinematics. Displacements of sensing joints will be converted, then delivered to driving joints to realize movements of the end-effector.

The amplitude of movement errors can be calculated by Eq.4.17. When EAF1 is used, movement errors on the end-effector are shown in Fig.4.14. When EAF2 is used, movement errors on the end-effector are shown in Fig.4.15. Original errors from Diving Joints are marked by gray line and errors after compensations are indicated by red line.

As well known from Fig.4.14 and 4.15, movement accuracies of the PM have been improved, and compared to EAF1, EAF2 is more effective.

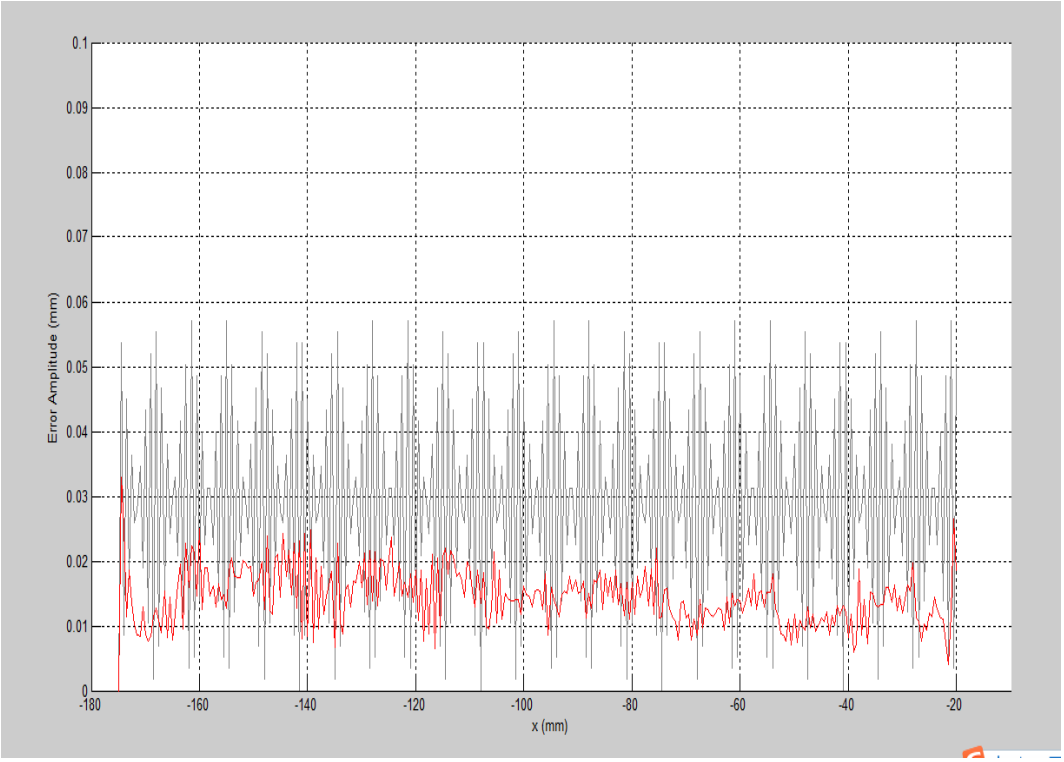

Fig. 4.14: Error on the end-effector by using the $\mathscr{W}_1$ and EAF1

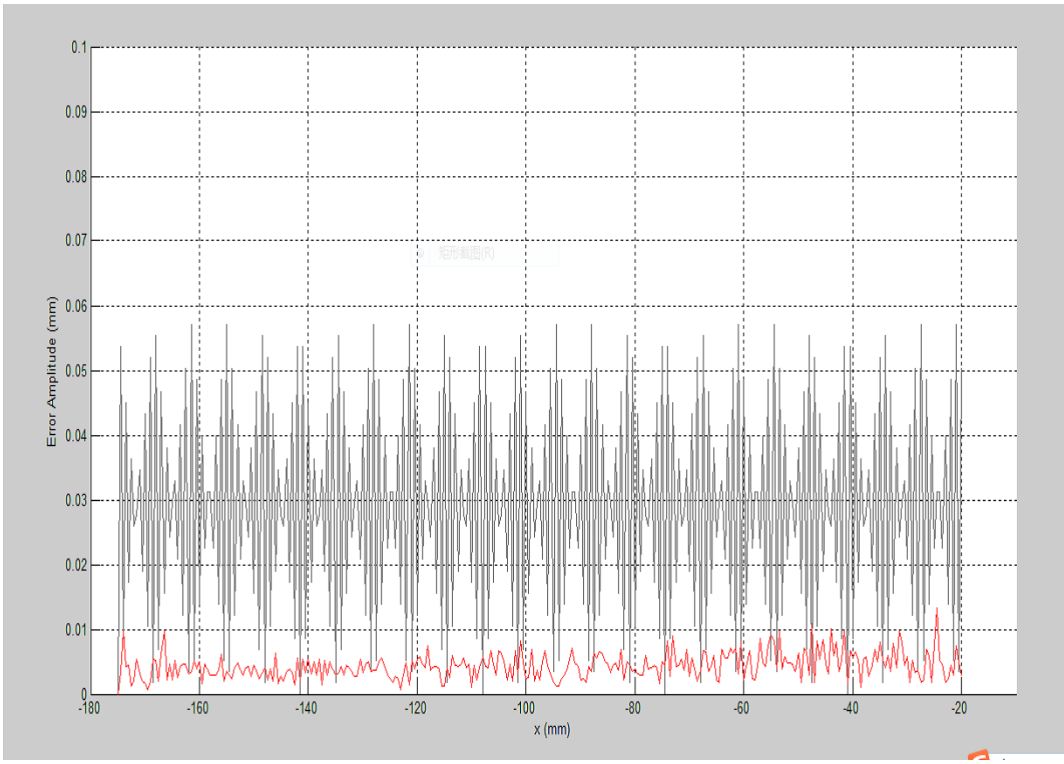

Fig. 4.15: Error on the end-effector by using the $\mathscr{W}_1$ and EAF2

(c) Improving movement accuracy of the PM by $\mathscr{W}_2$

In $\mathscr{W}_2$, all joints with better error performances will be used. Referring to Fig.4.3, angles of sensing joints will be used to calculate angles of other joints, results of calculation will be averaged to use. Displacements of sensing joints will be converted into displacements of driving joints, then averaged, finally delivered to driving joints to realize movements of the end-effector.

When EAF1 is used, movement errors on the end-effector are shown in Fig.4.16. When EAF2 is used, movement errors on the end-effector is shown in Fig.4.17. Similarly original errors from driving joints are marked by gray line and errors after compensations are indicated by red line. It will be known from Fig.4.16 and 4.17 that movement accuracies of the PM have been improved by $\mathscr{W}_2$. Compared to EAF1, EAF2 is more effective.

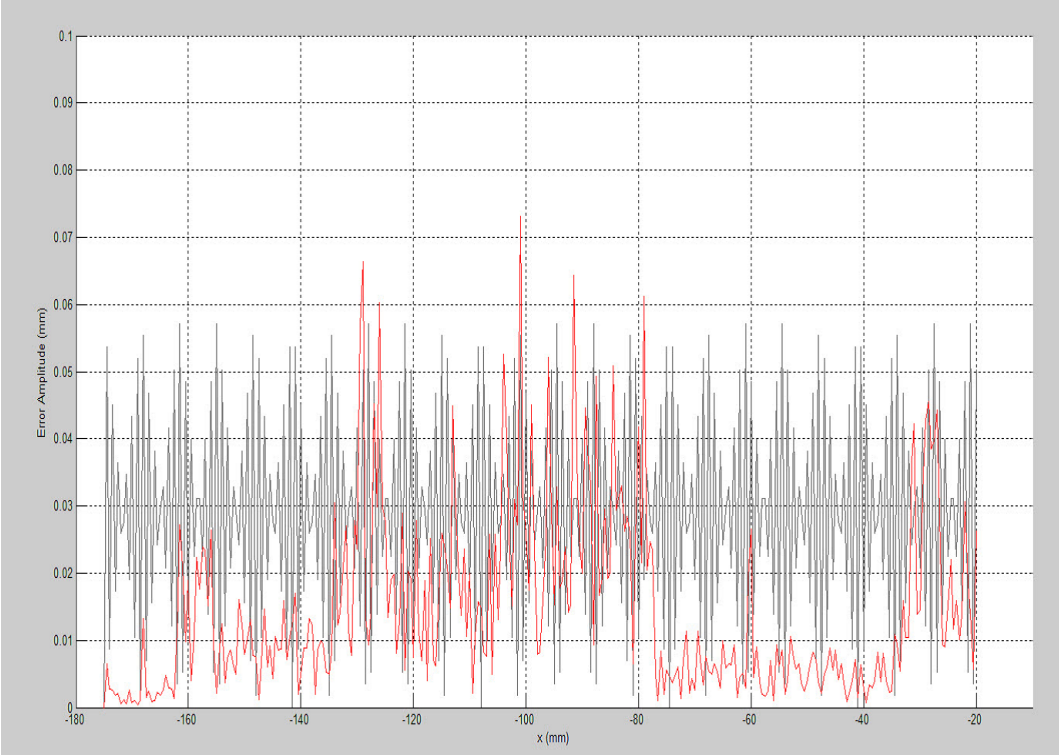

Fig. 4.16: Error on the end-effector by using the $\mathscr{W}_2$ and EAF1

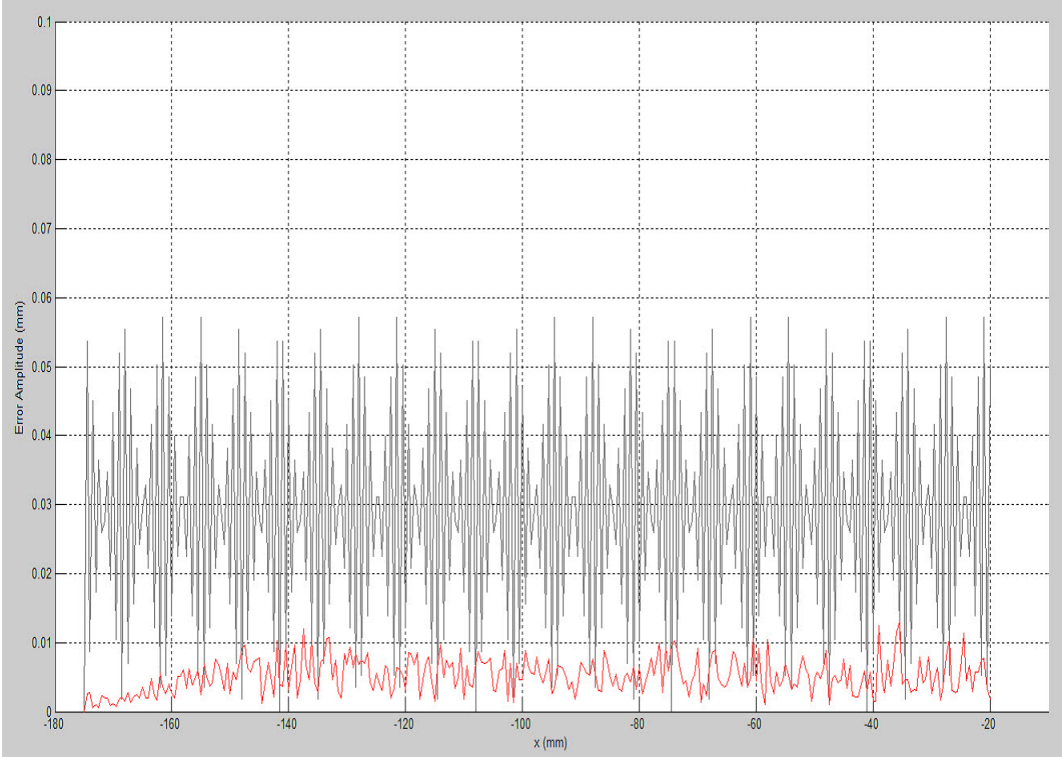

Fig. 4.17: Error on the end-effector by using the $\mathscr{W}_2$ and EAF2

Chapter 5

Conclusions

This thesis discussed direct kinematics and movement accuracy of PMs. Firstly it presents a set of methods to establish universal direct kinematic relations, which is to distinguish active joints and passive joints by using a pair of selection matrices, then derive the kinematic relation from active joints to all joints from the velocity constraint of PMs, finally get the direct kinematic relation from active joints to the end-effector. In the kinematics discussion, mechanism DOF, end-effector DOF, redundancy and manipulability of PMs have been already defined and discussed. Two main contributions in this part are a set of direct kinematic relation and a conclusion with reference to the manipulability of PMs, which the manipulability of PMs can be changed by selecting different active joints. The former can be applied to all PMs and will be utilized in kinematic analysis, design and optimization of architecture, decision of workspace in PMs, and the later gave one wide prospect for new research and new application of PMs.

Then one set of methods to improve movement accuracy of PM was presented, which is to equip redundant sensors to joints, pick out active joints with better movement information, convert their movement information, then transfer them to driving joints to realize movements of the end-effector. Error evaluation to different active joints, selections of sensing joints and use have been discussed. By movement simu-

lations, the validity of this set of methods has been verified. The movement accuracy of PMs has been improved, and some regions unusable for accuracy deterioration can be reused by using this set of methods. It is also expect to reduce the cost from design, manufacture for realization of accurate movements.

REFRENCE

[1] J. Tlusty, J. Ziegert and R. Ridgeway, “Fundamental Comparison of the Use of Serial and Parallel Kinematics for Machine Tools,” CIRP Annals-Manufacturing Technology, vol. 48, no. 1, pp. 331∼356, 1999.

[2] M. Weck and D. Steumer, “Parallel Kinematics Machine Tool-Current State and Future Potentials”, CIRP Annals-Manufacturing Technology, vol. 51, no. 2, pp. 671∼681, 2002.

[3] M. Uchiyama, K. Iimura, F. Pierrot, K. Unno and O. Toyama, “Design and Control of a Very Fast 6-DOF Parallel Robot,” Proceedings of the 1992 IMACS/SICE International Symposium on Robotics, Mechatronics and Manufacturing Systems, pp. 473∼478, 1992.

[4] A. Nahvi, J. M. Hollerbach and V. Hayward, “Calibration of a Parallel Robot Using Multiple Kinematic Closed Loops,” Proceedings of the 1994 IEEE International Conference on Robotics and Automation, vol. 1, pp. 407∼412, 1994.

[5] H. Zhuang, J. Yan and O. Masory, “Calibration of Stewart Platforms and Other Parallel Manipulators by Minimizing Kinematic Residuals,” Journal of Robotic Systems, vol. 15, no. 7, pp. 395∼405, 1998.

[6] J. Kim and F. C. Park, “Direct Kinematic Analysis of 3-RS Parallel Mechanism,” Mechanism and Machine Theory, vol. 36, no. 10, pp. 1121∼1134, 2001.

[7] S. Joshi and L.-W. Tsai, “A Comparison Study of Two 3-DOF Parallel Manipulators: One with Three and the Other with Four Supporting Legs,” IEEE Transactions on Robotics and Automation, vol. 19, no. 2, pp.200∼209, 2003.

[8] Q.-C. Li, Z. Huang and J. M. Herv*é*, “Type Synthesis of 3R2T 5-DOF Parallel Mechanisms Using the Lie Group of Displacements,” IEEE Transactions on Robotics and Automation, vol. 20, no. 2, pp. 173∼180, 2004.

[9] Q. Jin and T.-L. Yang, “Synthesis and Analysis of a Group of 3-Degree-Of-Freedom Partially Decoupled Parallel Manipulators,” ASME Journal of Mechanical Design, vol. 126, no. 2, pp. 301∼306, 2004.

[10] R. D. Gregorio, “Direct Position Analysis in Analytical Form of Parallel Manipulators Generating Structures with Topology SR-2PS,” Proceedings of the 2004 ASME Design Engineering Technical Conference, vol. 2, pp.115∼121, 2004.

[11] Y.-F. Fang and L.-W. Tsai, “Structure Synthesis of a Class of 3DOF Rotational Parallel Manipulators,” IEEE Transactions on Robotics and Automation, vol. 20, no. 1, pp. 117∼121, 2004.

[12] X. W. Kong and C. M. Gosselin, “Type Synthesis of Three Degree-of-Freedom Spherical Parallel Manipulators,” The International Journal of Robotics Research, vol. 23, no. 3, pp. 237∼245, 2004.

[13] X. W. Kong and C. M. Gosselin, “Type Synthesis of 3T1R 4DOF Parallel Manipulators Based on Screw Theory,” IEEE Transactions on Robotics and Automation, vol. 20, no. 2, pp. 181∼190, 2004.

[14] B. Hu and J.-J Yu, “Statics and Stiffness Model of Serial-Parallel Manipulator Formed by *k* Parallel Manipulators Connected in Series” ASME Journal of Mechanisms and Robotics, vol. 4, no. 2, 021012, 2012.

[15] I. Ebrahimi, J. A. Carretero and R. Boudreau, “3-PRRR Redundant Planar Parallel Manipulator: Inverse Displacement, Workspace and Singularity Analyses,” Mechanism and Machine Theory, vol. 42, no. 8, pp. 1007∼1016, 2007.

[16] S. Dutré, H. Bruyninckx and J. D. Schutter, “The Analytical Jacobian and Its Derivative for a Parallel Manipulator,” Proceedings of the 1997 IEEE International Conference on Robotics and Automation, vol.4, pp. 2961∼2966, 1997.

[17] D. Kim, W. K. Chung and Y. Youm, “Singularity Analysis of 6-DOF Manipulators with the Analytical Representation of the Determinant,” Proceedings of the 1999 IEEE International Conference on Robotics and Automation, vol. 2, pp. 889∼894, 1999.

[18] D. Kim, W. K. Chung and Y. Youm,“Analytic Jacobian of In-Parallel Manipulators,” Proceedings of the 2000 IEEE International Conference on Robotics and Automation, vol. 3, pp. 2376∼2381, 2000.

[19] C.M. Gosselin and J. Angeles, “Singularity Analysis of Closed-Loop Kinematic Chains,” IEEE Transactions on Robotics and Automation, vol. 6, no. 3, pp. 281∼290, 1990.

[20] J.-W. Zhao, K.-C. Fan, T.-H. Chang and Z. Li, “Error Analysis of a Serial-Parallel Type Machine Tool,” The International Journal of Advanced Manufacturing Technology, vol.19, pp.174∼179, 2002.

[21] Q.-S. Xu and Y.-M. Li, “Accuracy-Based Architecture Optimization of a 3-DOF Parallel Kinematic Machine,” Proceedings of the 2006 IEEE International Conference on Automation Science and Engineering, pp. 63∼68, 2006.

[22] J. Meng, D.-J. Zhang and Z.-X. Li, “Accuracy Analysis of Parallel Manipulators With Joint Clearance,” ASME Journal of Mechanical Design, vol. 131, no. 1, 011013: pp. 1∼9, 2009.

[23] J. Wang and O. Masory, “On the Accuracy of a Stewart Platform - Part I: The Effect of Manufacturing Tolerances,” Proceedings of the 1993 IEEE International Conference on Robotics and Automation, vol. 1, pp. 114∼120, 1993.

[24] I. S. M. Khalil, E. Globovic and A. Sabanovic, “High Precision Motion Control of Parallel Robots with Imperfections and Manufacturing Tolerances,” Proceedings of the 2011 IEEE International Conference on Mechatronics, pp. 39∼44, 2011.

[25] T. Yoshikawa, “Foundations of Robotics,” MIT Press, 1990.

[26] J. Phillips, “Freedom in Machinery,” vol. 1 (1984) and vol. 2 (1990) Combined, Cambridge University Press, 2006.

[27] J. Ryu and J. Cha, “Volumetric Error Analysis and Architecture Optimization for Accuracy of HexaSlide Type Parallel Manipulators,” Mechanism and Machine Theory, vol. 38, pp. 227∼240, 2003.

[28] Y. Yu and W.-Y. Liang, “Manipulability Inclusive Principle for Hip Joint Assistive Mechanism Design Optimization,” The International Journal of Advanced Manufacturing Technology, vol. 70, no. 5, pp. 929∼945, 2014.

[29] Y. Yu and Z.-W. Pei, “Kinematics Analysis and Manipulability of Closed-Loop Parallel Manipulator with Redundancy,” Proceedings of the 8th World Congress on Intelligent Control and Automation, pp. 2042∼2046, 2010.

[30] Z.-W. Pei and Y. Yu, “A Novel Method to Improve the Movement Accuracy of Parallel Mechanisms,” Proceedings of the 2014 IEEE International Conference on Robotics and Biomimetics, pp. 1169∼1174, 2014.

Acknowledgment

First and foremost I offer my sincerest gratitude to Professor Yong Yu, who has supported me throughout my work with your patience and knowledge. Your attentive guidance, valuable comments and encouragements enabled me to complete this research, without you this thesis would not have been completed.

I would also like to express my gratitude to Professor Mutsumi Watanabe and Professor Ryota Hayashi, thank you for spending an amount of time and patience on my seminars, your valuable advices gave me a lot of inspiration, pushed me forward along the path of this research.

Especially I want to thank Professor Tsutomu Nozaki, thank you for helping me in life, thank you for giving me lots of advices about life, thank you for bringing me to Japan, making me obtain a chance to taste different foreign culture, and to experience different life.

I also want to thank Mr. Irisa, Hisatome and Yano who have ever worked with me, your kindness and friendship made me feel very warm.

Finally, deeply thank my wife for your endless patience and constant supports throughout my graduate study.